Analysis of transcriptional regulation by RcsB homo- and heterodimers in *Escherichia coli*

Inaugural-Dissertation

zur

Erlangung des Doktorgrades

der Mathematisch-Naturwissenschaftlichen Fakultät

der Universität zu Köln

vorgelegt von

Hans Derk Pannen

aus Geldern

Berichterstatter:
(Gutachter)

Prof. Dr. Karin Schnetz

Prof. Dr. Jürgen Dohmen

Tag der mündlichen Prüfung: 27. Oktober 2015

Zusammenfassung....1
Abstract....2
1. Introduction....3
1.1. The Rcs phosphorelay and its cognate response regulator RcsB....4
1.2. Auxiliary regulators of RcsB belong to the FixJ/NarL-family....7
1.3. Aims of this thesis....11
2. Results....12
2.1. Homo- and heterodimer formation of RcsB....12
2.2. Establishment of reporter systems....14
2.2.1. RcsB-RcsB activates P*rprA* in a phosphorylation dependent manner....15
2.2.2. RcsA-RcsB activates P*wza* in a phosphorylation dependent manner....18
2.2.3. BglJ-RcsB reporter system....21
2.2.4. MatA-RcsB activates Pmat_{CFT073} in a phosphorylation independent manner....21
2.2.5. Search for potential DctR targets....26
2.2.6. Triple reporter system....29
2.3. Relevance of particular residues of RcsB for specific RcsB dimers....31
2.3.1. Identification of relevant amino acids within RcsB....31
2.3.2. The relevance of particular residues of RcsB varies with its interaction partner....33
2.4. Expression and stability of RcsB mutants....38
2.5. Protein-protein interaction of RcsB mutants....40
2.6. Mechanism of transcriptional activation....42
2.6.1. Interaction studies of RcsB with RNA polymerase by a bacterial two-hybrid system....42
2.6.2. Overexpression of the RNA polymerase α subunit....45
3. Discussion....52
3.1. Model....53
3.2. Homo- and heterodimerization of RcsB regulates a variety of cellular functions....55
3.3. RcsB regulates targets dependent and independent of phosphorylation....56
3.4. Residues within and close to active site of RcsB play a role for phosphorylation dependent activation....57
3.5. The mechanism of transcriptional activation by BglJ-RcsB depends on the promoter....58
4. Materials and Methods....61
4.1. Material....61
4.1.1. Bacterial strains, plasmids and oligonucleotides....61
4.1.2. Media, buffers and antibiotics....74
4.1.3. Enzymes, kits and chemicals....75
4.2. Methods....76
4.2.1. Standard molecular techniques....76
4.2.2. $CaCl_2$ competent cells and transformation....76
4.2.3. Electro-competent cells and electroporation....77
4.2.4. Mutagenesis PCR....77
4.2.5. Random mutagenesis screen....78
4.2.6. Promoter replacement and gene deletion....78

4.2.7. Preparation of lysate and transduction 79
4.2.8. Chromosomal integration 79
4.2.9. RcsB structure prediction 80
4.2.10. β-galactosidase assay 81
4.2.11. Motility assays 81
4.2.12. RNA isolation 81
4.2.13. Urea PAGE 81
4.2.14. cDNA synthesis 82
4.2.15. Microarray analysis 82
4.2.16. qPCR analysis 82
4.2.17. SDS PAGE and western blotting 83
4.2.18. Strep-protein interaction experiment (SPINE) 85

5. References 87

Abbreviations 95

Figure Index 96

Table Index 97

Danksagung 98

Erklärung 99

Zusammenfassung

Der FixJ/NarL-typ Transkriptionsfaktor RcsB ist der Response-Regulator des Rcs-Phosphorelays, einem komplexen Signaltransduktionssystem, welches die Integrität der bakteriellen Zellhülle überwacht. RcsB reguliert die Expression zahlreicher Loci die mit Motilität, Biofilmbildung und verschiedenen Stressantworten assoziiert sind. Dabei wird die Aktivität von RcsB durch zwei Mechanismen gesteuert: Erstens durch das Rcs-System, welches einen konservierten Aspartatrest in der Empfängerdomäne von RcsB phosphoryliert. Zweitens wird die Aktivität von RcsB durch Interaktion mit verschiedenen Hilfsproteinen gesteuert. Solche sind RcsA (Regulation der Kapselsynthese), BglJ (pleiotropischer Regulator, aktiviert *bgl u*nd *leuO*) sowie GadE (Säurestress). Diese Hilfsproteine gehören ebenfalls zur Familie der FixJ/NarL-Transkriptionsfaktoren. Zudem wurden zwei weitere Transkriptionsfaktoren der FixJ/NarL-Familie identifiziert, welche mit RcsB interagieren: MatA (kontrolliert Synthese der Mat-Pili) und DctR (in einem Acid-Stress-Island kodiert).

In dieser Arbeit wurden die Voraussetzungen der transkriptionellen Aktivierung durch RcsB-Homo- und Heterodimere analysiert. Zu diesem Zweck wurden geeignete Reportersysteme für RcsB-Homodimere und RcsB-Heterodimere mit RcsA und MatA entwickelt und getestet. Die Ergebnisse zeigen, dass MatA RcsB als Dimerisierungpartner benötigt um den *mat*-Promoter des UPEC-Stammes CFT073 zu aktivieren. Die Aktivierung erfolgt hierbei unabhängig von einer RcsB-Phosphorylierung. Zudem wurde gezeigt, dass MatA-RcsB die Motilität in *E. coli* K-12 hemmt. Des Weiteren bestätigen die Daten, dass die transkriptionelle Aktivierung durch RcsA-RcsB und RcsB-RcsB von einer RcsB-Phosphorylierung abhängt. In dieser Arbeit wurden außerdem bestimmte Aminosäuren der Empfängerdomäne von RcsB identifiziert, welche für die Aktivierung durch spezifische Dimere notwendig sind. Hierbei hat sich gezeigt, dass RcsB-Homodimere und RcsA-RcsB-Heterodimere -solche, deren Aktivität phosphorylierungsabhängig ist- die größte Ähnlichkeit aufweisen. Alle relevanten Aminosäuren sind innerhalb oder nahe des aktiven Zentrums lokalisiert und tragen vermutlich zur Strukturveränderung bei, welche durch Phosphorylierung induziert wird. Weitere Ergebnisse zum Mechanismus der transkriptionellen Aktivierung deuten daraufhin, dass einige Promotoren durch Interaktion von BglJ-RcsB und RNA-Polymerase in einem Pre-Recruitment-Mechanismus aktiviert werden.

Abstract

The FixJ/NarL-type transcription factor RcsB is the response regulator of the Rcs phosphorelay, a complex signal transduction system that senses perturbations of the bacterial cell envelope. RcsB regulates expression of multiple loci related to motility, biofilm formation, and various stress responses. The activity of RcsB is controlled by two mechanisms. First, the Rcs phosphorelay controls RcsB activity by phosphorylating a conserved aspartate residue within its receiver domain. Second, RcsB activity is modulated by interaction with auxiliary proteins, such as RcsA (regulation of capsule synthesis), BglJ (pleiotropic regulator, activating *bgl* and *leuO*), and GadE (acid stress response). These auxiliary regulators likewise belong to the FixJ/NarL transcription factor family and their activity depends on RcsB. Previously, RcsB was demonstrated to interact with two additional transcriptional regulators of the FixJ/NarL-family, MatA (control of the Mat pili expression) and DctR (encoded in the acid stress island).

In this work, determinants for transcriptional activation by RcsB homo- and heterodimers were analyzed. To this end, suitable reporter systems for RcsB homodimers and RcsB heterodimers with RcsA, and MatA were established. The results show that MatA requires RcsB as a dimerization partner for activating the *matA* promoter of UPEC strain CFT073 and that activation is independent of RcsB phosphorylation. In addition, it was shown that MatA-RcsB is able to repress the motility of *E. coli* K-12. Moreover, the results confirmed that transcriptional activation by RcsA-RcsB and RcsB-RcsB is phosphorylation dependent. This work also identified particular residues of the RcsB receiver domain being relevant for transcriptional activation by a specific dimer where RcsB homodimers and RcsA-RcsB heterodimers that are depending on RcsB phosphorylation possess the most similar properties. All relevant amino acids are located close to the active site, suggesting an important role for the structural change that is elicited by phosphorylation. Finally, data respective the mechanism of transcriptional activation, suggest that at some promoters BglJ-RcsB activates transcription by direct contacts to the RNA polymerase in a pre-recruitment mechanism.

1. Introduction

Bacteria are highly adaptive organisms with a large number of genes and pathways that allow exploiting a plenty of different environments. The central element of adaptation to a particular environment is the ability to modulate the expression of a gene subset in response to specific signals (Stephenson *et al.*, 2000). This response requires signal transduction systems for recognition and interpretation of signals, and the conversion of these signals resulting in a specific transcriptional regulation. For this purpose bacteria possess two-component signal transduction systems (TCS) that sense environmental stimuli and adjust the expression of specific genes appropriately. Two-component systems can also be found in eukaryotic organisms (Stock *et al.*, 2000). A typical two-component system consists of a sensor histidine kinase (HK) with an input and phosphorylation domain as well as a response regulator (RR) with an N-terminal receiver domain and a C-terminal output domain. Signal sensing by the input domain of the sensor histidine kinase triggers its autophosphorylation at a conserved histidine residue. From this histidine residue the phosphoryl group is transferred to a conserved aspartate residue within the receiver domain of its cognate response regulator, whose phosphorylation affects its output function (Stock *et al.*, 2000). Response regulators exist presumably in equilibrium between active and inactive state, while phosphorylation favors the active conformation and shifts the balance (Stock *et al.*, 2000). Beside prototypical two-component systems, a variety of bacteria possess more complex two-component systems. One more complex two-component system is the Rcs phosphorelay (Rcs = **R**egulator of **c**apsule **s**ynthesis) in *Escherichia coli* and other members of the *Enterobacteriaceae*, whose response regulator is RcsB. RcsB is a versatile transcription factor possessing the rare feature of homo- and heterodimerization with auxiliary regulators. RcsB is involved in many regulatory networks related to motility, cell division and various stress responses (Majdalani & Gottesman, 2005). In this work the determinants of transcriptional activation by RcsB are analyzed.

1.1. The Rcs phosphorelay and its cognate response regulator RcsB

The Rcs phosphorelay (Figure 1) is a complex two-component signal transduction system that was originally identified as a regulatory system of colanic acid capsule biosynthesis in *Escherichia coli* (Gottesman *et al.*, 1985). Nowadays the Rcs system is recognized as a key regulator of motility, biofilm formation, and various stress responses in *Enterobacteriaceae* and plays an important role in the control of lifestyle transition from a planktonic cell to a sessile cell in a biofilm (Evans *et al.*, 2013, Farris *et al.*, 2010, Laubacher & Ades, 2008, Majdalani & Gottesman, 2005). In many bacterial pathogens the Rcs phosphorelay is involved in controlling expression of virulence determinants. In enterohemorrhagic *E. coli*, for example, the Rcs system controls expression of genes at the locus of enterocyte effacement (LEE) that promote attachment to host cells (Tobe *et al.*, 2005). In *Salmonella enterica* serovar Typhimurium the Rcs system regulates the *Salmonella* pathogenicity island 2 (SPI-2) encoding a type III secretion system to transfer effector proteins into host cells (Wang *et al.*, 2007). In addition, the Rcs system has been implicated in pathogenicity in *Yersinia enterocolitica*, *Erwinia amylovora* and other pathogens (Hinchliffe *et al.*, 2008, Wang *et al.*, 2009, Majdalani & Gottesman, 2005). The Rcs phosphorelay consists of the inner membrane-bound histidine kinase RcsC and the response regulator RcsB (Figure 1). In addition to these two components, the Rcs system possesses the inner membrane-bound phosphotransfer protein RcsD, the outer-membrane lipoprotein RcsF and the inner membrane protein IgaA (YrfF) (Figure 1) (Cho *et al.*, 2014, Castanie-Cornet *et al.*, 2006, Majdalani & Gottesman, 2005). The core proteins RcsB, RcsC and RcsD are encoded at a single locus of the *E. coli* genome. The genes *rcsD* and *rcsB* form an operon which is immediately adjacent to *rcsC* but in a convergent orientation (Majdalani & Gottesman, 2005). Rcs-inducing conditions are, predominantly, perturbations of the cell wall and outer membrane by impaired lipopolysaccharide (LPS) synthesis through deletion of *rfaD* (Parker *et al.*, 1992) and *galU* (Girgis *et al.*, 2007), outer membrane protein (OMP) misfolding through deletion of *surA* (Castanie-Cornet *et al.*, 2006), and antibiotic-mediated peptidoglycan stress by β-lactam antibiotics such as amdinocillin (Laubacher & Ades, 2008). The lipoprotein RcsF is involved in sensing these perturbations and activating signaling, while IgaA inhibits the signaling cascade (Cho *et al.*, 2014, Farris *et al.*, 2010).

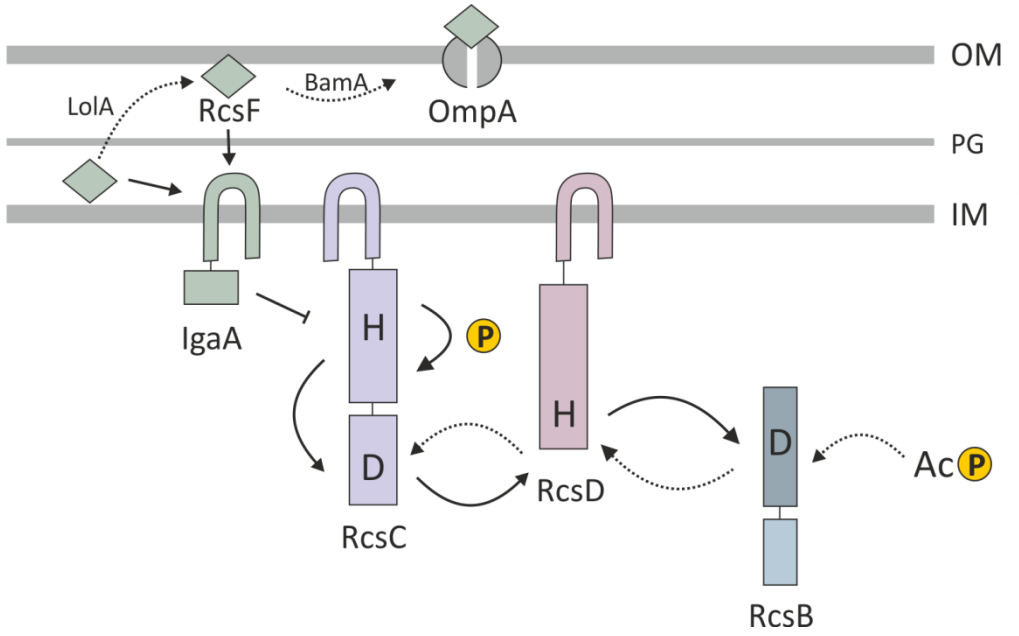

Figure 1. Model of activation and phosphotransfer of the Rcs phosphorelay
The lipoprotein RcsF is translocated from the inner membrane (IM) to the outer membrane (OM) by LolA (dashed arrows). At the OM RcsF binds BamA which funnels it to OmpA (dashed arrows). OmpA displays RcsF to the cell surface. By defects of the Lol system or the Bam machinery, RcsF interacts with IgaA inducing the autophosphorylation activity of the histidine kinase domain (H) of RcsC. The phosphotransfer of the active system is indicated by curved black arrows. From the histidine kinase domain, the phosphoryl group is transferred to the receiver domain (D) of RcsC, to the histidine phosphotransfer protein RcsD and in turn to the receiver domain of the response regulator RcsB. RcsB can also be phosphorylated unspecifically by acetyl phosphate (AcP) which is removed by the phosphatase activity of the uninduced Rcs system in reversible phosphotransfer direction (dashed curved arrow).

Both RcsF and IgaA are acting upstream of RcsC and RcsD (Figure 1) (Laubacher & Ades, 2008, Evans *et al.*, 2013, Cho *et al.*, 2014). On a molecular level, RcsF monitors lipoprotein transport through the periplasm and the β-barrel assembly. The chaperone LolA escorts lipoproteins including RcsF from the inner to the outer membrane (Figure 1). Defective LolA-mediated transport causes RcsF accumulation at the inner membrane what activates the Rcs system through IgaA which in turn induces *lolA* expression (Tao *et al.*, 2012, Cho *et al.*, 2014). At the outer membrane, RcsF monitors the β-barrel assembly machinery (Bam) by interacting with BamA. Active BamA funnels RcsF to the outer membrane porin OmpA that exposes RcsF to the cell surface (Figure 1) (Cho *et al.*, 2014). Disruption of this machinery results in RcsF accumulation in the periplasm where RcsF can activate the Rcs system by interaction with IgaA (Cho *et al.*, 2014). Both RcsC and RcsD are anchored to the inner membrane and exhibit a cytoplasmic part (Figure 1). The cytoplasmic part of RcsC includes a sensor kinase domain which is autophosphorylated at a conserved histidine residue upon activation of the signaling cascade. From this histidine, the phosphate is transferred to a

conserved aspartate residue within the receiver domain of RcsC. In the next step of the phosphorelay cascade the phosphate is transferred to a conserved histidine residue in the histidine-phosphotransfer domain of RcsD, and from there to the receiver domain of RcsB (Majdalani & Gottesman, 2005). Notably, in the absence of a stimulus, RcsB can be phosphorylated by acetyl-phosphate as a phosphoryl group donor (Figure 1) (Hu *et al.*, 2013). RcsC and RcsD have a phosphatase activity to remove the phosphate from RcsB in reversible phosphotransfer reactions (Figure 1) (Majdalani *et al.*, 2002, Majdalani *et al.*, 2005).

The complexity of the output that is generated by the Rcs phosphorelay via the response regulator RcsB is likewise high and involves additional protein components. RcsB is a 216 amino acid protein with an N-terminal receiver domain containing the phosphorylation site (D56) and a C-terminal DNA binding domain (Henikoff *et al.*, 1990, Gao *et al.*, 2007). The receiver domain comprises residues 5 to 124 and the DNA-binding domain residues 144 to 209 with a FixJ/NarL-type typical helix-turn-helix-DNA-binding motif (HTH) from residue 151 to 194 (Majdalani & Gottesman, 2005, Pristovsek *et al.*, 2003). As canonical bacterial response regulators, RcsB can regulate target genes as a homodimer (Majdalani & Gottesman, 2005). Dependent on phosphorylation, RcsB activates transcription of multiple loci including *rprA*, encoding the small regulatory RNA RprA, the cell division genes *ftsZ* and *ftsA*, *bdm* coding for a protein involved in biofilm formation, as well as *osmB* and *osmC*, encoding an osmotically inducible lipoprotein and peroxidase (Majdalani & Gottesman, 2005, Francez-Charlot *et al.*, 2005). RcsB binding sites, that were mapped for *osmC* and *bdm* locate just upstream of the -35 promoter region, probably requiring interaction with RNA polymerase for activation (Sturny *et al.*, 2003, Francez-Charlot *et al.*, 2005, Majdalani & Gottesman, 2005).

Strikingly, in addition to forming homodimers, RcsB interacts with auxiliary transcriptional regulators including RcsA, GadE, BglJ, MatA, and DctR that likewise exhibit a DNA-binding domain of the FixJ/NarL-type (Majdalani & Gottesman, 2005, Castanie-Cornet *et al.*, 2010, Venkatesh *et al.*, 2010, Fabisch, 2008). The interactions of RcsB with the auxiliary partners alter the DNA-binding specificity (Venkatesh *et al.*, 2010, Castanie-Cornet *et al.*, 2010, Wehland & Bernhard, 2000) and thus extend the regulatory repertoire of the Rcs system to the control of multiple loci related to motility and biofilm formation, various stress responses, cell surface components, and additional functions (Majdalani &

Gottesman, 2005, Clarke, 2010). Although heterodimerization of response regulators is a common feature in Eukaryotes, it is very rare in bacteria. To date, the only described example for heterodimerization of bacterial response regulators beside RcsB are BldM and WhiI in the filamentous bacteria *Streptomyces* (Al-Bassam *et al.*, 2014). Notably, BldM and WhiI likewise belong to the FixJ/NarL family of transcriptional regulators.

1.2. Auxiliary regulators of RcsB belong to the FixJ/NarL-family

E. coli has 18 proteins with a FixJ/NarL-type typical HTH-motif, of which RcsA, GadE, BglJ, MatA and DctR were shown to interact with RcsB (Fabisch, 2008). Their targets and cellular roles are summarized in Table 1 and their relations in Figure 2. RcsA is a 207 amino acids long protein whose intracellular concentration is generally low. The amount of the RcsA protein is limited by its rapid degradation by Lon, an ATP-dependent protease (Stout *et al.*, 1991). Moreover, the expression of *rcsA* is repressed by HNS (Sledjeski & Gottesman, 1995). However, RcsA was reported to activate its own expression together with RcsB (Ebel & Trempy, 1999, Wehland & Bernhard, 2000). The small RNA DsrA was found to activate *rcsA* expression by anti-silencing HNS repression (Sledjeski & Gottesman, 1995). Together with RcsB, RcsA activates expression of loci such as the *cps/wza* gene cluster and *yjb* operon for exopolysaccharide production, or *rcsA* expression itself (Stout *et al.*, 1991, Ferrieres *et al.*, 2007). The *flhDC* operon encoding the flagella master regulator is repressed by RcsA-RcsB (Soutourina & Bertin, 2003, Francez-Charlot *et al.*, 2003). RcsA-RcsB heterodimers regulate their targets by binding a specific DNA sequence, called RcsAB box, which is located around 100 bp upstream of the transcription start site of *wza* as well as *rcsA* and downstream of the promoter of *flhDC* (Wehland & Bernhard, 2000, Francez-Charlot *et al.*, 2003). The activity of the RcsA-RcsB heterodimer depends on phosphorylation of RcsB (Majdalani & Gottesman, 2005).

Table 1. Cellular roles of RcsB homo- and heterodimers

Transcription factor	Role	Target genes[1]	Source
RcsB/RcsB	cell division, biofilm formation, general stress response	*ftsAZ*, *bdm*, *osmC*, *osmB*, *rprA*, *gadA*	(Carballes *et al.*, 1999, Francez-Charlot *et al.*, 2005, Sturny *et al.*, 2003, Majdalani *et al.*, 2002, Castanie-Cornet *et al.*, 2010)
RcsA[2]/RcsB	capsule production	*wza*, *rcsA*, *flhDC*, *csg*	(Stout & Gottesman, 1990, Ebel & Trempy, 1999, Francez-Charlot *et al.*, 2003, Vianney *et al.*, 2005)
BglJ[2]/RcsB	pleiotropic role	*bgl*, *leuO*, other targets	(Venkatesh *et al.*, 2010, Stratmann *et al.*, 2012, Salscheider *et al.*, 2013)
GadE[2]/RcsB	acid stress resistance	*gadA/BC*	(Castanie-Cornet *et al.*, 2010)
MatA[2]/RcsB	fimbriae	*mat*, *flhDC*	(Lehti *et al.*, 2012b, Lehti *et al.*, 2012a, Lehti *et al.*, 2013)
DctR[2]/RcsB	acid stress?	?	(Masuda & Church, 2003)

[1]activated targets in green, repressed targets in red

[2]HNS repressed

BglJ is a 225 amino acid transcriptional regulator that is encoded in an operon together with YjjQ, another transcription factor belonging to the FixJ/NarL-family (Stratmann *et al.*, 2008). Notably, YjjQ was also identified as a transcriptional repressor of the *flhDC* operon and other targets (Wiebe *et al.*, 2015). Expression of *yjjQ-bglJ* is repressed by HNS and activated by the LysR-type transcription factor LeuO that antagonizes HNS-mediated repression (Stratmann *et al.*, 2008). Interestingly, BglJ-RcsB heterodimers in turn activate *leuO* expression and hence BglJ and LeuO form a small regulatory network (Stratmann *et al.*, 2012). Furthermore, BglJ-RcsB activates expression of the *bgl* operon, encoding proteins for the uptake and utilization of aryl-β,D-glucosides and more than 10 additional loci (Venkatesh *et al.*, 2010, Stratmann *et al.*, 2012, Salscheider *et al.*, 2013). For regulation of expression, BglJ-RcsB was proposed to act in the context of the promoter as a class I activator interacting with RNA polymerase or as an HNS antagonist. At the *bgl* promoter BglJ-RcsB acts synergistically with CRP (Salscheider *et al.*, 2013). Moreover, a consensus DNA-binding motif was defined that suggested a DNA phasing- and orientation-dependent positioning of the BglJ-RcsB heterodimer in relation to the transcription start site which varies with the promoter

(Salscheider *et al.*, 2013). Unlike RcsA-RcsB, the activity of BglJ-RcsB is independent of RcsB phosphorylation (Venkatesh *et al.*, 2010, Stratmann *et al.*, 2012).

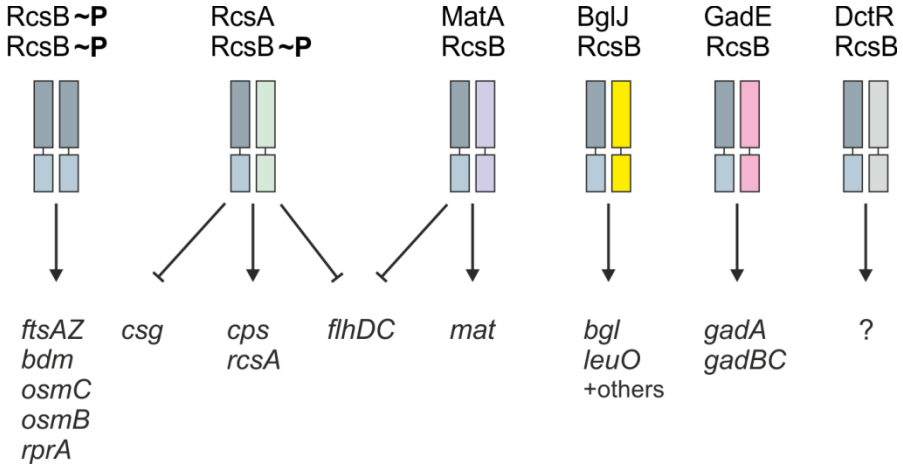

Figure 2. Targets of RcsB homo- and heterodimers in *E. coli*.
RcsB homodimers activate *ftsAZ, bdm, osmC, osmB,* and *rprA*. RcsA-RcsB activates wza*, rcsA* and represses *csg* and *flhDC*. MatA-RcsB activates *mat* in NMEC and represses *flhDC.* BglJ-RcsB activates several loci including *bgl* and *leuO.* GadE-RcsB activates *gadA* and *gadBC*. Direct targets of DctR-RcsB are unknown.

GadE, the central activator of glutamate-dependent acid resistance, is encoded by the *gadE-mdtEF* operon located within the acid fitness island. GadE's expression is negatively regulated by HNS (Tucker *et al.*, 2002, Tramonti *et al.*, 2008, Sayed & Foster, 2009). Together with RcsB, GadE activates the expression of the *gadA*/*BC* genes in a phosphorylation independent manner by binding the GAD box located around -60 bp upstream of the transcription start. The genes *gadA* and *gadB* encode glutamate decarboxylases conferring resistance to extreme acidic conditions. Interestingly, phosphorylated RcsB represses expression of *gadA* as a homodimer by binding to a site upstream of the -10 promoter element (Castanie-Cornet *et al.*, 2010).

In a systematic approach, interaction of RcsB with all other 18 FixJ/NarL-type proteins in *E. coli* K-12 was previously investigated (Fabisch, 2008). These heterodimerization studies using the bacterial LexA-based two-hybrid system (Dmitrova *et al.*, 1998) revealed MatA and DctR as further interaction partners of RcsB (Fabisch, 2008). Notably, all FixJ/NarL-type proteins (except GadE and EvgA) that form heterodimers with RcsB do not form homodimers and *vice versa* (Fabisch, 2008). The one/two- hybrid analyses for EvgA showed homodimerization as well as heterodimerization with RcsB. For GadE neither homo- nor heterodimerization was detected under standard conditions, possibly due to acid-stress dependent dimerization behavior (Fabisch, 2008).

MatA (also termed EcpR) is a 196 amino acids long transcriptional regulator encoded as the first gene of the common *mat* fimbria operon (Lehti *et al.*, 2012a). Mat fimbriae are a common colonization factor promoting biofilm formation as well as bacterial adherence to epithelial cells (Lehti *et al.*, 2010, Lehti *et al.*, 2012b). MatA is the key activator of this operon in newborn meningitis-associated *E. coli* (NMEC) and enterohemorrhagic *E. coli* (EHEC) although the *mat* operon remains cryptic in the non-pathogenic *E. coli* K-12 and strains belonging to the lineages A and B1 (Martinez-Santos *et al.*, 2012, Lehti *et al.*, 2012a, Lehti *et al.*, 2012b, Lehti *et al.*, 2013). In NMEC and other *E. coli* strains belonging to the lineages B2, D, and E, MatA forms a positive autoregulatory circuit (Lehti *et al.*, 2013). However, also the MatA protein of *E. coli* K-12 strain MG1655 is fully functional (Lehti *et al.*, 2013). In addition to MatA, RcsB is required to activate *mat* expression in NMEC (Lehti *et al.*, 2012a, Lehti *et al.*, 2012b). Notably, the *mat* operon is repressed by HNS (Lehti *et al.*, 2012b, Lehti *et al.*, 2013). The *flhDC* operon is under negative control of MatA and hence the importance of MatA in the transition from planktonic to adhesive lifestyle is discussed (Lehti *et al.*, 2012a).

DctR is a 176 amino acids long predicted transcriptional regulator encoded in the *slp-dctR* operon whose expression is likewise repressed by HNS (Krin *et al.*, 2010). The gene *dctR* is a member of the *E. coli* acid fitness island (AFI) and its expression is activated by YdeO (Mates *et al.*, 2007, Masuda & Church, 2003). Deletion of *slp-dctR* abolishes YdeO-induced acid resistance (Masuda & Church, 2003). Slp and DctR were implicated in protection against metabolic end products under acidic conditions, however a direct target of DctR as a transcriptional regulator is not known (Mates *et al.*, 2007, Yamanaka *et al.*, 2014).

1.3. Aims of this thesis

For the viability of bacteria it is essential to fine-tune gene expression according to the environmental conditions. RcsB has the unique feature to interact with several auxiliary co-regulators and is able to activate and repress targets dependent on interaction partner and phosphorylation state. These different modes of regulation by RcsB imply specific recognition mechanisms between RcsB and auxiliary regulators. Thus, RcsB is a versatile transcription factor being involved in many regulatory networks that contribute to adjust gene expression in response to environmental conditions. So far the specific determinants for transcriptional activation by RcsB are poorly understood. The aims of this work were:

- To study a potential heterodimer formation of FixJ/NarL-type transcription factors
- To further characterize the RcsB regulon by identification of putative targets of MatA-RcsB and DctR-RcsB heterodimers
- To establish reporter systems to analyze transcriptional regulation by RcsB homo- and heterodimers
- To study the phosphorylation dependence of RcsB for activity of specific heterodimers
- To identify particular amino acid residues within RcsB which are important for the activity of RcsB as well as residues which are crucial for specific interaction with only one or a subset of the partners
- To study the mechanism of transcriptional activation by BglJ-RcsB

2. Results

To address the aims of this work, I applied following approaches:

- Analysis of heterodimer formation by bacterial LexA-based two-hybrid system
- Search for MatA and DctR targets by microarray analysis
- Analysis of MatA-RcsB effect on motility on soft agar plates
- Reporter construction by fusion of known target promoters to *lacZ*
- Analysis of the activity of RcsB mutants as homo- and heterodimers by β-galactosidase assays using the established reporter systems
- Stability test of RcsB mutants by western blotting
- Interaction analysis of RcsB mutants by strep-protein interaction experiment
- BglJ-RcsB-RNA polymerase interaction studies by a bacterial two-hybrid system as well as overexpression of the RNA polymerase α subunit + mutants

2.1. Homo- and heterodimer formation of RcsB

The FixJ/NarL-type transcriptional regulator RcsB is known to interact with auxiliary regulators such as RcsA, BglJ and GadE which also belong to the FixJ/NarL family (Majdalani & Gottesman, 2005, Castanie-Cornet *et al.*, 2010, Venkatesh *et al.*, 2010). In previous studies, homo- and heterodimerization of RcsB was analyzed using the bacterial LexA-based one/two-hybrid system (Dmitrova *et al.*, 1998). The one-hybrid reporter for examining homodimer formation consists of the native *sulA* promoter (+/+) fused to *lacZ* (Figure 3A). Only homodimers of proteins fused to the wild-type DNA-binding domain of the LexA repressor are able to bind to the *lexA* operator and repress P*sulA lacZ* expression. For analyzing heterodimer formation, the *sulA* promoter carries a hybrid *lexA* operator (408/+) with a mutation in one half-site (Figure 3B). Only heterodimers in which one partner is fused to the LexA wild-type DNA-binding domain and the other partner is fused to the $LexA_{408}$ mutant DNA-binding domain are able to bind the hybrid operator and repress P*sulA lacZ* expression (Dmitrova *et al.*, 1998).

A

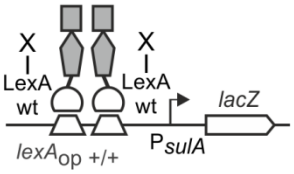

B

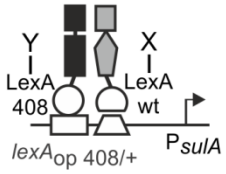

C

LexA408-fusion	Fold repr. / -IPTG / +IPTG	LexAwt-fusion RcsB	BglJ	RcsA	MatA	DctR
RcsB		9[a]	9[a]	8[a]	9[b]	12[b]
	-	2037	1779	3579	2200	1892
	+	237	203	441	254	164
BglJ		7[c]	NT	1[c]	1[c]	1[c]
	-	1809		1840	1752	1823
	+	252		1741	1908	1921
RcsA		NT	NT	NT	1	1
	-				1606	1636
	+				1612	2021
MatA		NT	NT	NT	NT	1
	-					1433
	+					1372

D

	LexAwt-fusion RcsB	BglJ	RcsA	MatA	DctR
Fold repr.	27[a]	5[a]	1[a]	1[b]	1.5[b]
-IPTG	2422	3237	2246	3184	3010
+IPTG	89	589	2177	2836	1924

Figure 3. Homo- and heterodimer formation by RcsB, BglJ, RcsA, MatA and DctR.
(A) In the LexA-based one/two-hybrid system, the *sulA* promoter *lacZ* fusion with the wild-type LexA +/+ operator was used to analyze homodimerization. For analysis of homodimerization, a fusion of the respective protein to the wild-type LexA DNA-binding domain was expressed from a plasmid under the control of the IPTG-inducible lac_{UV5} promoter (P_{UV5}). (B) The *sulA* promoter *lacZ* reporter fusion with a hybrid *lexA* 408/+ operator served as a reporter for heterodimerization. For heterodimerization analysis, fusions of one protein to the wild-type LexA DNA-binding domain and the potential interaction partner fused to the $LexA_{408}$ mutant DNA-binding domain were co-expressed from compatible plasmids. (C) Summary of the results for heterodimer formation by RcsB, BglJ. The fold repression of the *lexA*$op_{408/+}$ *sulA* promoter *lacZ* fusion is a measure of heterodimerization, and was calculated by dividing the expression levels (values given in smaller font size) of the *PsulA lacZ* reporter that were obtained without and with induction of the LexA-fusion proteins. For analyzing heterodimer formation of RcsA, MatA, and DctR with each other, strains S3440 (Δ*rcsB*) was co-transformed with plasmids encoding for $LexA_{WT}$-X and $LexA_{408}$-Y fusions, respectively. The following plasmids were used: pKEMK4 ($LexA_{WT}$-MatA), pKEMK1 ($LexA_{WT}$-DctR), as well as pKEDP59 ($LexA_{408}$-MatA) and pKEDP60 ($LexA_{408}$-RcsA). The cultures were grown in LB supplemented with antibiotics in the presence and absence of IPTG to an OD_{600} of 0.5. (D) Summary of homodimer formation of RcsB, BglJ, RcsA, MatA and DctR. The fold repression of the *sulA* promoter *lacZ* fusion with the *lexA* operator (*lexA*$op_{+/+}$) is a measure of homodimerization. Values indicated with [a] are taken from (Venkatesh *et al.*, 2010). Unpublished laboratory results are indicated with [b] from (Fabisch, 2008) and [c] from (Dreck, 2013).

Previous analyses using the LexA-based two-hybrid system (Dmitrova *et al.*, 1998) demonstrated an interaction of RcsB also with MatA, and DctR, respectively (Figure 3C) (Fabisch, 2008). Analyses using the LexA-based one-hybrid system demonstrated that these interaction partners of RcsB partners do not form homodimers (Figure 3D). Since RcsB interacts with RcsA, BglJ, MatA, and DctR, these proteins may form heterodimers in other combinations as well. In previous experiments, heterodimer formation between BglJ with RcsA, MatA, or DctR, respectively, was not observed (Figure 3C) (Dreck, 2013). Here I tested heterodimer formation between RcsA and MatA, or DctR, respectively, and between MatA and DctR using the bacterial LexA-based two hybrid system.

The two-hybrid assays for heterodimer formation of RcsA, MatA and DctR were conducted in a *ΔrcsB* background strain carrying the *sulA* 408/+ hybrid promoter fused to *lacZ*. This strain (S3440) was co-transformed with a plasmid harboring RcsA or MatA fused to the $LexA_{408}$ DNA-binding domain together with a plasmid harboring one of the other FixJ/NarL-type proteins MatA or DctR fused to the wild-type $LexA_{WT}$ DNA-binding domain. Neither the co-induction of $LexA_{408}$-RcsA with $LexA_{WT}$-MatA or $LexA_{WT}$-DctR, respectively, nor the co-induction of $LexA_{408}$-MatA with $LexA_{WT}$-DctR resulted in a repression, suggesting that RcsA, MatA and DctR do not form heterodimers with each other (Figure 3C). Taken together, these data combined with the previous findings show that RcsB forms heterodimers with RcsA, BglJ, MatA, and DctR, and that these interaction partners neither form homodimers nor heterodimers with each other.

2.2. Establishment of reporter systems

To study the regulatory effect of RcsB homo- and heterodimers, appropriate reporter systems for RcsB-RcsB, RcsA-RcsB, MatA-RcsB and DctR-RcsB remained to be established. To this end, the promoter regions of specific targets were fused to *lacZ*, integrated, and their activation tested in different strain backgrounds. Given that for MatA and DctR no targets are known in *E. coli* K-12, I performed a Microarray analysis. Furthermore, I investigated whether transcriptional activation by RcsB homodimers or heterodimers with RcsA, BglJ, and MatA depends on RcsB phosphorylation. For this, I expressed wild-type RcsB or mutants D56E, D56N, and D56A in the appropriate reporter strains. RcsB-D56E mimics phosphorylated RcsB, and RcsB-D56N and -D56A mimic non-phosphorylated inactive RcsB (Scharf, 2010). In all reporter strains, the chromosomal *lacZ* gene was deleted.

2.2.1. RcsB-RcsB activates P*rprA* in a phosphorylation dependent manner

For analyzing the RcsB homodimer activity, first a P*ftsA lacZ* fusion was tested as a reporter. This fusion, which was constructed before, comprises the promoter region (-70 to +30) of the cell division gene *ftsA* that is activated by RcsB (Carballes *et al.*, 1999), fused to the reporter gene *lacZ* (constructed by Öztürk, Figure 4A). Previously, this reporter was tested in Δ*rcsB* Δ*lacZ* strain T818 (Öztürk, 2010). This strain was transformed with empty plasmid pKESK22 or plasmids expressing wild-type RcsB and mutants D56E, D56N, D56A, or M88A (pKETS6, pKETS7, pKETS8, pKES235 and pKES232) and β-galactosidase activities were determined. RcsB-D56E mimics phosphorylated RcsB, and RcsB-D56N and -D56A mimic non-phosphorylated inactive RcsB (Scharf, 2010). In RcsB mutant M88A, methionine at position 88 is replaced by alanine. At this position, response regulators except for RcsB carry usually a conserved small residue such as alanine or glycine (Bourret, 2010). Compared to the empty vector control, the plasmidically expressed wild-type *rcsB* did not activate the *ftsA* promotor (Öztürk, Figure 4B). The finding may be due to non-induced Rcs signaling resulting in an equilibrium shift to unphosphorylated RcsB in the cytoplasm. Accordingly, the RcsB mutant D56A, mimicking inactive RcsB, did not activate the promoter and RcsB-D56N only slightly. RcsB-D56E, mimicking phosphorylated RcsB, as well as RcsB-M88A, activated the promoter around 5-fold compared to the control plasmid (Öztürk, Figure 4B).

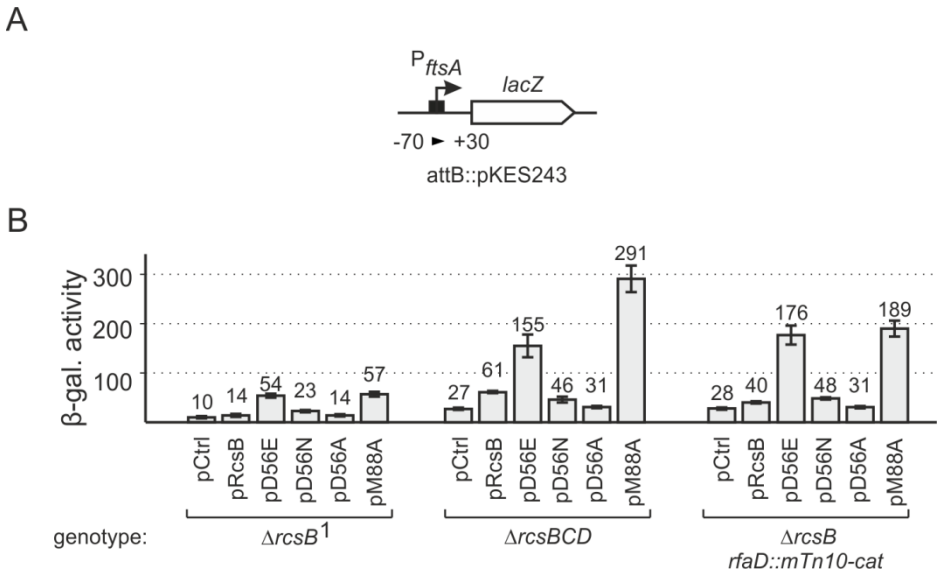

Figure 4. Analysis of the P*ftsA lacZ* reporter in different strain backgrounds
(A) The *ftsA* promoter region from -70 to +30 relative to the transcription start site was fused to *lacZ* on plasmid pKES243 and integrated into the *attB* site of the chromosome of different strains. These reporter strains were transformed with empty plasmid pKESK22 (pCtrl), wild-type RcsB (pKETS6) or RcsB-mutants D56E, D56N, D56A and M88A (pKETS7, pKETS8, pKES235, and pKES232) expressing plasmids and reporter expression levels were determined. (B) P*ftsA lacZ* expression levels in Δ*rcsB* Δ*lacZ* strain T818, Δ*rcsBCD* Δ*lacZ* strain T868 and Δ*rcsB* Δ*lacZ rfaD*::mTn-*cat* strain T866. Cultures for β-galactosidase assays were grown in LB medium to an OD_{600} of 0.5, supplemented with 1 mM IPTG and 25 µg/ml of kanamycin. Values obtained for Δ*rcsB* strain (indicated with [1]) are unpublished laboratory results from Öztürk, 2010.

Based on these previous results, I constructed two P*ftsA lacZ* reporter strains to potentially increase RcsB phosphorylation. The first reporter strain Δ*rcsBCD* Δ*lacZ* (T868) lacks both the sensor kinase RcsC and the phosphotransfer protein RcsD to avoid RcsB dephosphorylation by the Rcs system. In the second reporter strain Δ*rcsB* Δ*lacZ rfaD*::mTn10-cat (T866), *rfaD* is mutated by transposon insertion. Mutation of *rfaD* which is involved in lipopolysaccharide (LPS) synthesis (Pegues *et al.*, 1990) was reported to activate Rcs signaling (Parker *et al.*, 1992). Each reporter strain was transformed with an empty plasmid or plasmids expressing wild-type RcsB and mutants D56E, D56N, D56A, or M88A and β-galactosidase activities were determined. In the Δ*rcsBCD* Δ*lacZ* strain, wild-type RcsB activated expression approximately 2-fold to 61 units compared to the empty vector control with 27 units (Figure 4B). RcsB mutants D56E and M88A activated P*ftsA lacZ* up to 155 units and 291 units, respectively (Figure 4B). RcsB mutant D56N activated expression only slightly with 46 units and RcsB-D56A did not activate P*ftsA lacZ* expression (Figure 4B). In the Δ*rcsB* Δ*lacZ rfaD*::mTn10-*cat* strain wild-type RcsB only slightly activated expression from 28 units for the empty vector control to 40 units (Figure 4B). RcsB mutants D56E and M88A activated the P*ftsA lacZ* up to

176 units and 189 units, respectively. RcsB mutant D56N activated expression only slightly with 40 units and RcsB-D56A did not activate P*ftsA lacZ* expression (Figure 4B). In none of the three reporter strain backgrounds the P*ftsA lacZ* expression was more than approximately 2-fold upregulated by wild-type RcsB and around 6-fold by RcsB-D56E compared to the control. Thus the P*ftsA lacZ* fusion did not prove to be optimal for further analyses and a reporter was needed which is strongly activated by wild-type RcsB that allows distinguishing smaller differences.

Therefore the promoter of *rprA* (-124 to +4) encoding the small RNA RprA whose expression is activated by RcsB (Majdalani *et al.*, 2002) was fused to the *lacZ* reporter gene and this construct was integrated into the chromosome of different strain backgrounds (Figure 5A).

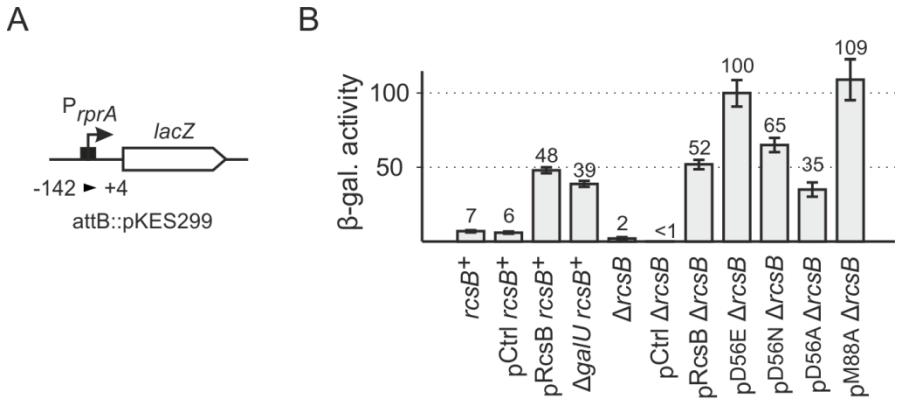

Figure 5. P*rprA lacZ* as a reporter for studying activation by RcsB
(A) The *rprA* promoter region from -142 to +4 relative to the transcription start site was fused to *lacZ* on plasmid pKES299 and integrated into the *attB* site of the chromosome. (B) The expression levels of the P*rprA lacZ* reporter were determined in *rcsB*$^+$ Δ*lacZ* strain T2023, *rcsB*$^+$ Δ*galU* Δ*lacZ* strain T2041, and Δ*rcsB* Δ*lacZ* strain T1052. For complementation, *rcsB* was expressed from plasmid pKETS6. RcsB derivatives D56E, D56N, D56A and M88A from plasmids pKETS7, pKETS8, pKES235, and pKES232, respectively. Empty cloning vector pKESK22 served as control (pCtrl). Cultures for β-galactosidase assays were grown in LB medium to an OD_{600} of 0.5, if transformed supplemented with 1 mM IPTG and 25 µg/ml of kanamycin.

In the *rcsB*$^+$ strain T2023 the P*rprA lacZ* expression was poorly activated (7 units, Figure 5B). In a Δ*galU* strain that cannot produce UDP-D-glucose, the Rcs system is constitutively activated (Girgis *et al.*, 2007). Deletion of *galU* in the *rcsB*$^+$ background (T2041) activated P*rprA lacZ* expression up to 39 units (Figure 5B). In the Δ*rcsB* strain (T1052) P*rprA lacZ* expression is very low (2 units, Figure 5B) and when transformed with control plasmid pKESK22 completely off (<1 unit, Figure 5B). Complementation of Δ*rcsB* strain with wild-type *rcsB* (pKETS6) induced P*rprA lacZ* expression up to 52 units (Figure 5B). RcsB mutants D56E and M88A activated the promoter up to 100 units and 109 units, respectively, and RcsB

derivative D56N and D56A activated the *rprA* promoter up to 65 and 35 units, respectively. This lower activity for the inactive RcsB-D56A mutant confirms an at least partial phosphorylation dependent activation. Although activation of P*rprA* by RcsB homodimers is phosphorylation dependent, the complementation with wild-type *rcsB* partially overcomes the requirement for induction of the Rcs signaling cascade. In the Δ*rcsB* strain, plasmidically expressed wild-type RcsB activates the P*rprA* more than 50-fold and RcsB-D56E more than 100-fold compared to the control plasmid, allowing to distinguish also small differences. Taken together, the P*rprA lacZ* reporter in the Δ*rcsB* strain proved to be appropriate for the analysis of transcriptional activation by RcsB and mutants. The results also confirmed a phosphorylation dependent activation by RcsB homodimers.

2.2.2. RcsA-RcsB activates P*wza* in a phosphorylation dependent manner

To analyze the activity of RcsA-RcsB heterodimers, a P*wza lacZ* reporter was constructed and analyzed in various strain backgrounds, each carrying a *lacZ* deletion. For this purpose the *wza* promoter (-202 to +346) was fused to *lacZ,* and integrated into the *attB* site of the chromosome. The promoter is derived from the *wza-wca* gene cluster of capsule production that is activated by RcsA-RcsB in a phosphorylation dependent manner (Gupte *et al.*, 1997, Majdalani & Gottesman, 2005). This P*wza lacZ* reporter was tested in a Δ*rcsB* strain background. Since the activation of P*wza* was reported to be phosphorylation dependent, the P*wza lacZ* reporter was also tested in a Δ*rcsBCD* strain background lacking RcsC and RcsD to avoid RcsB dephosphorylation by the Rcs system as well as a Δ*rcsB rfaD*::mTn10-cat strain background with an *rfaD* mutation which is supposed to activate the Rcs system. Expression of *rcsA* is repressed by HNS and autoregulated by RcsA-RcsB (Sledjeski & Gottesman, 1995, Majdalani & Gottesman, 2005) and the intracellular RcsA concentration is low because RcsA is a target of the Lon protease (Torres-Cabassa & Gottesman, 1987). This is why in certain strains the native *rcsA* promoter was replaced by the strong phage λ P_L promoter or weak P16 promoter causing constitutive expression and avoiding HNS repression as well as circumventing autoregulation. Overall the P*wza lacZ* reporter was tested in strains with a different combination of these above-described features that are summarized in Figure 6.

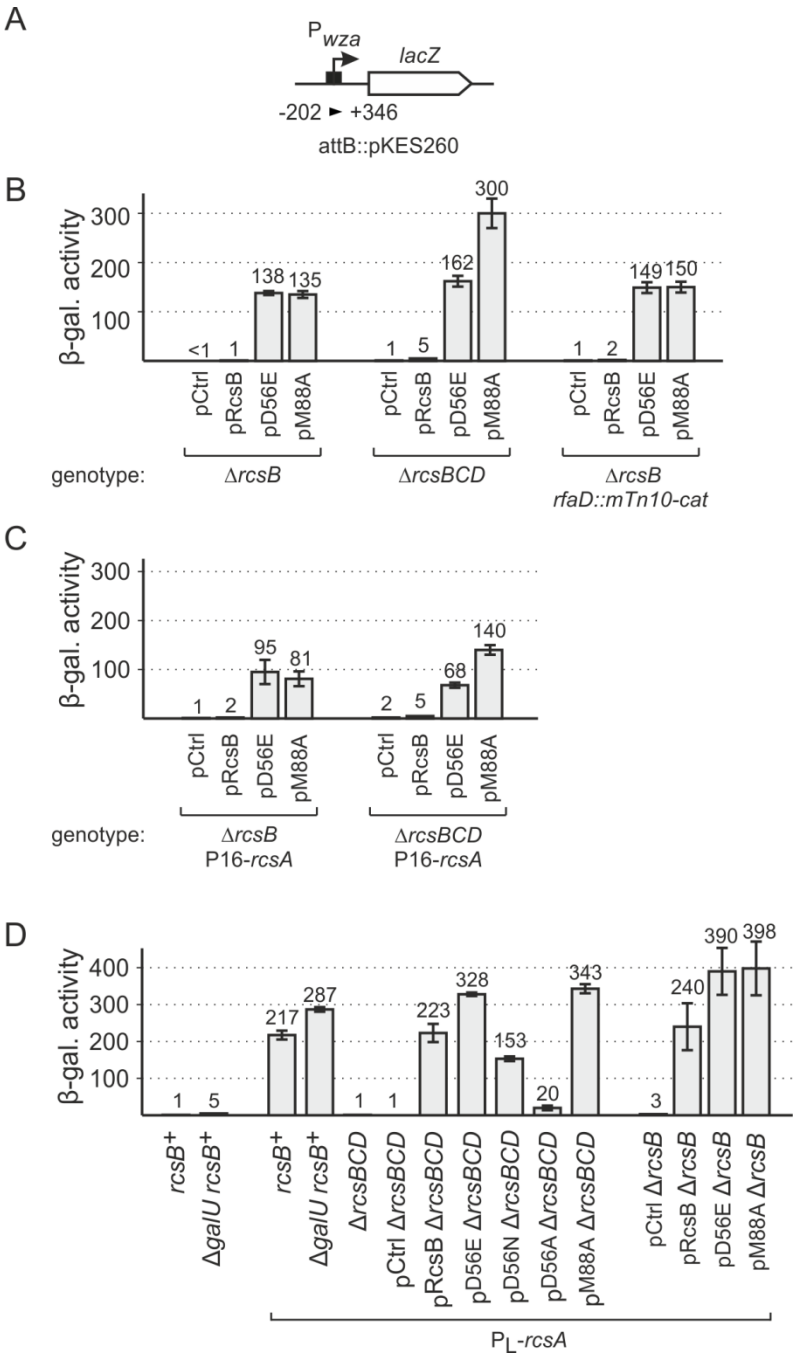

Figure 6. P*wza lacZ* as a reporter for studying activation by RcsA-RcsB

(A) The *wza* promoter region from -202 to +346 relative to the transcription start site was fused to *lacZ* on plasmid pKES260 and integrated into the *attB* site of the chromosome of different strains. These reporter strains were transformed with empty plasmid pKESK22 (pCtrl), RcsB wild-type (pKETS6) or RcsB-mutants D56E and M88A (pKETS7, pKES232) expressing plasmids and reporter expression levels were determined. Cultures for β-galactosidase assays were grown in LB medium to an OD_{600} of 0.5, if transformed supplemented with 1 mM IPTG and 25 µg/ml of kanamycin. (B) P*wza lacZ* expression levels in Δ*rcsB* Δ*lacZ* strain T864, Δ*rcsBCD* Δ*lacZ* strain T921 and Δ*rcsB* Δ*lacZ rfaD::mTn-cat* strain T919. (C) P*wza lacZ* expression levels in Δ*rcsB* Δ*lacZ* $rcsA_{P16}$ strain T929 and Δ*rcsBCD* Δ*lacZ* $rcsA_{P16}$ strain T979. (D) Expression levels of the P*wza lacZ* reporter in $rcsB^+$ Δ*lacZ* $rcsA_{PL}$ strain T2039, $rcsB^+$ Δ*galU* Δ*lacZ* $rcsA_{PL}$ strain T2045, Δ*rcsBCD* Δ*lacZ* $rcsA_{PL}$ strain T963, and Δ*rcsB* Δ*lacZ* $rcsA_{PL}$ strain T927. RcsB and derivatives D56E, D56N, D56A, and M88A were expressed from plasmids pKETS6, pKETS7, pKETS8, pKES235 and pKES232.

Each reporter strain was transformed with empty plasmid pKESK22 or plasmids expressing wild-type RcsB (pKETS6) and mutants D56E, D56N, D56A, and M88A (pKETS7, pKETS8, pKES235, pKES232) and the reporter expression was measured by β-galactosidase assays. The results are summarized in Figure 6. In strains with the native *rcsA* promoter (Δ*rcsB* strain T864, Δ*rcsBCD* strain T921 and Δ*rcsB rfaD::mTn-cat* strain T919, Figure 6B), the reporter expression levels upon complementation with wild-type *rcsB* were not significantly higher compared to the control. In strains with *rcsA* under the control of the weak constitutive P16 promoter (Δ*rcsB* P16-*rcsA* strain T929 and Δ*rcsBCD* P16-*rcsA* strain T979), the reporter expression levels upon complementation with wild-type *rcsB* were also not significantly higher compared to the control (Figure 6C), similar to the strains with the native *rcsA* promoter. RcsB mutants D56E and M88A activated the promoter strongly in the strains with native *rcsA* promoter and the weak constitutive P16 promoter (Figure 6B and C). Interestingly, the activation by RcsB-D56E and M88A was higher in the strains with the native *rcsA* promoter compared to the strains with constitutive *rcsA* expression controlled by P16 (Figure 6B and C). This can be explained by autoinduction of the native *rcsA* promoter. In the *rcsB*$^+$ P_L-*rcsA* strain T2039 P*wza lacZ* was strongly activated compared to the *rcsB*$^+$ strain (217 units and 1 unit, Figure 6D). Activation of the Rcs system by deletion of *galU* in the *rcsB*$^+$ background (T2042) did not strongly activate P*wza lacZ* expression (5 units, Figure 6D). Deletion of *galU* in the *rcsB*$^+$ P_L-*rcsA* background (T2045) induced P*wza lacZ* expression up to 287 units (Figure 6D). In the Δ*rcsBCD* P_L-*rcsA* strain T963, plasmidic wild-type RcsB expression activated expression 223-fold compared to the untransformed strain and the strain harboring an empty plasmid (223 versus 1 units, Figure 6D). RcsB mutant D56N and D56A activated P*wza lacZ* up to 153 and 20 units, and RcsB mutants D56E and M88A activated the promoter up to 328 units and 343 units, respectively (Figure 6D). The low activity of the RcsB-D56A mutant compared to wild-type RcsB demonstrates the RcsB phosphorylation dependence of transcriptional activation by RcsA-RcsB.

When *rcsA* is constitutively expressed under P_L control in the presence of RcsB, capsule production is activated and colonies of the strains exhibit a mucoid phenotype on LB plates (Figure 7, middle photo). In a Δ*rcsB* strain constitutive *rcsA* expression is not able to induce the mucoid phenotype, confirming that capsule production depends on both, RcsA and RcsB (Figure 7, right photo). Since induction of Rcs signaling by deletion of *galU* in the wild-type background is not sufficient to activate P*wza*, we continued our experiments in

Δ*rcsBCD ΔlacZ* P_L-*rcsA* reporter strain T963, although a Δ*rcsB* P_L-*rcsA* reporter strain (T927) yielded comparable results (Figure 6D). Collectively, RcsA-RcsB activates P*wza* in a phosphorylation dependent fashion.

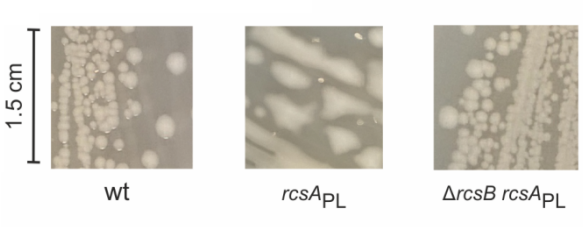

Figure 7. The mucoid phenotype depends on RcsB and RcsA.
E. coli wt strain S4197 (left) and PL-*rcsA* strain T2039 (middle) and Δ*rcsB* PL-*rcsA* strain T927 (right). Only the presence of RcsA together with RcsB is able to induce the mucoid phenotype (middle photo).

2.2.3. BglJ-RcsB reporter system

A reporter system for analyzing BglJ-RcsB has already been established. The *leuO* promoter was fused to *lacZ* and chromosomally integrated in a Δ*rcsB* $bglJ_C$ Δ*lacZ* strain, in which a miniTn10 transposon was inserted in *yjjQ* leading to constitutive expression of *bglJ* (Stratmann *et al.*, 2012). The *yjjQ-bglJ* operon is usually repressed by HNS (Stratmann *et al.*, 2008).

2.2.4. MatA-RcsB activates Pmat_{CFT073} in a phosphorylation independent manner

Two-hybrid results suggested that the DNA-binding transcriptional regulator MatA (EcpR) forms heterodimers with RcsB whereas it does not form homodimers. It was recently shown that activation of the HNS repressed *mat* operon by MatA in NMEC strain IHE3034 and other *E. coli* strains depends on the specific sequence of the *mat* regulatory region. This sequence of the regulatory region is divergent between the *E. coli* lineages B2, D, and E as compared to the A and B1 lineages, while the nucleotide sequence of the *matABCDEF* coding region is highly conserved among all *E. coli* strains (Lehti *et al.*, 2013). To establish a suitable reporter system for studying MatA-RcsB activity in *E. coli* K-12, I first performed a microarray analysis. However, the analysis did not reveal any specific target locus of MatA in *E. coli* K-12. The ten highest upregulated loci are summarized in Table 2. According to the average fluorescence intensities the expression of these loci is low and the results might be unspecific. The average intensities of three housekeeping genes *rrsA*, *ihfB* and *rpoD* detected in this microarray analysis are listed in Table 2 as reference.

Table 2. Summary of MatA microarray analysis results

probe position[a]	dir.[b]	gene	gene position	function	fold change	average intensities[c] (pCtrl/pMatA)
3866477-3866882	<<	*ibpB*	3866469-3866897	small heat shock protein	7.5	8.97/11.97
1460475-1460889	>>	*paaI*	1460471-1460893	phenylacetyl-CoA thioesterase	5.5	7.89/10.30
1459157-1460454	>>	*paaH*	1459054-1460481	3-hydroxyadipyl-CoA dehydrogenase	4.2	8.56/10.55
1460988-1462030	>>	*paaJ*	1460893-1462098	β-ketoadipyl-CoA thiolase	3.8	9.16/11.03
2794269-2795549	>>	*gabP*	2794253-2795653	aminobutyrate transporter	3.3	7.04/8.69
310109-310657	>>	*matB*	310084-310671	Mat fibrillin subunit	3.2	7.82/9.48
1826119-1826877	<<	*ydjS*	1825955-1826923	succinylglutamate desuccinylase	3.2	8.10/9.89
3703015-3703486	<<	*dppD*	3702865-3703848	dipeptide transporter	3.2	9.16/10.79
2793213-2793315	>>	*gabT*	2792735-2794015	aminobutyrate aminotransferase	3.0	8.52/9.92
14273-15112	>>	*dnaJ*	14168-15298	chaperone	2.9	11.69/13.25
housekeeping genes						
224773-224815	>>	*rrsH*	223771-225312	16S ribosomal RNA	1.0	15.23/15.23
963844-964109	>>	*ihfB*	963051-963335	integration host factor, β subunit	1.0	12.86/12.90
3213085-3213830	>>	*rpoD*	3211069-3212910	RNA polymerase, σ70	1.5	12.37/12.93

Summary of the ten highest MatA-regulated loci (p value < 0.05).

[a] Positions of probes and genes are given as coordinates of U0096.3 genome.

[b] 'dir' describes the orientation of the probe (<< for lower strand, >> for upper strand).

[c] Average intensities of the strain harboring control (left) or MatA expressing plasmid (right)

Therefore, I constructed a *lacZ* fusion of the *mat* promoter and regulatory region from UPEC strain CFT073 encompassing position -552 to +68 relative to the T1 transcription start site, similar to a NMEC *matA* promoter reporter gene fusion described before (Lehti *et al.*, 2013). The NMEC strain IHE3034 and the UPEC strains CFT073 both belong to the same phylogenetic B2 subgroup of *E.coli* (Lehti *et al.*, 2013), and accordingly, the *matA* upstream region of strains IHE 3034 and CFT073 exhibit an almost identical nucleotide sequence while the sequence of strain K-12 differs (Figure 8).

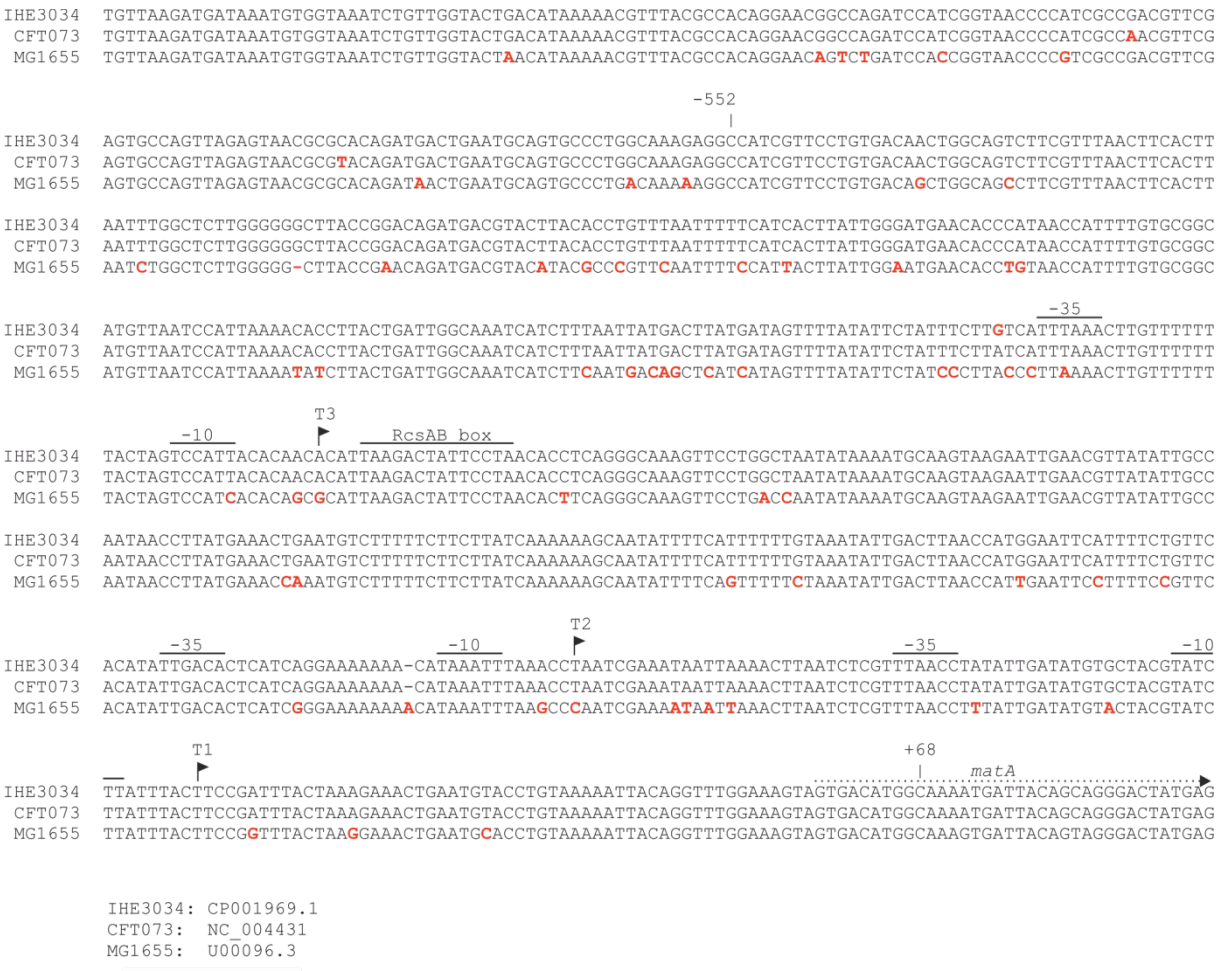

Figure 8. Sequence alignment of *matA* upstream region of *E. coli* strains IHE3034, CFT073 and MG1655.

Three different promoters with transcriptional start sites (T1, T2, T3) as well as the -35 and -10 promoter elements are indicated. The main promoter P2 contains an RcsAB box (Lehti *et al.*, 2013). Nucleotides that differ from the IHE3034 sequence are indicated in red. For the reporter the $matA_{CFT073}$ promoter region from -552 to +68 relative to the T1 transcription start site was fused to *lacZ.*

Here, I used the P$matA_{CFT073}$ *lacZ* reporter to test regulation by RcsB and MatA (Figure 9A). This reporter was integrated into the chromosome of *rcsB*$^+$ strain (T1749) and an isogenic Δ*rcsB* strain (T1747) as well as in isogenic P_L-*matA* and P_L-*matA* Δ*rcsB* strains background (T1986 and T1987). In the two latter strains the native HNS repressed *mat* promoter in the K-12 genome was replaced by the phage λ P_L promoter causing constitutive expression of *matA.* The P$matA_{CFT073}$ *lacZ* fusion exhibited basal expression levels of 167 units in the *rcsB*$^+$ strain, i.e. in the presence of RcsB, in which chromosomal *matA* is not expressed (strain T1749) (Figure 9B). In the presence of MatA and RcsB (P_L-*matA rcsB*$^+$ strain T1986) the expression level of the P$matA_{CFT073}$ *lacZ* reporter increased to 1367 units (Figure 9B). However, upon expression of *matA* (allele P_L-*matA*) in the Δ*rcsB* strain (T1987) the activity of

the P*mat lacZ* reporter was very low (89 units, Figure 9B). Complementation of this P_L-*matA* Δ*rcsB* strain with *rcsB* using plasmid pKETS6 triggered an increase of P*mat lacZ* expression to 2468 units (Figure 9B). Similar results were obtained for *rcsB*$^+$ strain T1749 and Δ*rcsB* strain with MatA expressed from plasmid pKEDP51 (Figure 9B). Taken together, the results demonstrate that both proteins MatA and RcsB are required for activating the $matA_{CFT073}$ promoter indicating that a MatA-RcsB heterodimer activates the *mat* promoter.

Next, I assessed whether activation by MatA-RcsB depends on RcsB phosphorylation. To this end, the reporter strain T1987 (P_L-*matA* Δ*rcsB*) was transformed with a plasmid encoding RcsB-D56E (pKETS7) mimicking phosphorylated RcsB and RcsB-D56A (pKES235) that mimics the non-phosphorylated inactive RcsB (Scharf, 2010). Upon complementation with *rcsB*-D56E and *rcsB*-D56A the expression levels were 3207 units and 2177 units, respectively (Figure 9B). The moderate difference in activation of P*mat* by the RcsB-D56 mutants and wild-type RcsB (2468 units) suggest that transcriptional activation of the $matA_{CFT073}$ promoter by MatA-RcsB heterodimers is only weakly dependent on RcsB phosphorylation. These results are in accordance with expression studies in NMEC strain IHE3034, where deletion of the Rcs phosphorelay genes *rcsC* and *rcsD* did not affect *mat* expression (Lehti *et al.*, 2012b).

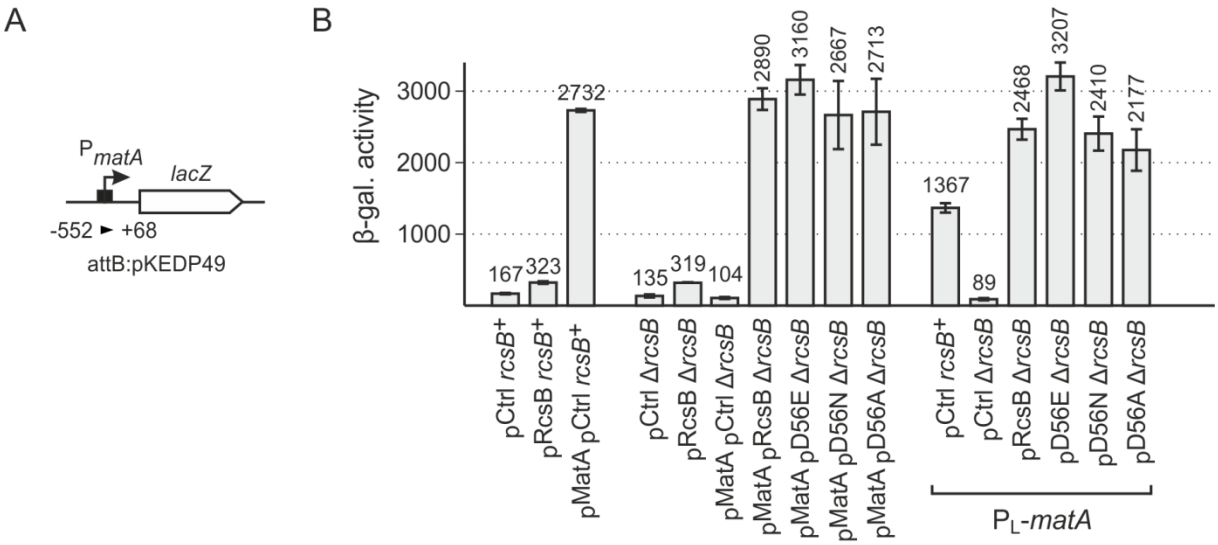

Figure 9. MatA-RcsB activates the *matA*$_{CFT073}$ promoter.
(A) The *matA*$_{CFT073}$ promoter region from -552 to +68 relative to the T1 transcription start site was fused to *lacZ* on plasmid pKEDP49 and integrated into the *attB* site of the chromosome. (B) The expression levels of the P*matA*$_{CFT073}$ *lacZ* reporter were determined in *rcsB*$^+$ Δ*lacZ* strain T1749, Δ*rcsB* Δ*lacZ* strain T1747, P$_L$-*matA* *rcsB*$^+$ Δ*lacZ* strain T1986 and P$_L$-*matA* Δ*rcsB* Δ*lacZ* strain T1987. For complementation, *rcsB* was expressed from plasmid pKETS6. RcsB derivatives D56E, D56N, and D56A were expressed from plasmids pKETS7, pKETS8 and pKES235, respectively. Empty vector pKESK22 serves as control (pCtrl). MatA was expressed from plasmid pKEDP51 (pMatA). Cultures for β-galactosidase assays were grown in LB medium to an OD_{600} of 0.5, if necessary supplemented with 1 mM IPTG and 50 µg ml^{-1} of ampicillin and/or 25 µg/ml of kanamycin.

Recently it was shown that ectopic expression of *matA* impairs the swimming behavior of *E. coli* strains IHE3034 (NMEC) and MG1655 (K-12) presumably by repression of the *flhDC* operon encoding the master regulator of flagella synthesis $FlhD_4C_2$ (Lehti *et al.*, 2012a). Here, I tested whether this repression of motility by ectopically expressed MatA depends on RcsB. To this end, 3 µl of an overnight culture of motile *E. coli* K-12 *rcsB*$^+$ strain T1241 was spotted to the center of a soft agar plate (0.2 % agar), and the motility radius was measured after growth of 5 hours at 37°C. The motility radius of the *rcsB*$^+$ K-12 strain T1241 was approximately 16 mm (Figure 10). When this strain was transformed with a plasmid expressing *matA* under control of the *tac* promoter (pKEDP30), its motility on soft agar plates supplemented with 0.2 mM IPTG was completely abolished (Figure 10). The motility of an isogenic Δ*rcsB* strain (U89) was similar to the *rcsB*$^+$ strain (16 mm, Figure 10), and this Δ*rcsB* strain remained motile upon additional expression of *matA* (18 mm, Figure 10). These data demonstrate that inhibition of motility by MatA requires RcsB, indicating that MatA-RcsB heterodimers repress motility.

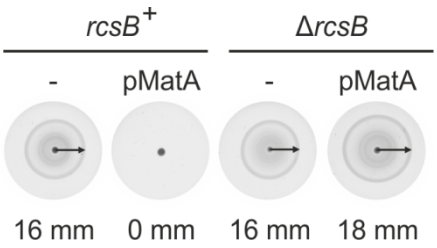

Figure 10. MatA-RcsB inhibits motility.
Motility of *rcsB*$^+$ strain T1241 and Δ*rcsB* strain U89 and of transformants of these strains ectopically expressing MatA under the control of P_{tac} (pKEDP30) was determined. Overnight cultures were grown in LB medium, if transformed supplemented with 1 mM IPTG and 25 µg ml^{-1} kanamycin. 3 µl of each culture was spotted on the center of a 0.2 % soft agar plate containing 0.2 mM IPTG and 25 µg ml^{-1} kanamycin for transformants, and the plates were incubated at 37°C for 5 hours. The plates were scanned and the motility radii that are indicated by arrows were measured. Image scale: Reduced by 1:4 of original size.

2.2.5. Search for potential DctR targets

Our two-hybrid analyses identified DctR as a further FixJ/NarL-type protein that interacts with RcsB (Fabisch, 2008). Gene *dctR* (*yhiF*) presumably forms an operon with the upstream gene *slp* encoding a lipoprotein (Tucker *et al.*, 2003). Both DctR and Slp play a role in protection against organic-acids that are metabolic end products under acidic conditions (Mates *et al.*, 2007). The expression of *slp-dctR* is activated by YdeO, a regulator of genes involved in the cellular response to acid resistance (Masuda & Church, 2003). However, as no target locus of DctR is known (Mates *et al.*, 2007), to analyze the relevance of the DctR-RcsB protein interaction in gene regulation I first needed to identify a DctR target. For this I performed a microarray analysis and compared the transcriptome of *E. coli* K-12 strain BW30270 harboring a plasmid encoding DctR under control of the IPTG inducible *tac* promoter (pKEDP31) to the same strain harboring vector pKESK22 as control. The expression of *dctR* was induced by addition of IPTG for 30 minutes in the exponential growth phase. The transcript analysis revealed that 57 loci were more than 10-fold upregulated (with p value < 0.05). At ten of these 57 loci, the microarray probe set mapped within an annotated gene (Table 3). However, the expression of these ten targets is low according to the average intensities. The average fluorescence intensities were in the range of 6.85 for *ypjC* and 8.39 for *yaiV* upon DctR expression (see Table 3). The average intensities of three housekeeping genes *rrsA*, *ihfB* and *rpoD* detected in this microarray analysis are listed in Table 3 as reference.

Table 3. DctR upregulated loci determined by microarray analysis

probe position[a]	dir.[b]	gene	gene position	function	fold change	average intensities[c] (pCtrl/pDctR)
3657577-3658135	<<	*arrS*	3657986-3658054	small regulatory RNA	18.4	3.78/7.82
4260607-4261264	>>	*yjbM*	4260599-4261306	predicted protein	16.0	3.94/7.70
2991310-2991759	>>	*ygeG*	2991268-2991759	predicted chaperone	14.0	4.18/7.84
2990556-2990915	>>	*ygeF*	2990554-2991043	hypothetical protein	13.9	4.27/7.96
2784529-2784724	<<	*ypjC*	2783638-2785011	pseudo	13.5	3.46/6.85
4250967-4252274	>>	*yjbI*	4250703-4252283	pseudo	13.4	4.77/8.28
1096019-1096776	>>	*ycdU*	1095843-1096829	predicted inner membrane protein	12.9	4.51/8.05
394477-395129	>>	*yaiV*	394506-395129	predicted DNA-binding transcriptional regulator	10.4	5.12/8.39
2989936-2990345	<<	*yqeK*	2989935-2990360	hypothetical protein	10.3	3.78/6.96
3633574-3634438	<<	*yhiL*	3632852-3634458	pseudo	10.3	4.67/7.74
housekeeping genes						
224773-224815	>>	*rrsH*	223771-225312	16S ribosomal RNA	1.0	15.23/15.20
963844-964109	>>	*ihfB*	963051-963335	integration host factor, β subunit	1.0	12.86/12.86
3213085-3213830	>>	*rpoD*	3211069-3212910	RNA polymerase, σ70	1.4	12.37/12.79

Summary of all significantly DctR-regulated loci (> 10-fold, p value < 0.05).
[a] Positions of probes and genes are given as coordinates of U0096.3 genome.
[b] 'dir' describes the orientation of the probe (<< for lower strand, >> for upper strand).
[c] Average intensities of the strain harboring control (left) or DctR expressing plasmid (right)

Of these 10 loci I selected six loci (*ycdU*, *ygeF*, *ygeG*, *yjbI*, *yjbM*, *ypjC*) to validate the microarray data by qRT-PCR. None of the six targets was significantly upregulated by DctR under the same growth conditions. Since DctR is encoded in an acid stress island, the qRT-PCR experiment was repeated with RNA obtained from transformants that were grown in acidic conditions (LB MES pH 5.5, supplemented with 1 mM IPTG for 30 minutes). Loci *ygeF, ycdU and yjbM* exhibited an around 10-fold, 5-fold, and 2.5-fold upregulation by DctR, respectively, when bacteria were grown at pH 5.5 but not when grown at pH 7.0 (Figure 11A). The expression of loci *ygeG*, *yjbI*, and *ypjC* was not upregulated in the presence of DctR, neither in bacteria grown at pH 7 nor at pH 5.5. Loci *ygeF* and *ycdU* were further analyzed by qPCR (Figure 11B). For this, RNA was isolated from *rcsB*$^{+}$ strain S3974 and Δ*rcsB* strain T73, harboring either control vector pBAD24 or DctR expression vector pKEDP57 grown at pH 5.5. However, the determined fold change was unspecific and the absolute expression levels reflected by the Ct values were very low (Figure 11B). The effect of DctR on *ygeF* expression was also analyzed by β-galactosidase assays. For this, the promoter region of *ygeF* (-193 to +12 rel. to start codon) was fused to *lacZ* on pKEDP61 and integrated into the chromosome of Δ*lacZ* strain (resulting T2017) and Δ*lacZ* P_{L}-*dctR* strain (resulting T2016).

The *lacZ* data showed no differences of P*ygeF* activation upon *dctR* expression, neither at pH 7.0 nor at pH 5.5. In addition, the effect of DctR on *arrS* expression was analyzed by β-galactosidase assays. The expression of gene *arrS* encoding the 69 nt long small RNA ArrS (Aiso *et al.*, 2011) was not analyzed by qPCR because of its short length it was difficult to design an adequate primer pair. For the construction of the promoter *lacZ* fusion, the promoter region of *arrS* (-311 to +10 rel. to the transcription start) was fused to *lacZ* resulting plasmid pKEDP52. The *rcsB*$^+$ Δ*lacZ* strain S4197 and P_L-*dctR rcsB*$^+$ Δ*lacZ* strain T1841 were transformed with plasmid pKEDP52 harboring P*arrS lacZ* and β-galactosidase assays were performed. The *lacZ* data showed no differences of P*arrS* activation upon *dctR* expression, neither at pH 7.0 nor at pH 5.5. Taken together, a certain target gene activated by DctR could not be identified in *E. coli* K-12.

A

	pH 5.5		pH 7.0	
locus	control	+ DctR	control	+ DctR
ycdU	1	4.7	0.8	0.8
ygeF	1	10.2	1.3	1.3
ygeG	1	1.1	0.3	0.3
yjbI	1	1.1	0.3	0.4
yjbM	1	2.6	0.7	0.7
ypjC	1	0.3	1.0	0.6

B

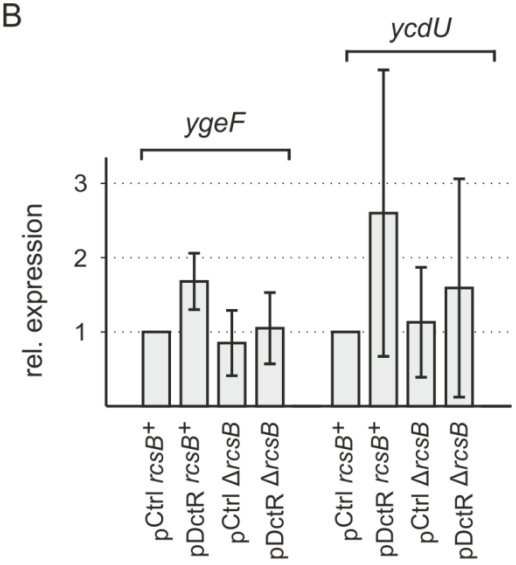

Figure 11. Influence of DctR and pH on expression.
qRT-PCR analysis of chromosomal loci expression. Cultures were inoculated in LB-MES (pH 5.5) and LB-MOPS (pH 7.0) supplemented with 25 µg ml^{-1} kanamycin or 50 µg ml^{-1} of ampicillin to an OD_{600} of 0.05 for exponential growth. At an OD_{600} of 0.3 IPTG was added to a final concentration of 1 mM and cultures were grown for additional 30 min. For first-strand cDNA synthesis, random hexameric DNA oligonucleotides were used. Quantitative PCR was performed using serial dilutions of cDNA and loci specific primers. Ct values were normalized to *rpoD* expression determined with primers T247 and T248. (A) RNA was isolated from cultures of strain S3839 (*rcsB+*), harboring either control vector pKESK22 (-DctR) or DctR expression vector pKEDP31 (DctR). Expression level is given as fold-change compared with the wild-type control (S3839 harboring pKESK22) grown at pH 5.5. Rel. expression indicates values of 1 experiment. (B) RNA was isolated from cultures of *rcsB+* strain S3974 and Δ*rcsB* strain T73, harboring either control vector pBAD24 (pCtrl) or DctR expression vector pKEDP57 (pDctR) grown at pH 5.5 in LB-MES supplemented with 50 µg ml^{-1} of ampicillin and 0.2 % arabinose. Expression level is given as fold-change compared with the control (S3974 harboring pBAD24). Rel. expression indicates values of at least 3 experiments.

2.2.6. Triple reporter system

To find single amino acid substitutions within RcsB that potentially impair interaction with specific partners, so far a plasmid expressing randomly mutated *rcsB* was transformed into a Δ*rcsB* Δ*lacZ* $bglJ_C$ reporter strain carrying the BglJ-RcsB activated *leuO* promoter fused to *lacZ* (T572). The transformants were screened on X-gal indicator plates, and clones exhibiting a Lac-negative phenotype were characterized. These RcsB mutants were then characterized for transcriptional activation of targets that are activated by RcsA-RcsB and RcsB-RcsB, respectively. For improving the efficiency of this screen, I designed a triple reporter strain with features that allow for analysis of transcriptional activation by RcsB-RcsB, RcsA-RcsB and BglJ-RcsB in the same strain.

In this Δ*rcsB* Δ*lacZ* strain *rcsA* is constitutively expressed under the control of the P_L promoter. RcsA, together with plasmid provided RcsB, activates colonic acid capsule production, and the cells become mucoid (Gupte *et al.*, 1997). The *bglJ* gene is as well constitutively expressed and with a functional version of RcsB, BglJ-RcsB heterodimers activate expression of the *bgl* operon (Venkatesh *et al.*, 2010) and the colonies exhibit the Bgl positive phenotype on BTB salicin indicator plates. The third feature of this triple reporter strain is the integrated P*rprA lacZ* fusion which is activated by RcsB-RcsB homodimers that allows screening for the Lac phenotype on X-gal indicator plates. The relevant genotype of this triple reporter strain (T1751) is shown in Figure 12A.

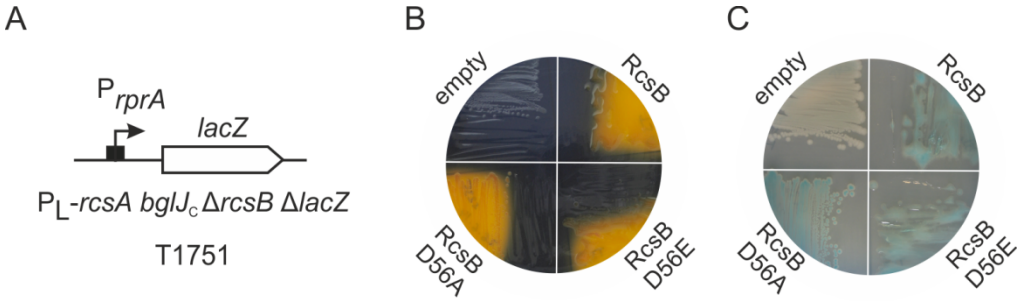

Figure 12. Triple reporter system for RcsB mutagenesis screen
(A) Relevant phenotype of the triple reporter strain T1751. The P*rprA lacZ* fusion is integrated into the *attB* site of a Δ*rcsB* Δ*lacZ* strain with *rcsA* under the control of the constitutive P_L promoter and expressing *bglJ* constitutively. (B) Phenotypic assay of strain T1751 transformed with empty vector (pKESK22) or vectors expressing wild-type RcsB and mutants D56E and D56A (pKETS6, pKETS7, and pKES235) on BTB salicin plates (kanamycin, IPTG) and on (C) X-gal plates (kanamycin, IPTG).

For testing this reporter system, strain T1751 was transformed either with empty plasmid pKESK22 or plasmids expressing wild-type RcsB and mutants D56E and D56A (pKETS6, pKETS7 and pKES235) and the transformants were plated on BTB salicin plates (Figure 12B)

and LB X-gal plates (Figure 12C) both containing kanamycin for selection and IPTG for induction of *rcsB* expression. In the absence of RcsB (empty vector pKESK22), colonies of the reporter strain exhibited the Bgl negative (transparent colonies) and Lac negative (white colonies) phenotype with non-mucoid colonies, indicating that neither expression of *bgl* nor of the *lacZ* reporter and the capsule genes was induced. Upon complementation with wild-type *rcsB* or derivatives D56E or D56A, all transformants showed the Bgl phenotype on BTB salicin plates (yellow colonies, Figure 12B), indicating that expression of *bgl* was induced by BglJ-RcsB and that induction is independent on RcsB phosphorylation. Upon complementation with wild-type *rcsB* or derivatives, all transformants exhibited a Lac positive phenotype on X-gal plates, albeit only slightly (light blue colonies, Figure 12C). Wild-type RcsB and RcsB-D56E but not RcsB-D56A were able to induce a mucoid phenotype, indicating that capsule gene expression is induced by RcsA-RcsB in an RcsB phosphorylation dependent manner (Figure 12B and C). Taken together, this phenotypic screening reflects the results obtained by β-galactosidase assays, in detail the RcsB phosphorylation independence for transcriptional activation by BglJ-RcsB and the distinct RcsB phosphorylation dependence for transcriptional activation by RcsA-RcsB. However, the at least partly RcsB phosphorylation dependence of transcriptional activation by RcsB homodimers that was found in the β-galactosidase assays is indistinguishable in the phenotypic assay. Summarized this triple reporter is a suitable tool for performing random mutagenesis screens for RcsB mutants that impair the activity of BglJ-RcsB, RcsA-RcsB or RcsB-RcsB, nevertheless the effect of the RcsB mutants on transcriptional activation needs to be further studied by quantitative methods such as β-galactosidase assays. Notably, the results show that RcsB homodimers as well as RcsA-RcsB and BglJ-RcsB heterodimers are simultaneously active, suggesting that RcsB forms homodimers and heterodimers with BglJ and RcsA at the same time, when BglJ and RcsA are present in the cell.

2.3. Relevance of particular residues of RcsB for specific RcsB dimers

Our results demonstrated that MatA-RcsB heterodimers are active independent of RcsB phosphorylation, as shown previously for BglJ-RcsB (Venkatesh *et al.*, 2010, Salscheider *et al.*, 2013). In contrast, the activity of RcsA-RcsB heterodimers and RcsB homodimers is phosphorylation-dependent (Majdalani & Gottesman, 2005, Clarke, 2010). To study the determinants for transcriptional activation by RcsB homo- and heterodimers, I identified particular residues of RcsB being relevant for transcriptional activation in the context of interaction partner. For this, RcsB mutants were specifically constructed or isolated from a mutagenesis screen and tested in the appropriate reporter systems.

2.3.1. Identification of relevant amino acids within RcsB

To identify particular amino acids of RcsB that are important for its activity together with the auxiliary proteins, a construction of RcsB mutants as well as a random mutagenesis screen was performed in which 31 RcsB residues were replaced obtaining 36 different mutants. These RcsB residues were selected as follows: (1) By a bioinformatics based analysis in which 38 RcsB protein sequences from various Proteobacteria were aligned (Kay Hofmann, Milteny Biotech), presumably surface-exposed amino acids were chosen. In this analysis, the amino acid residues I14, Y64, D66, R76, H77, and M88 were presumed as notably surface exposed (Figure 13C). (2) By a comparison of RcsB with conserved features of response regulators, amino acids of the highly conserved active quintet which includes D56, D11, T87, and K109 were chosen (Bourret, 2010). (3) In addition the highly conserved and presumably structurally important residues P60 and G67 were selected (Figure 13A). (4) Residues K180 and S184 (Figure 13E) were selected because of their location in the DNA-recognition helix α9 from which K180 was shown to be critical for DNA-binding activity (Thao et al., 2010). (5) Residues I199 and N203 (Figure 13E) are located in helix α10 of the C-terminal domain which is involved in dimerization of the NarL C-terminal domain (Maris et al., 2002). (6) On the basis of a structure prediction (see below), presumably surface exposed residues of the α4-β5-α5 surface that has been defined as dimerization interface in response regulators of the PhoB-type, were chosen (Gao & Stock, 2010, Bourret, 2010). This group comprises residues L95, S96, L99, D100, E104, I106, L108, T114, D115 and K118 (Figure 13B). (7) In a non-saturated random mutagenesis screen for inactive RcsB mutants, D11G, L41P, S58P, D62G, D66N, V98A (Figure 13D), F162C and F162S (Figure 13E) were isolated.

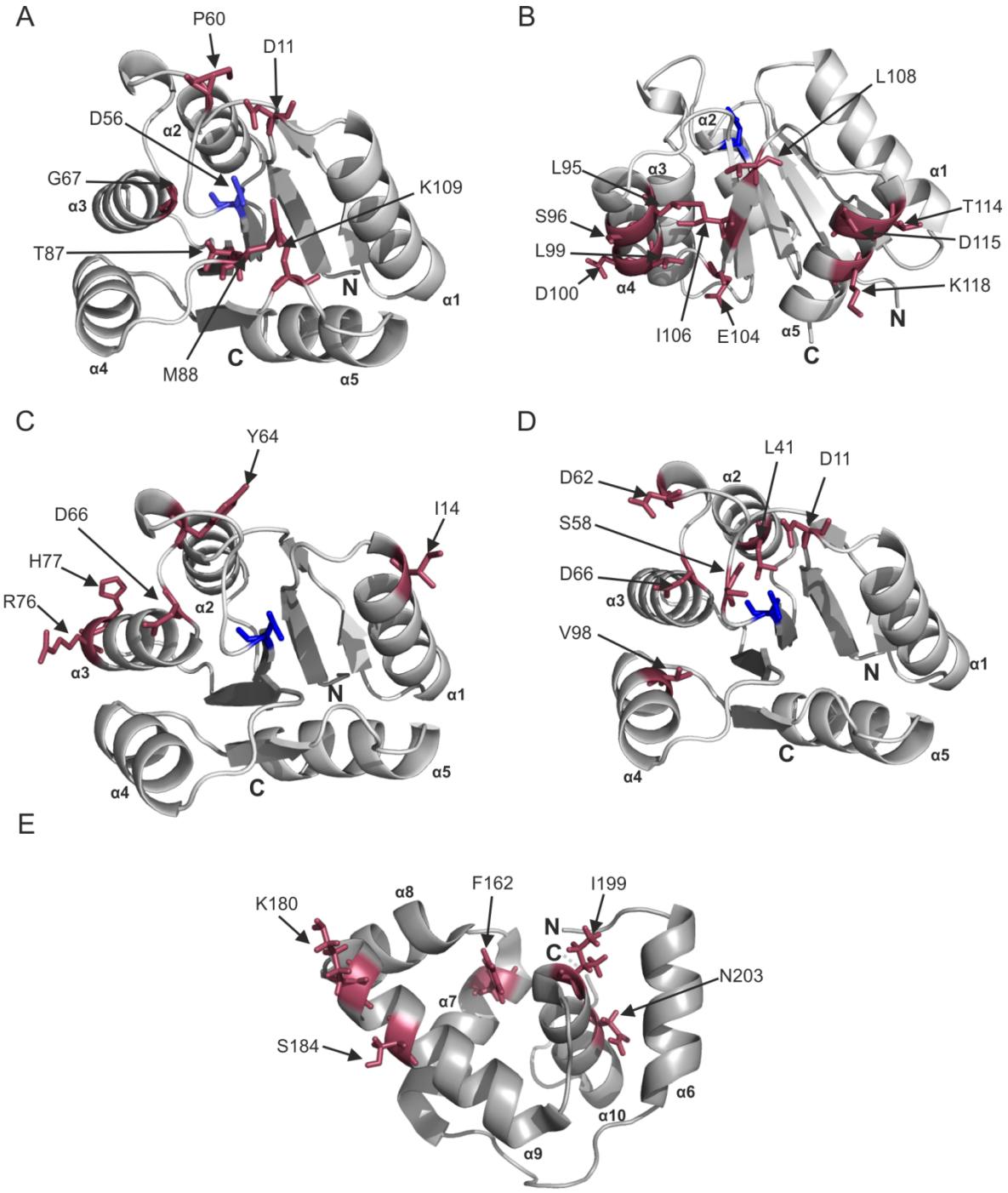

Figure 13. Structural model of the receiver domain of RcsB.
Structural model of the receiver domain and DNA-binding domain of RcsB. The model of the receiver domain was predicted by the PHYRE2 server (Kelley & Sternberg, 2009) on the basis of the crystal structure of NarL (Schnell *et al.*, 2008). The phosphorylation site is marked in blue. The DNA-binding domain was solved for RcsB of *Erwinia amylovora* (Pristovsek *et al.*, 2003). Mutated residues are marked in red. (A) Top view on the active site with active quintet and highly conserved residues indicated. The α helices are labelled from 1-5. (B) Side view on the α4-β5-α5-surface with surface exposed amino acids indicated. (C) Top view on the active site with amino acids indicated that were predicted to be surface exposed by bioinformatics based analysis. (D) Top view on the active site with amino acids being found in a random mutagenesis screen. (E) RcsB DNA-binding domain. Helices α8 and α9 constitute the HTH motif.

Receiver domains of two-component response regulators typically exhibit a $(\beta\alpha)_5$ topology with five parallel β sheets in the center surrounded by two α helices on the one and three on the other side (Bourret, 2010). The structure of the RcsB receiver domain has not been solved. Therefore, I used the PHYRE2 server (Kelley *et al.*, 2015) to predict a structural model of the RcsB receiver domain on the basis of the crystal structure of NarL (Schnell *et al.*, 2008), comprising residues 1-125 (Figure 13A-D). The structural model suggests that in RcsB, the active quintet group comprises the amino acid residue D56 that can become phosphorylated, as well as D10, D11, T87, M88 and K109. Of these the three aspartate residues D10, D11, and D56 presumably coordinate the metal ion that is essential for the phosphoryl group chemistry and hence for receiver domain function (Bourret, 2010). Interestingly, at the position corresponding to methionine residue 88 in RcsB, in other bacterial response regulators there is often a small amino acid such as alanine or glycine conserved (Bourret, 2010). Additional conserved residues within the receiver domains are amino acids P60 and G67 (Figure 13A). The structure of the DNA-binding domain was solved for RcsB derived from *Erwinia amylovora* comprising amino acids 129-215 by NMR spectroscopy (Pristovsek *et al.*, 2003). Helices α8 and α9 (residues 151-194) were identified as the central HTH DNA-binding motif which is stabilized by helix α7 (Pristovsek *et al.*, 2003).

According to their possible function, the RcsB mutants can be divided into five groups with exchanged amino acids (i) belonging to the active quintet of the receiver domain (D56, D11, T87, K109), (ii) being highly conserved within receiver domains of response regulators (P60, G67, M88), (iii) being surface exposed on α-helices or β-sheets (I14, R76, H77, L95, S96, L99, D100, E104, I106, L108, T114, D115, K118), (iv) other residues being non-exposed or located within loops (L41, S58, D62, Y64, D66, V98), and (v) residues within the DNA-binding domain (F162, K180, S184, I199, N203).

2.3.2. The relevance of particular residues of RcsB varies with its interaction partner

The results demonstrated that the phosphorylation dependence of RcsB for transcriptional activation varies with its interaction partner. Phosphorylation of response regulators at the conserved aspartic acid residue is considered to induce a structural change that stabilizes the active form (Gao & Stock, 2010) and affects the α4-β5-α5 surface that has been defined as dimerization interface of PhoB-type response regulators (Gao & Stock, 2010, Bourret, 2010). Helix α1 has been identified as dimerization surface in NarL-type response regulators (Trajtenberg *et al.*, 2014). The finding that some RcsB-heterodimers are active independent

of RcsB-phosphorylation suggests that for these, the phosphorylation-induced structural change is not important indicating that they interact differently or that the active form of that particular heterodimer is more stable. Here I analyzed if particular amino acids of the receiver domain of RcsB are important for its activity together with the auxiliary proteins. The RcsB mutants were analyzed in reporter strains with P*rprA lacZ* (T1052) for RcsB homodimer activity, P*wza lacZ* (T963) for RcsA-RcsB activity, P*leuO lacZ* (T572) for BglJ-RcsB activity and P*matA lacZ* (T1987) for MatA-RcsB activity. These reporter strains were transformed with low-copy plasmids coding for wild-type RcsB and mutants. To allow data comparison the expression levels directed by the respective *lacZ* reporter fusions were standardized to those obtained in presence of the active RcsB derivative D56E which were defined as 100 %. A brief summary of the data obtained for (i) active quintet, (ii) highly conserved and (iii) α/β-surface exposed residues is as follows (Figure 14). First, mutation of residues of the active quintet including D56, D11, T87, and K109 has the highest impact on the phosphorylation dependent RcsA-RcsB heterodimer and on RcsB. Among these mutants only K109A has strong impact on BglJ-RcsB and MatA-RcsB. Second, of the three mutants of conserved amino acid residues P60A, G67A, and M88A the latter (M88A) results in high activity of all RcsB homo-/heterodimers. In other response regulators a small amino acid is highly conserved at position M88 (Bourret, 2010). The M88A mutation may stabilize the active conformation of RcsB. G67A has a strong impact on RcsB, RcsA-RcsB, and BglJ-RcsB, but not on MatA-RcsB, while P60A affects only the phosphorylation dependent RcsB and RcsA-RcsB. Third, mutation of the presumably α/β-surface exposed residues that are located close to the phosphorylation site (including L95A, I106A, L108A, and D115A) reduce the activity of RcsB and RcsA-RcsB and have little to no impact on BglJ-RcsB and MatA-RcsB. Mutation of I14 to alanine renders all dimers inactive (Figure 14). Residue I14 is located on α helix 1 which has been identified as dimerization surface in NarL-type response regulators (Trajtenberg et al., 2014). The data suggest that α helix 1 may constitute the dimerization interface in RcsB. The results obtained for (iv) other residues being non-surface exposed on α-helices or located in loops are as follows: The majority of mutations abolishes or significantly impairs the activity of RcsB homodimers or heterodimers with RcsA or BglJ, while those mutants tested for MatA-RcsB did not have an effect (Figure 14). D66A has a strong impact on RcsA-RcsB and also affects RcsB-RcsB but neither BglJ-RcsB nor MatA-RcsB.

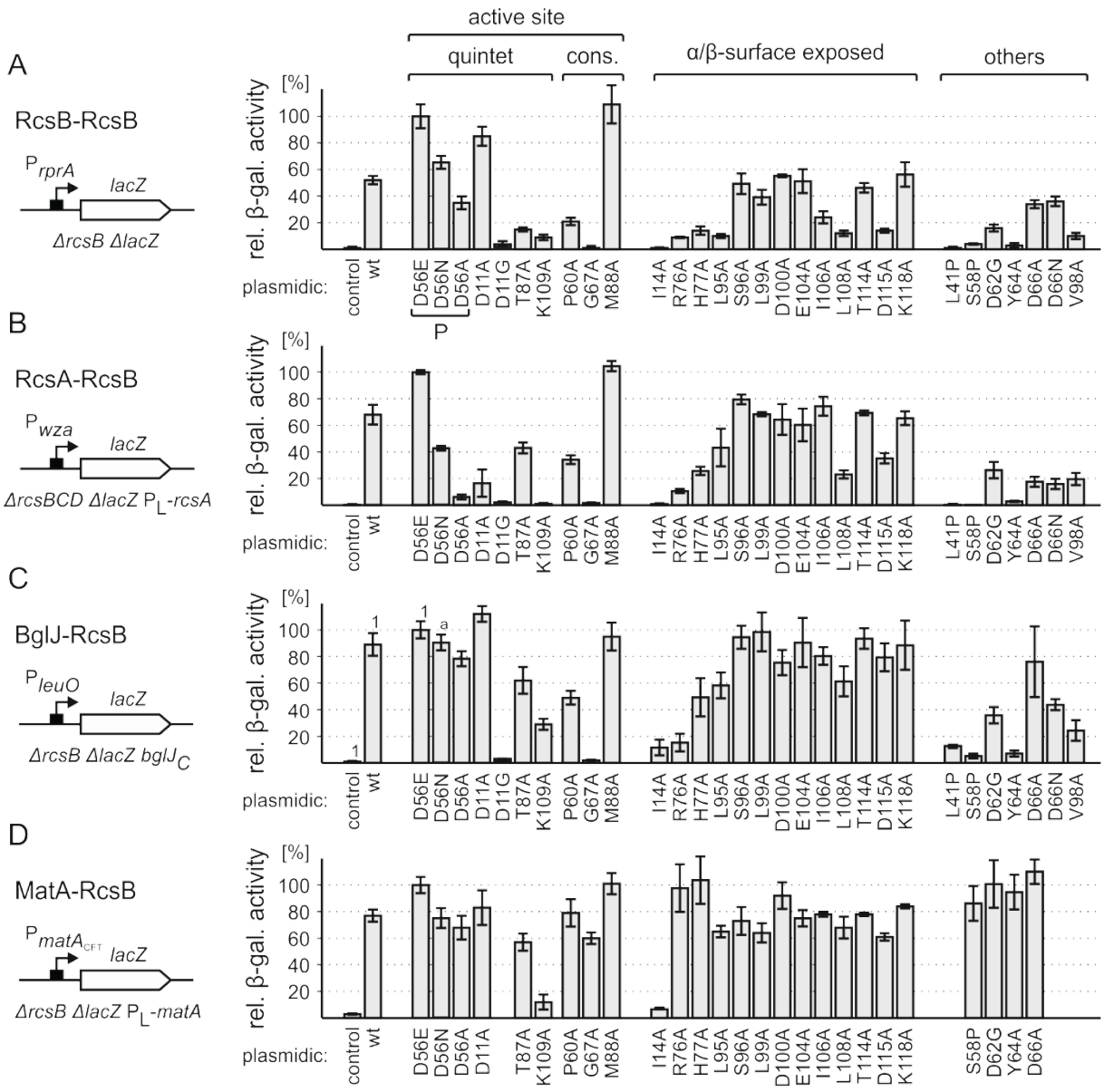

Figure 14. Effects of active site, α/β-surface exposed, and other residues on transcriptional activation.

Each strain was transformed with empty plasmid pKESK22 or plasmids expressing RcsB-wild-type and –mutants (pKETS6-8, pKES229-235, pKES271-275, pKESL111-120, pKEDP41, pKEDP43-47) and β-galactosidase activities were determined. The values obtained for RcsB-D56E were defined as 100 %. The phosphorylation site is marked with P. Cultures for β-galactosidase assays were grown in LB medium to an OD_{600} of 0.5 supplemented with 1 mM IPTG and 25 µg ml^{-1} of kanamycin. (A) Test system for monitoring the activity of RcsB mutants for RcsB homodimers: *rprA* promoter *lacZ* fusion integrated into *attB* site in a Δ*rcsB* Δ*lacZ* background (T1052). (B) Test system for analyzing RcsA-RcsB: *wza* promoter *lacZ* fusion in Δ*rcsBCD* Δ*lacZ* P_L-*rcsA* background expressing rcsA constitutively (T963). (C) Test system for BglJ-RcsB: *leuO* promoter *lacZ* fusion in Δ*rcsB* Δ*lacZ* $bglJ_C$ background expressing *bglJ* constitutively (T572). (D) Test system for MatA-RcsB: $matA_{CFT73}$ promoter *lacZ* fusion in Δ*rcsB* Δ*lacZ* P_L-*matA* background expressing *matA* constitutively (T1987). [a] Values are taken from Stratmann et al. 2012. [b] Values for L95A, S96A, L99A, D100A, E104A, I106A, L108A, T114A, D115A, and K118A mutants tested in strains T1052, T963, and T572 are unpublished laboratory results (Gausling, 2014).

The results obtained for (v) residues within the DNA-binding domain are briefly summarized below (Figure 15). The vast majority of mutations completely abolishes or significantly impairs the activity of RcsB homodimers or heterodimers with RcsA or BglJ. K180A, being located within α9 of the DNA binding domain completely abolishes activity of all dimers. Its location is in the HTH motif close to the turn to α8 and hence presumably affects the DNA-binding ability of RcsB. Mutated F162, found in the mutagenesis screen as F162C and F162S completely abolishes activity of all tested dimers. F162 is located at α7 that is important for stabilizing the HTH motif α8 and α9 by hydrophobic interaction (Figure 13E). The mutants putatively disturb the integrity of the HTH motif.

Taken together, RcsB homodimers and RcsA-RcsB heterodimers that are depending on RcsB phosphorylation possess the most similar properties. According to the structural model (Figure 13) all mutations located in the receiver domain that reduce or impair their activity are located in close vicinity to the active site supporting the predicted model. These residues are presumably important for the structural change that is elicited by phosphorylation. Therefore the active conformation of RcsB is likely essential for transcriptional activation by RcsB homodimers and heterodimers with RcsA. Interestingly, all residues found by the random mutagenesis screen with the exception of F162C and F162S are also close to the active site. For the activity of BglJ-RcsB dimers amino acid G67 plays a crucial role and K109 a partial role, whereas for the activity of MatA-RcsB only amino acid K109 is important. K109 and other amino acids being important for the activity of all dimers may be crucial for the structure. K180 is most probably crucial for DNA-binding. Another possibility for inactive RcsB mutants is reduced protein stability due to improper folding and rapid degradation which was addressed with a chloramphenicol chase experiment (see next section). Summarized, these results underscore the model that transcriptional regulation of RcsB homodimer and RcsA-RcsB heterodimer targets depends on Rcs signaling induced by cell envelope stress, while expression of MatA-RcsB and BglJ-RcsB target genes may not.

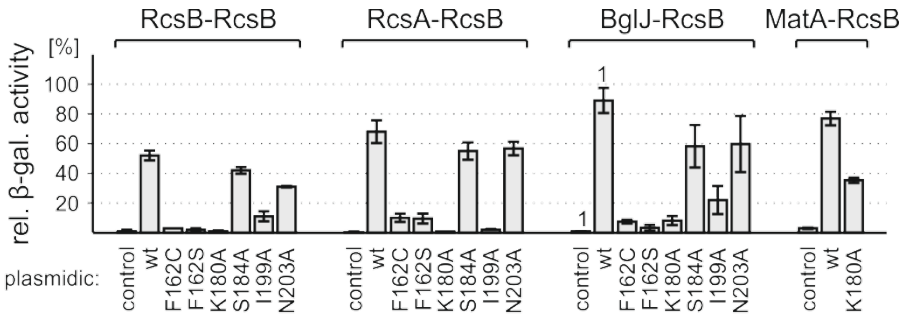

Figure 15. Effects of residues in DNA-binding domain on transcriptional activation.
Each strain was transformed with empty plasmid pKESK22 or plasmids expressing RcsB-wild-type and –mutants (pKETS6, pKES276-279, pKEDP40, pKEDP42) and β-galactosidase activities determined. Values of bars marked with [1] are taken from Stratmann et al. 2012. Cultures for β-galactosidase assays were grown in LB medium to an OD_{600} of 0.5 supplemented with 1 mM IPTG and 25 µg ml^{-1} of kanamycin. Analysis of RcsA-RcsB in reporter strain T1052, of RcsA-RcsB in strain T963, of BglJ-RcsB in strain T572, and of MatA-RcsB in strain T1987.

2.4. Expression and stability of RcsB mutants

The expression analyses using the *lacZ* reporters showed that several RcsB mutants were not able to activate gene expression as homodimers as well as heterodimers to the same extent as wild-type RcsB. The amino acid substitutions within RcsB could potentially influence correct folding of the mutant proteins leading to reduced stability by degradation. To find out, whether these RcsB mutants are instable and rapidly degraded, in a chloramphenicol chase experiment the protein stability was analyzed. To this end, plasmids were constructed for IPTG inducible expression of C-terminally HA-tagged RcsB mutants (Figure 16A). With these plasmids Δ*rcsB* strain T21 was transformed and cultures of these transformants were grown without induction of $rcsB_{HA}$ expression. At OD_{600} of 0.3 the first samples were taken. At the same time the expression was induced by adding IPTG (1 mM final concentration). The second sample was taken 30 minutes after induction. Immediately thereafter, chloramphenicol (200 µg/ml) was added to inhibit protein synthesis. After further 30 minutes the third sample was taken. The samples were analyzed by western blot analysis. The results demonstrate that all proteins were expressed to comparable amounts. However, the stability of the K109A mutant was reduced in comparison to the wild-type (Figure 16B). The K109A mutant was inactive in all tested reporter systems for RcsB homodimers and heterodimers with RcsA, BglJ and MatA. According to the structure prediction (Figure 13A), K109 resides in the center of the receiver domain and hence could play an important role for the integrity of the structure.

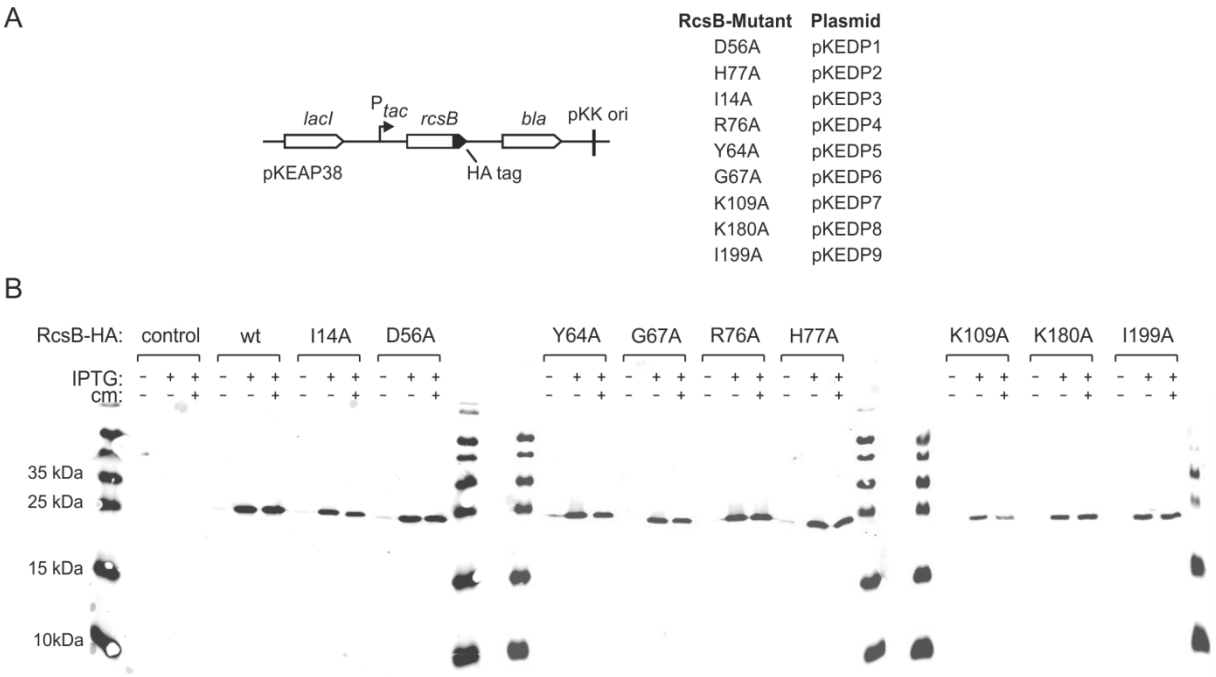

Figure 16. Stability assays of RcsB and its mutants by western blot analysis.
(A) Features and list of plasmids expressing HA tagged wild-type RcsB and mutants. (B) The plasmidic expression of HA tagged RcsB or HA tagged RcsB mutants (pKEAP38, pKEDP1-9) was induced by IPTG and inhibited by chloramphenicol. Thus, the stability of the RcsB protein and its mutants should be monitored. Samples were taken before induction (- IPTG, - cm), 30 minutes after induction (+ IPTG, - cm) and 30 minutes after inhibition by chloramphenicol (+ IPTG, + cm). For the empty vector control no HA tagged protein could be detected. For the RcsB wild-type and its mutants, no or very weak bands appear for the samples taken from cultures without IPTG induction of expression. The difference of the intensity between the bands obtained from cultures after IPTG induction (+ IPTG, - cm) and after inhibition of protein synthesis (+ IPTG, + cm) give information about the stability of each RcsB mutant. For the RcsB mutant K109A, the (+ IPTG, + cm) band is weaker than the (+ IPTG, - cm) band, indicating that this RcsB mutant exhibits a reduced stability.

2.5. Protein-protein interaction of RcsB mutants

To analyze whether the mutant RcsB proteins are still able to interact with each other and with the co-regulators RcsA as well as BglJ and form stable homo- and heterodimers, respectively, the *SPINE* method (*Strep-Protein-Interaction-Experiment*) was applied (Herzberg *et al.*, 2007). For this purpose, two different expression vectors were transformed into strain T73 (Δ*rcsB*). One contained an HA-tagged RcsB version, the other one the Strep-tagged interaction partner RcsB, BglJ, or RcsA (Figure 17A). In brief, exponential cultures (1000 ml LB medium containing ampicillin and kanamycin) were inoculated from a fresh overnight culture and grown to an OD_{600} = 0.8 and at this point the expression of the Strep- and HA-tagged proteins were induced by adding IPTG (1 mM final concentration). One hour after induction of protein synthesis, the crosslinking agent formaldehyde was added, which stabilizes the interactome, i.e. all interacting proteins including those being tagged, are crosslinked. A protein lysate obtained from these cultures was applied on a Strep-tactin gravity flow column, thereby the Strep-tagged RcsB protein and consequently the putative HA-tagged interaction partner were purified. The eluate was boiled for reversion of the crosslinks and analyzed by western blot (Figure 17). Figure 17A shows the results for analysis of RcsB-RcsB interaction. All RcsB mutants seem to interact with each other. Also the HA-tagged RcsB-D56A mutant that mimics inactive RcsB was detected in the eluate, indicating that the dimerization behavior of RcsB is phosphorylation independent. However the quantification of the interaction turned out to be difficult. The interaction between BglJ and RcsB for specific RcsB mutants could also be shown by the *SPINE* method. Therefore Strep-tagged RcsB or RcsB mutants, respectively, were plasmidically expressed together with an HA-tagged BglJ (Figure 17B) in the strain T175 (Δ*rcsB* Δ*yjjP-yjjQ-bglJ*) under the same conditions as for RcsB-RcsB homomers. The protein lysates obtained from these cultures were purified on a strep tactin columns, potential crosslinking between BglJ-HA and RcsB-Strep was reversed by boiling and analyzed by western blot analysis. In the control experiment, at which BglJ-HA is expressed in the absence of RcsB-Strep, BglJ-HA can only be detected in the lysate but not in the eluate, indicating that BglJ-HA is indeed purified via the interaction with RcsB-Strep (Figure 17B). However, the interaction appears to be weaker than between RcsB-RcsB.

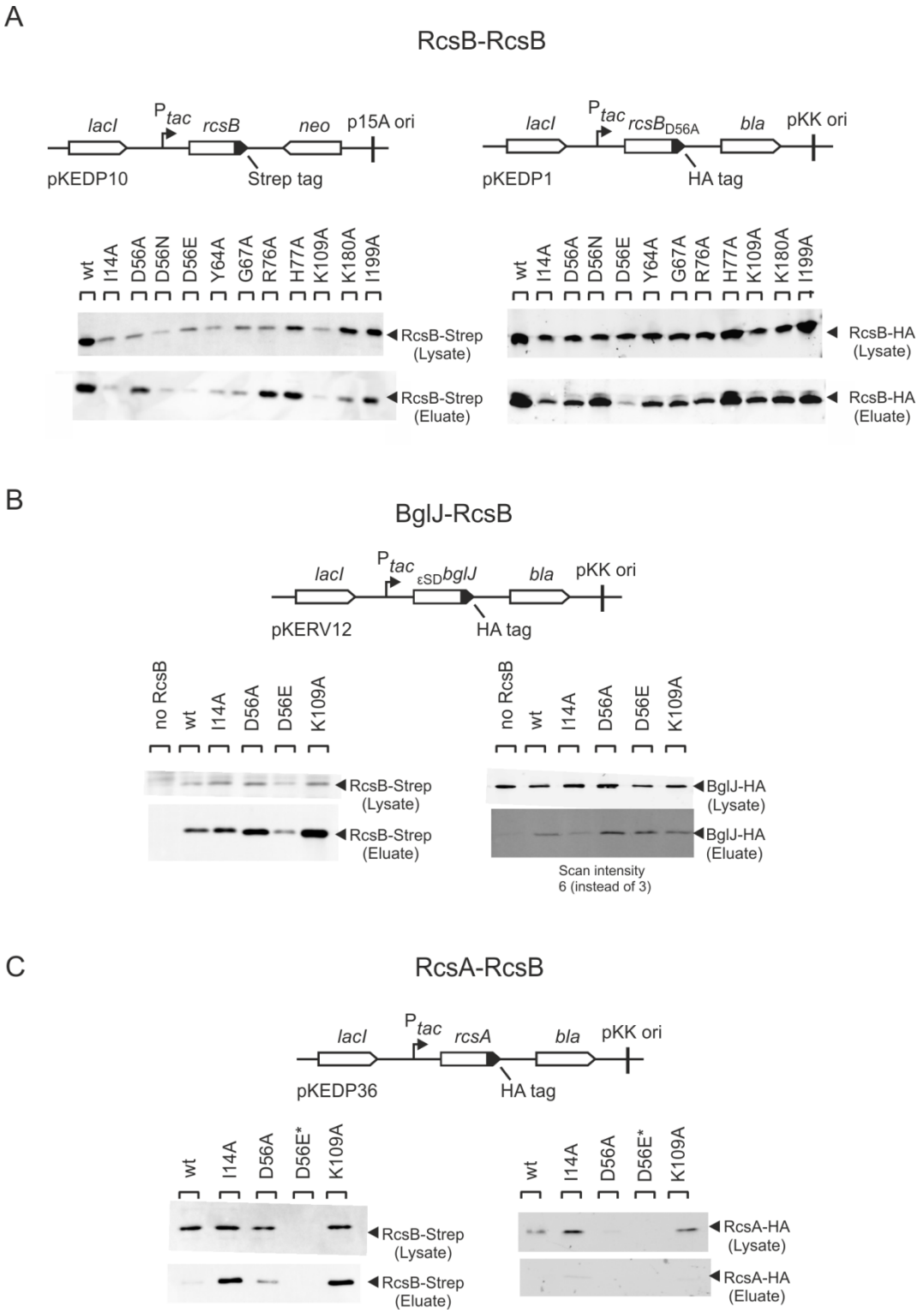

Figure 17. RcsB protein interaction studies by *SPINE*.
Features of plasmids and western blots of protein lysate and eluate obtained from SPINE analyses. Each western blot was developed with rat anti-HA as primary and fluorescence labeled anti rat as secondary antibody. The Strep-tagged proteins were visualized with Strep-MAB-HRP-conjugate antibodies via chemiluminescence. (A) For analyzing RcsB-RcsB interaction, RcsB-Strep expressing plasmids pKEDP10-21 and RcsB-HA expressing plasmids pKEAP38, pKEAP43-44, and pKEDP1-9 were used. RcsB-Strep and RcsB-HA were expressed in strain T73 (Δ*rcsB*). (B) For analyzing BglJ-RcsB interaction, RcsB-Strep (pKEDP10-21) and BglJ-HA (pKERV12) were expressed in strain T175 (Δ*rcsB* Δ*yjjP-yjjQ-bglJ*). (C) For analyzing RcsA-RcsB interaction, RcsB-Strep and RcsA-HA (pKEDP36) were expressed in strain T1338 (Δ*rcsB* Δ*rcsA*).

This observation might be due to BglJ-HA forming inclusion bodies upon high overexpression resulting in growth defects. On pKERV12 the native RBS of BglJ is replaced by an epsilon element and Shine-Dalgarno sequence (εSD) enhancing protein synthesis initiation (Figure 17B). For RcsA-RcsB interaction, HA-tagged RcsA was expressed together with Strep-tagged RcsB and its mutants under the same conditions as for RcsB-RcsB homomers. The protein lysates obtained from these cultures were also purified on a strep tactin columns, potential crosslinking between RcsA and RcsB reversed by boiling and analyzed by western blot analysis. Only two weak RcsA bands could be seen in the anti-HA immunostained western blot for the eluate (Figure 17C). The interaction between RcsA and RcsB appears to be weaker than for BglJ-RcsB. The fact that in the RcsA-RcsB interaction experiment no bands could be detected - neither for RcsB-D56E-Strep nor for RcsA-HA tested with RcsB-D56E – may be caused by a difficulty in pelleting the cultures. RcsA-RcsB activates expression of the capsule genes causing a mucoid phenotype of colonies on plates. Pellets obtained by centrifugation of liquid cultures immediately resuspended in the remaining medium. Taken together, for assessing a protein-protein interaction between RcsB-Strep and RcsB-HA, BglJ-HA, and RcsA-HA, *SPINE* proves to be difficult.

2.6. Mechanism of transcriptional activation

In recent studies, the mechanism of activation by BglJ-RcsB of several target genes was analyzed. Therefore the BglJ-RcsB binding site was mapped at several loci and a consensus sequence motif was proposed. It was suggested that activation by BglJ-RcsB is DNA phasing dependent at some loci, such as it was shown for P*molR* and proposed for P*ynbA* (Salscheider *et al.*, 2013). As activation of several promoters by BglJ-RcsB is DNA helical turn dependent, BglJ-RcsB might interact with RNA polymerase. To study a potential interaction between BglJ-RcsB and RNA polymerase, I followed two approaches as follows: A bacterial two-hybrid system and the overexpression of the RNA polymerase α subunit.

2.6.1. Interaction studies of RcsB with RNA polymerase by a bacterial two-hybrid system

Interaction of RcsB with the alpha subunit of RNA polymerase was tested with a bacterial two-hybrid system (Dove & Hochschild, 2004). In this system, either the RcsB-HTH domain or the whole RcsB was fused to the cI domain of phage λ (plasmids pKEKD23, pKEDP38 and pKEDP39, Figure 18B). The λ cI domain binds to the λ operator being located 62 bp upstream of the transcription start of the reporter construct in strain S3773 (Figure 18A). Transcription

of the *lacZ* reporter gene is only induced if there are direct contacts between RcsB or RcsB-HTH, respectively, and the αCTD domain of the RNA polymerase (Figure 18A). As a positive control served the plasmids pAC λcI-β 831-1057, encoding for a fusion of amino acids 831–1057 of RNA polymerase β subunit to λcI under PlacUV5 control, and pBR α-σ70 D581G, encoding for a fusion of amino acids 528-613 of σ^{70} (with a D581G substitution) to RNA polymerase α-subunit under PlacUV5 control. Plasmids pAC λcI and pBR α(NTD) served as negative control. Expression of both positive control plasmids is necessary for activation of the promoter, mediated by λ cI binding to the λ operator and interacting with the RNA polymerase. The positive control plasmids exhibited a transcriptional activation of the reporter, with expression levels of 245 units uninduced and 1246 units induced (200 µM IPTG final concentration). The negative control plasmids resulted in 81 and 106 units, respectively. In a second setup RcsB HTH was fused to the N-terminal domain (αNTD) and the αCTD was fused to λ cI (plasmids pKEKD24 and pKEDP50, Figure 18B). These constructs were plasmidically expressed under the control of the *lacUV* promoter applying 200 µM IPTG final concentration as well as without induction (Figure 18C). Also varying IPTG concentrations (from 10 µM to 1 mM) were tested. For none of the different setups activation of the reporter promoter could be detected. Taken together, by this bacterial two-hybrid system an interaction between RcsB and RNA polymerase could not be detected.

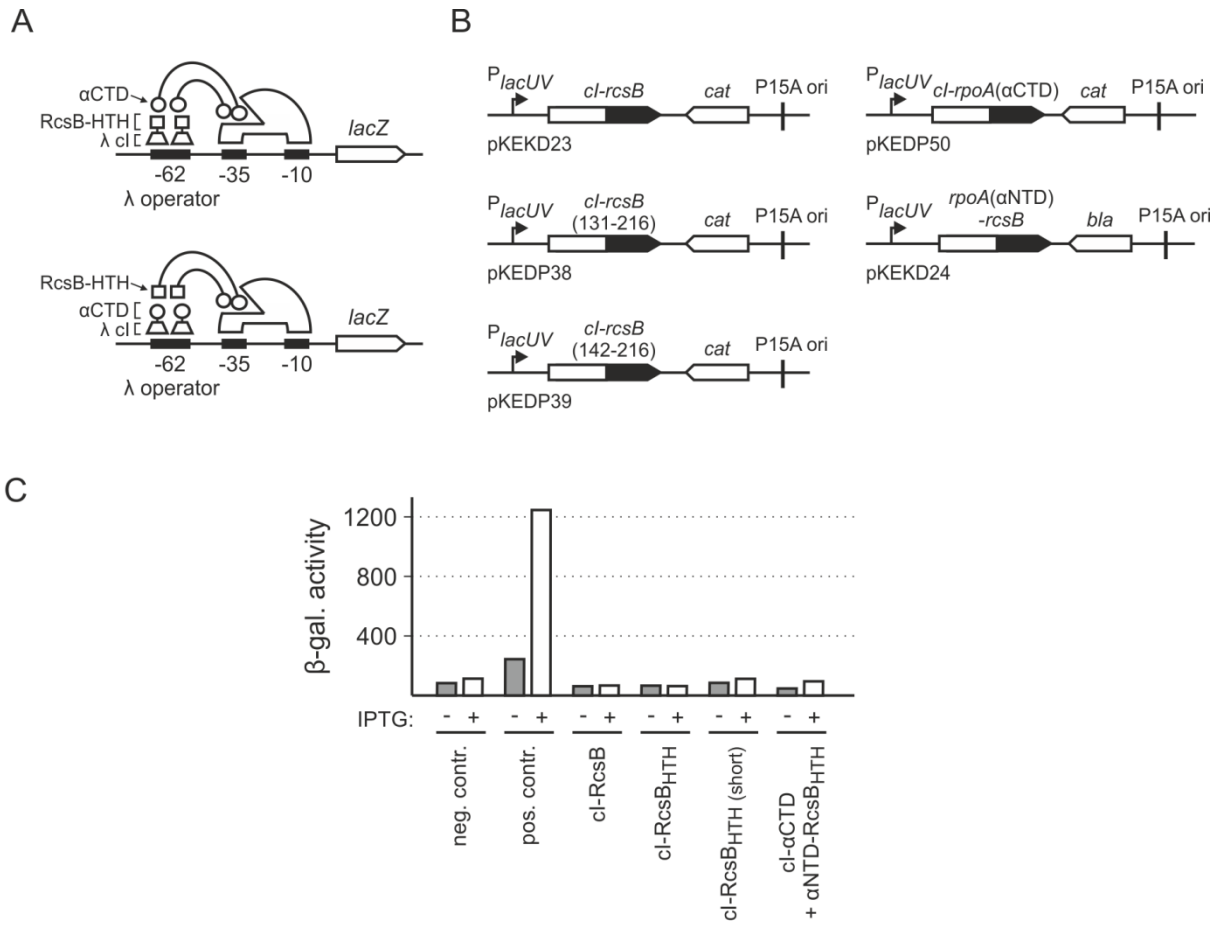

Figure 18. Experimental setup, used plasmids and results for RcsB-RNA polymerase interaction by bacterial two-hybrid analyses.

(A) Schematic overview of the bacterial two-hybrid system. RcsB and RcsB HTH respectively were fused to λ cI (top) or the αCTD was fused to λ cI and RcsB HTH to α NTD (bottom). If RcsB/RcsB HTH and αCTD interact, the reporter gene *lacZ* is expressed and the β-galactosidase activity can be measured in reporter strain S3773. (B) Features of plasmids pKEKD23, pKEDP38, pKEDP39, pKEDP50 and pKEKD24 used for the bacterial two-hybrid experiment. All constructs were expressed under the control of P_{UV5}. (C) β-galactosidase assay results in miller units for induction with 200 µM IPTG final concentration. The induced positive control plasmids pAC λcI-β 831-1057 and pBR α-σ70 D581G exhibited a promotor induction of 1246 units. Plasmids pAC λcI + pBR α(NTD) served as negative control. For none of the different setups activation of the reporter promoter could be detected.

2.6.2. Overexpression of the RNA polymerase α subunit

In a second approach to analyze potential BglJ-RcsB interaction with RNA polymerase, the complete α subunit as well as a truncated version lacking the αCTD of the RNA polymerase was plasmidically expressed. The idea of this approach is depicted in Figure 19. If BglJ-RcsB interacts with the αCTD to activate certain promoters, the expression of a reporter gene should be activated in case of overexpression of the wt α subunit (Figure 19A). Overexpression of the αNTD, a truncated version lacking the αCTD should reduce reporter gene expression (Figure 19B). Such mutant RNA polymerase holoenzymes are unable to induce transcription activation by cAMP/CRP at some type I CRP-dependent promoters, such as *lac* and *uxuAB* (Igarashi et al. 1991).

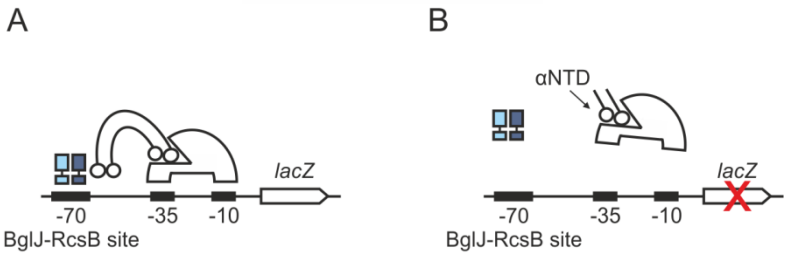

Figure 19. Idea of overexpressing RNA polymerase α subunit and αNTD in case of αCTD BglJ-RcsB interaction.
(A) Upon overexpression of wt α subunit, the RNA polymerase holoenzymes are able to activate the promoter due to direct contacts to BglJ-RcsB. (B) If αNTD is overexpressed, a given proportion of RNA polymerase holoenzymes is lacking the αCTD. The activation of the promoter is impaired.

For this approach the promoters of the HNS repressed genes *leuO* and *yidL* (Figure 20C) as well as of genes *molR*, *ynbA* (Figure 20D) were analyzed. All four promoters were shown to be a BglJ-RcsB target (Salscheider *et al.*, 2013). In addition, I analyzed P*rprA*, a promoter that is activated by RcsB homodimers (Figure 20B). Previous analyses demonstrated a phasing dependent activation of the *molR* promoter by BglJ-RcsB, and showed a BglJ-RcsB binding site in phase of the *ynbA* promoter. The BglJ-RcsB binding site at the *yidL* promoter was shown to be in reverse orientation and P*yidL* may not be activated by direct BglJ-RcsB RNA polymerase contacts (Salscheider *et al.*, 2013). The reporter strains carried *attB* integrated promoter *lacZ* fusions in a *bglJ*$_C$ background. For the analyses, the appropriate reporter strains were transformed with pBR derived high-copy plasmids expressing wt α subunit (pLAX185) or αNTD (pLAD235) under the control of the IPTG-inducible *lpp/lacUV* tandem promoter (Figure 20A) and β-galactosidase activities determined.

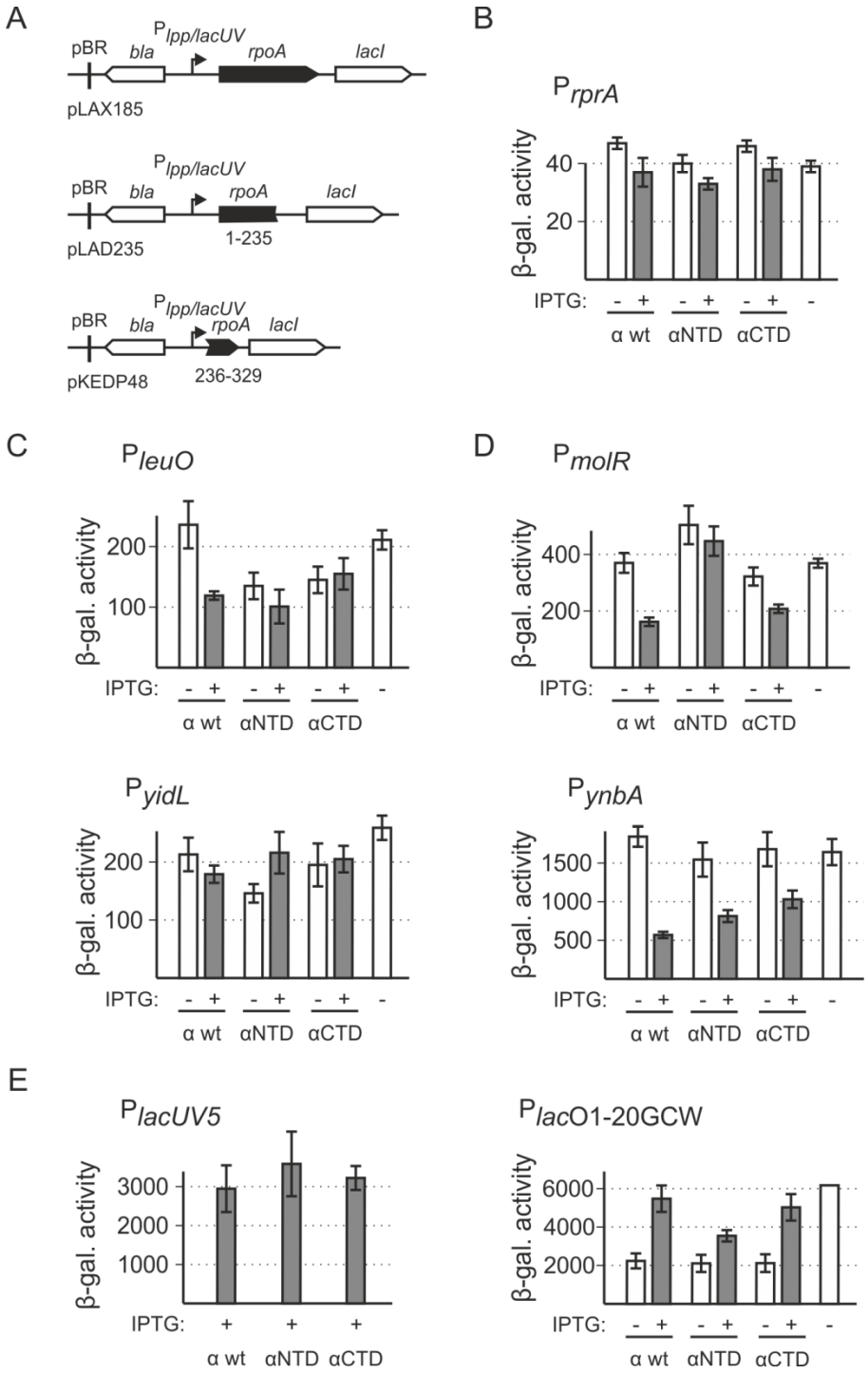

Figure 20. Effects of overexpression of the RNAP α subunit on different promoters.
(A) pBR derived high-copy plasmids harboring full-length *rpoA* (pLAX185) or the truncated αCTD (pKEDP48) or αNTD (pLAD235) under the control of the IPTG-inducible *lpp/lacUV* tandem promoter. The reporter strains were transformed with these plasmids and cultures for β-galactosidase assays were grown in LB medium to an OD_{600} of 0.5 optional supplemented with 1 mM IPTG and 50 µg ml^{-1} of ampicillin. Untransformed reporter strains served as control. (B) Results for P*rprA lacZ* fusion integrated into a *ΔlacZ ΔgalU* strain (T2043) for analyzing RNA polymerase interaction with RcsB homodimers, (C) Results for P*leuO* and P*yidL*, both HNS repressed, fused to *lacZ* and integrated in a *ΔlacZ ΔleuO bglJ*$_C$ strain background (T570, T1474) (D) Results for P*molR lacZ* and P*ynbA lacZ* integrated in a *ΔlacZ ΔleuO bglJ*$_C$ strain background (T1441, T1326). (E) Results for P*lacUV5* (strain S1906, negative control) and P*lacO1*-20GCW (strain T46, positive control).

Reporter strain S1906 with P*lacUV5 lacZ* served as negative control and strain T46 with P*lacO1*-20GCW as positive control with CRP-RNA polymerase interaction required for expression (Figure 20E). Cultures for β-galactosidase assays were grown in LB medium to an OD_{600} of 0.5 supplemented with 1 mM IPTG and 50 µg ml^{-1} of ampicillin.

First, the *rprA* promoter that is activated by RcsB homodimers was analyzed. Since activation of the *rprA* promoter is RcsB phosphorylation dependent, the analyses were conducted in a Δ*galU* strain. The results are shown in Figure 20B. The expression levels obtained for induced expression of full-length and truncated α subunits were similar to the control without plasmid. Consequently, a potential interaction between the RNA polymerase α subunit and RcsB homodimers could not be shown for the *rprA* promoter. Next, the promoters activated by BglJ-RcsB were analyzed. Interestingly, at the *leuO, molR,* and *ynbA* promoter the induction of wt α expression significantly reduced reporter gene expression levels (Figure 20C, D). Induction of αNTD expression causes reduced reporter gene expression levels for the *ynbA* promoter compared to no induction. Surprisingly, the induced expression of the wt α subunit caused a reduced reporter expression at the *molR* and *ynbA* promoter; however, expression of the αNTD had no influence on the level of the control, at least for P*molR*. These findings contradict the initial hypothesis that overexpression of αNTD lacking the αCTD should reduce the promoter activity if BglJ-RcsB interacts with RNA polymerase α subunit. Also the fact that the strain is merodiploid for *rpoA* (the chromosomal *rpoA* is present) as the gene is essential for viability, does not fully explain the results, although it could explain why the results obtained for overexpressing αNTD are on the same level as the control without plasmid (Figure 20D, top graph). The results obtained for the *molR* promoter upon expression of wt α subunit, although unexpected, can indeed be in accordance with the initial considerations. If the BglJ-RcsB dimer binds to the αCTD before the RNA polymerase holoenzyme binds to the *molR* promoter, overexpression of the full-length α subunit would outcompete RNA polymerase for interaction with BglJ-RcsB and thus reduce activation of the *molR* promoter (Figure 21B). To test this hypothesis, I expressed the αCTD (pKEDP48), a truncated version of the α subunit lacking αNTD. At P*molR,* induced αCTD overexpression activates the promoter on a similar level as α wt (Figure 20D, top graph), supporting the hypothesis of a pre-recruitment mechanism. At P*ynbA,* induced αCTD overexpression also reduced promoter activation, although the effect was less strong than

for wt α subunit (Figure 20D, bottom graph). A model explaining these results is depicted in Figure 21A and B.

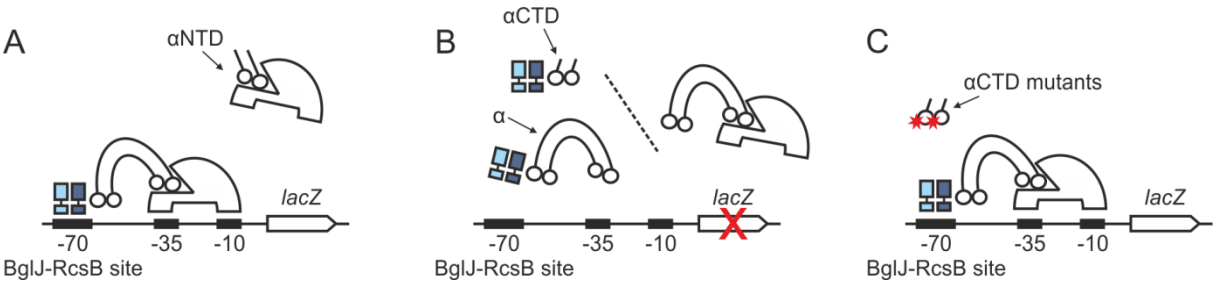

Figure 21. Potential model of P*molR* activation by BglJ-RcsB.
(A) Although αNTD is plasmidically expressed, P*molR* is activated by fully assembled RNA polymerase with the α subunit being encoded in the chromosome. (B) Overexpressed α subunit or αCTD bind BglJ-RcsB in a pre-recruitment mechanism and hinder fully assembled RNA polymerase to interact. P*molR* activation is decreased. (C) Overexpressed αCTD mutants have less ability to interact with BglJ-RcsB. The wild-type RNA polymerase is able to activate P*molR*.

The results above indicated for P*molR* a pre-recruitment mechanism, in which the BglJ-RcsB dimer binds to the αCTD before the RNA polymerase holoenzyme binds to the *molR* promoter. In this case, overexpression of the full-length α subunit or its C-terminal domain would hinder the RNA polymerase holoenzyme for interaction with BglJ-RcsB and thus reduce activation of the *molR* promoter (Figure 21B). To test this hypothesis, I repeated the analyses with plasmidically expressing different αCTD mutants. Each αCTD mutant carried a single alanine substitution of residues belonging to the 287 determinant that were previously shown to contact CRP during class I and class II CRP-dependent transcription (Savery *et al.*, 1998, Savery *et al.*, 2002). The location of residues belonging to the 287 determinant is indicated in Figure 22A and a list of plasmids harboring the αCTD mutants is given in Figure 22B. In case of a pre-recruitment mechanism, reduced contacts between BglJ-RcsB and ectopically expressed αCTD mutants would not hinder the RNA polymerase holoenzyme for interaction with BglJ-RcsB anymore. Consequently, in case of expressing αCTD mutants, reporter gene expression should increase compared to wild-type αCTD (Figure 22C). Here, I tested P*molR* and P*ynbA*, each having the BglJ-RcsB binding site in phase, as well as P*yidL* as a control with the BglJ-RcsB binding site in reverse orientation. To this end, the appropriate reporter strains were transformed with plasmids expressing the αCTD mutants T285A, E286A, V287A, E288A, L290A, G315A, R317A, and L318A. The β-galactosidase activities were determined without induction and with IPTG induction. The

results are summarized in Figure 22C-E. The statistical significance was calculated for each αCTD mutant compared to wild-type αCTD upon induction. Activation of P*molR* and P*ynbA* was significantly higher upon expression of each αCTD mutant compared to the wild-type αCTD (gray bars, Figure 22C and D). Activation of P*yidL* was similar for expression of αCTD mutants or wild-type αCTD (gray bars, Figure 22E). These results are in agreement with the initial hypothesis in which wild-type αCTD hinders RNA polymerase holoenzyme for interaction with BglJ-RcsB at P*molR* and P*ynbA*. Mutant αCTD proteins bind BglJ-RcsB with less affinity, the steric hindrance is reduced and P*molR* as well as P*ynbA* activation is higher. Taken together, these results support the model for P*molR* and P*ynbA* activation by direct contacts between the transcription factor BglJ-RcsB and the αCTD of the RNA polymerase.

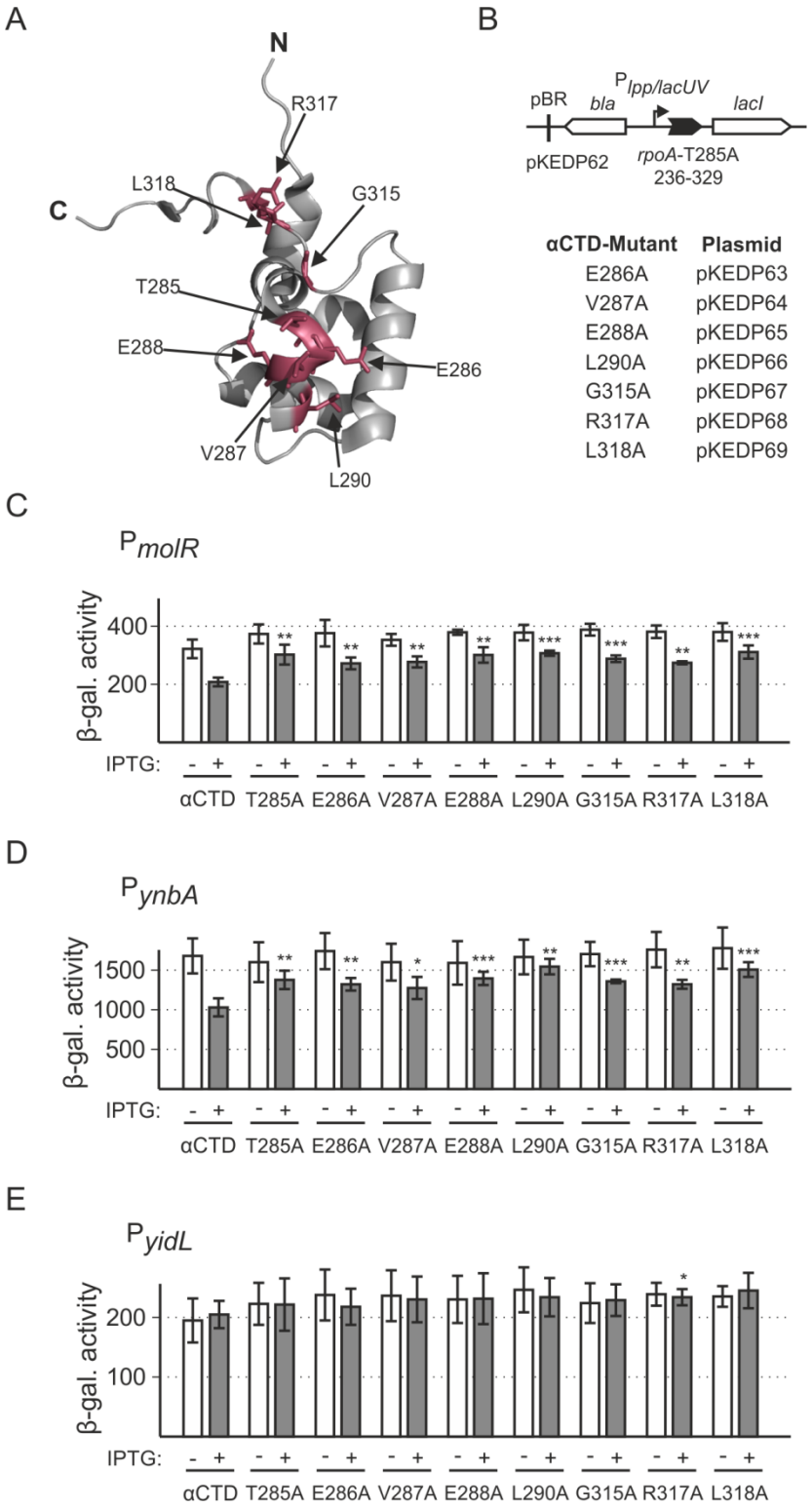

Figure 22. Effects of overexpression of αCTD mutants on P*molR*, P*ynbA*, and P*yidL*.
(A) Structure of the αCTD with residues belonging to the 287 determinant indicated. The structure of the *E. coli* αCTD was solved by X-ray crystallography comprising amino acids 245-329 (Lara-Gonzalez *et al.*, 2010). (B) pBR derived high-copy plasmids harboring αCTD (pKEDP48) or mutants T285A, E286A, V287A, E288A, L290A, G315A, R317A, and L318A (pKEDP62-69) under the control of the IPTG-inducible *lpp/lacUV* tandem promoter. The reporter strains were transformed with these plasmids and cultures for β-galactosidase assays were grown in LB medium to an OD_{600} of 0.5 supplemented with 50 µg ml^{-1} ampicillin and 1 mM IPTG in case of induction. (C) Results for P*molR* *lacZ* integrated in a *ΔlacZ ΔleuO bglJ*$_C$ strain background (T1441). (D) Results for P*ynbA* *lacZ*

integrated in a *ΔlacZ ΔleuO bglJ*$_C$ strain background (T1326). (E) Results for P*yidL* fused to *lacZ* and integrated in a *ΔlacZ ΔleuO bglJ*$_C$ strain background (T1474). Displayed values are means ± SD. The significance was calculated for each mutant compared to αCTD upon IPTG induction with *p < 0.05; **p < 0.01; ***p < 0.001.

3. Discussion

The Rcs phosphorelay is a key regulator of motility, biofilm formation, and various stress responses and its complex output is governed by the response regulator RcsB (Majdalani & Gottesman, 2005). Since RcsB is involved in the regulation of these highly energy-consuming processes, its output function has to be tightly regulated. Hence, the activity of RcsB is controlled on different levels: On the one hand it is controlled by its phosphorylation state and on the other hand RcsB can regulate target genes as a homodimer or heterodimers with RcsA, BglJ, GadE (Majdalani & Gottesman, 2005, Venkatesh *et al.*, 2010, Castanie-Cornet *et al.*, 2010). Recently RcsB was found to also interact with MatA and DctR. This study provides molecular insights into homo- and heterodimer formation of RcsB. I established suitable reporter systems for analyzing transcriptional activation by RcsB homodimers, and by RcsB heterodimers with RcsA, and MatA. The results demonstrate that RcsB together with MatA fully activates the *matA* promoter of UPEC strain CFT073 and moreover, that MatA-RcsB is able to repress the motility of *E. coli* K-12, suggesting that a MatA-RcsB heterodimer regulates expression. Furthermore, the results demonstrate that transcriptional activation by MatA-RcsB heterodimers is independent of RcsB phosphorylation. An RcsB phosphorylation-independent mechanism was also shown for BglJ-RcsB (Stratmann *et al.*, 2012). The data confirmed that RcsA-RcsB and RcsB-RcsB act in a phosphorylation dependent manner. In a systematic approach I found amino acid residues within the receiver domain of RcsB that are required for transcriptional activation by RcsB homodimers and heterodimers with RcsA, those transcription factors depending on RcsB phosphorylation. All mutations that reduce or impair the activity are located in close vicinity to the active site. These residues are presumably important for the structural change that is elicited by phosphorylation. Additionally, the triple reporter results demonstrated that RcsB homodimers as well as RcsA-RcsB and BglJ-RcsB heterodimers are simultaneously active, suggesting that RcsB forms homodimers and heterodimers at the same time, if the auxiliary regulators are present. Finally, I found indications that at some promoters BglJ-RcsB heterodimers activate transcription presumably by an interaction with the RNA polymerase in a pre-recruitment mechanism.

3.1. Model

The results of this work together with previous publications suggest the following model (Figure 23A): The Rcs phosphorelay monitors the lipoprotein transport through the periplasm and the β-barrel assembly in *E. coli*. Rcs signaling is activated by cell envelope stress conditions. Upon activation of the Rcs system by perturbations of the cell envelope, RcsB is phosphorylated at the conserved phosphorylation site D56 resulting in structural changes of the RcsB protein. Phosphorylated RcsB can regulate the expression of target genes by binding the promoter region as a homodimer or as a heterodimer with RcsA. However, RcsB phosphorylation is not sufficient for activation of RcsA-RcsB targets. For regulation of RcsA-RcsB targets, *rcsA* expression needs to be induced presumably by additional factors. BglJ-RcsB and MatA-RcsB regulate their target genes independent of RcsB phosphorylation and hence independent of the Rcs signaling cascade. Activation of BglJ-RcsB and MatA-RcsB targets might rather be controlled by activation of *bglJ* and *matA* expression. For DctR no certain target genes are known. For RcsB homodimers and heterodimers with RcsA, especially amino acid residues within and in close proximity to the active site play a role (Figure 23B,C). These residues are presumably important for the structural change that is elicited by phosphorylation.

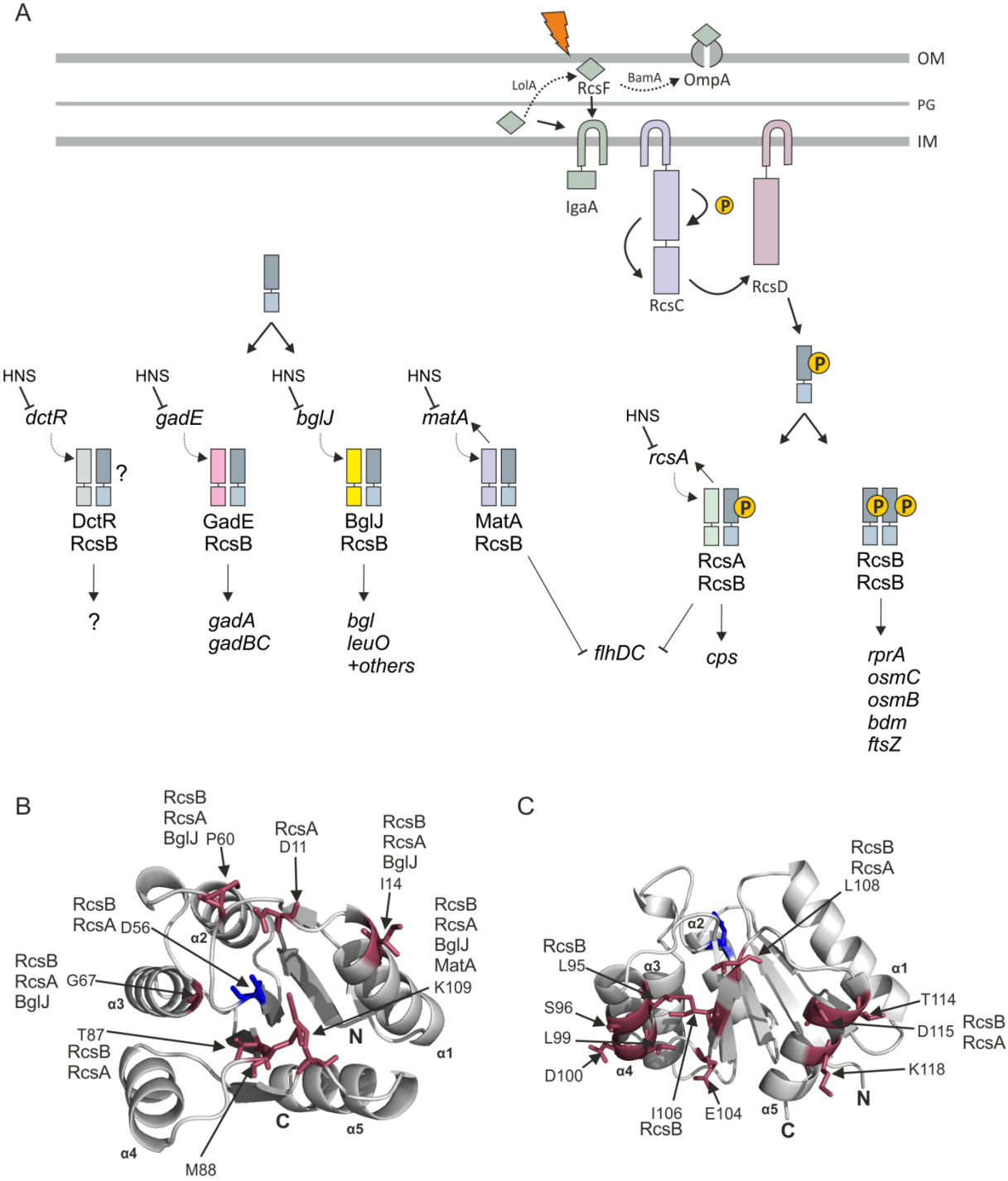

Figure 23. Model of RcsB involved in different regulatory networks.

(A) The Rcs phosphorelay monitors lipoprotein transport through the periplasm by the Lol system and β-barrel assembly by the Bam machinery. It is activated by cell envelope stress conditions. Upon induction of the Rcs system by cell envelope stress (jagged arrow), RcsB becomes phosphorylated via RcsC and RcsD. As a homodimer or heterodimer with RcsA, phosphorylated RcsB regulates its specific set of target genes. MatA-RcsB and BglJ-RcsB as well as GadE-RcsB regulate their target genes independent of RcsB phosphorylation and act uncoupled from the Rcs signaling. Genes *rcsA*, *bglJ*, *matA*, *gadE*, and *dctR* are HNS repressed. Genes *rcsA* and *matA* are autoactivated. (B) The predicted structure of the receiver domain with active site residues and (C) α4β5α5 surface exposed residues. All mutations that reduce or impair their activity of the phosphorylation-dependent partners are located in close vicinity to the active site. These residues are presumably important for the structural change that is elicited by phosphorylation.

3.2. Homo- and heterodimerization of RcsB regulates a variety of cellular functions

Heterodimerization of bacterial response regulators is rare, so that to date, the only known example beside RcsB in *Enterobacteriaceae* is BldM and WhiI in *Streptomyces* (Al-Bassam *et al.*, 2014). Notably, BldM and WhiI likewise belong to the FixJ/NarL family of transcriptional regulators. The BldM homodimer and BldM/WhiI heterodimers play key roles in the morphological differentiation. Both, BldM and WhiI are atypical and orphan response regulators which are presumably not phosphorylated by cognate sensor kinases. BldM homodimers activate transcription of group I genes required for early stages of development, while BldM/WhiI heterodimers regulate expression of group II genes involved in the late stages of development. Since no targets of a potential WhiI homodimer are known, WhiI is thought to modulate BldM binding specificity through heterodimerization (Al-Bassam *et al.*, 2014).

Similarly, RcsB is able to form homo- and heterodimers with a set of transcriptional regulators of the FixJ/NarL family of DNA-binding proteins. RcsA, BglJ, MatA, DctR, and GadE were shown to form heterodimers with RcsB. These auxiliary proteins of RcsB likewise adjust RcsB binding specificity. According to this, the DNA-binding motifs for RcsB homodimers, and heterodimers with RcsA, BglJ and MatA are similar in only one half, which may be bound by RcsB, with the interaction partner of RcsB presumably binding to the other half (Wehland & Bernhard, 2000, Sturny *et al.*, 2003, Venkatesh *et al.*, 2010, Lehti *et al.*, 2013, Salscheider *et al.*, 2013). This ability of response regulators to form functional heterodimers with auxiliary proteins allows the combination of different signals to a highly specific output and thus provides an additional level of control. These various features of RcsB might be responsible for the importance of the Rcs system in lifestyle decisions and colonization. The primary niche of *E. coli* is the gastrointestinal tract of warm blooded animals. For effective colonization of the intestine, *E. coli* cells have to successfully cross the gastric barrier and survive acidic challenges. For that reason, the inverse regulation of motility and stress responses as well as biofilm formation seems to be important for colonization. Accordingly, RcsB is essential for successful colonization of the intestinal tract of mice (Lasaro *et al.*, 2014). Together with GadE, RcsB is involved in activation of acid stress genes (Hommais *et al.*, 2004, Castanie-Cornet *et al.*, 2010). Additionally, RcsA-RcsB heterodimers repress the *flhDC* operon encoding the flagella master regulator (Soutourina & Bertin, 2003, Francez-Charlot *et al.*, 2003). In addition, MatA was shown to repress *flhDC* (Lehti *et al.*, 2012a) and

this work demonstrates that inhibition of motility by MatA requires RcsB (see chapter 2.1.4., Figure 10). In the context of acid stress, repressing flagellum synthesis is necessary to close the proton entrance during flagellum motor functioning (Soutourina *et al.*, 2002). Furthermore, flagellin can trigger the host immune response (Haiko & Westerlund-Wikstrom, 2013) and therefore a repression of flagellum synthesis could be beneficial for colonization.

3.3. RcsB regulates targets dependent and independent of phosphorylation

Transcriptional regulation triggered by RcsB homodimers and RcsA-RcsB heterodimers was reported to be phosphorylation dependent (Majdalani & Gottesman, 2005) and my data also provided evidence for a phosphorylation-dependent mechanism (see chapter 2.1.1. and 2.1.2.). The activity of BglJ-RcsB and MatA-RcsB heterodimers is independent of RcsB phosphorylation (see chapter 2.1.4. and (Venkatesh *et al.*, 2010)). The RcsB-RcsB target genes such as *rprA*, *bdm*, or *ftsAZ* play a role in the general stress response, biofilm formation, or cell division, respectively, and are accordingly involved in energy-consuming processes (Francez-Charlot *et al.*, 2005, Majdalani & Gottesman, 2005). Since gene *rcsB* is expressed under standard growth conditions, it is coherent that this set of RcsB homodimer targets is regulated in response to RcsB phosphorylation by the Rcs system (see chapter 2.2.1, Figure 5) that is induced by cell envelope stress. BglJ-RcsB and MatA-RcsB heterodimers activate transcription independent of RcsB phosphorylation (see chapter 2.2.2, Figure 6 and 2.2.4, Figure 9). The genes *rcsA*, *bglJ*, and *matA* are HNS repressed under standard conditions. The specific function of BglJ and MatA in gene regulation is uncoupled from Rcs signaling. Thus, activation of their own expression might in turn play a key role in activating their set of target genes. Regulation of *bglJ* is likely a subject of a feedback control mechanism in which the LysR-type transcription factor LeuO activates *yjjQ-bglJ* expression. On the other hand, BglJ-RcsB activates *leuO* expression (Stratmann *et al.*, 2008) and BglJ and LeuO form a small regulatory network in *E. coli* (Stratmann *et al.*, 2012). Gene *matA* is the first gene of the *mat* operon. In the lineages A and B1, such as laboratory strain MG1655 the *mat* operon is cryptic (Lehti *et al.*, 2013). In NMEC and other *E. coli* strains belonging to the lineages B2, D, and E, MatA forms a positive autoregulatory circuit (Lehti *et al.*, 2013) most likely activating expression as a MatA-RcsB heterodimer (see chapter 2.1.4.). Furthermore, the integration host factor (IHF) has been shown to be essential for counteracting HNS repression at the *mat* promoter (Martinez-Santos *et al.*, 2012), and binding sites for CRP

(cAMP-receptor protein) and Lrp (leucine-responsive protein) in the *mat* promoter region have been identified (Grainger *et al.*, 2005, Cho *et al.*, 2008, Lehti *et al.*, 2013). This indicates that additional factors are involved in *mat* regulation beside MatA-RcsB. Environmental signals inducing *mat* expression are low pH and elevated acetate concentrations mimicking the host environment, but also low temperature (Lehti *et al.*, 2013). Expression of *rcsA* is repressed by HNS and autoactivated by RcsA-RcsB. In addition, the RcsA concentration is limited by its degradation by the ATP-dependent Lon protease (Majdalani & Gottesman, 2005). In contrast to MatA-RcsB, autoactivation of *rcsA* depends on RcsB phosphorylation. Rcs signaling alone is presumably not sufficient to activate *rcsA* expression. I tested if deletion of *galU,* which was reported to induce Rcs signaling, has a positive effect on *wza* expression. In the Δ*galU* mutant strain *wza* expression was not strongly induced, supposedly due to low RcsA concentrations (see chapter 2.1.2., Figure 6). This is why also additional activators of *rcsA* expression, such as the small RNA DsrA were discussed (Sledjeski & Gottesman, 1995). Taken together, *rcsA* expression is repressed by HNS and activated by RcsA-RcsB and possibly by additional factors such as DsrA. This complex activation of *rcsA* expression ensures tight regulation being necessary since *rcsA* overexpression driven by the P_L promoter (see 2.1.2., Figure 6) or stabilizing RcsA in *lon* mutant cells (Ebel & Trempy, 1999) is sufficient to induce the mucoid phenotype by expressing capsule genes, a highly energy-consuming process.

3.4. Residues within and close to active site of RcsB play a role for phosphorylation dependent activation

This work identified particular residues of the RcsB receiver domain being relevant for transcriptional activation in the context of interaction partner. I used the crystal structure of the receiver domain of NarL to predict the structure of the receiver domain of RcsB (see chapter 2.2, Figure 13). NarL exhibits a canonical $(\beta\alpha)_5$ topology which is conserved among bacterial response regulators. According to the prediction, the active quintet residues that play a role in phosphoryl group chemistry are located central on the top of the α helices and β sheets. The active site residues are particularly important for the activity of the phosphorylation dependent RcsB-RcsB and RcsA-RcsB dimers, supporting the structure prediction. Receiver domains typically undergo phosphorylation-mediated conformational changes, at which the α4-β5-α5 face is the locus of the greatest difference between active and inactive conformation (Gao & Stock, 2010). Accordingly, the activity of BglJ-RcsB and

MatA-RcsB, those being independent of RcsB phosphorylation, are not significantly affected by exchange of amino acids comprising the α4-β5-α5 surface. Therefore the α4-β5-α5 surface is likely not the dimerization interface of RcsB although there remains a possibility that the dimerization surface varies with the interaction partner. However, the α4-β5-α5 residues being relevant for the activity of RcsB homodimers and RcsA-RcsB heterodimers are located in close proximity to the active site. Summarized, the amino acids relevant for RcsB homodimers and RcsA-RcsB heterodimers, those depending on RcsB phosphorylation are presumably important for the structural change that is triggered by phosphorylation. A similar approach, in which mutations of particular amino acids of a potential interaction surface were evaluated for transcriptional activation, was previously conducted for the DesR response regulator of *Bacillus subtilis* (Trajtenberg *et al.*, 2014). In contrast, potential interaction interfaces were identified before on the basis of crystallographic data. The receiver domain of DesR varies from the canonical $(\beta\alpha)_5$ topology of response regulators with six central β sheets surrounded by six α helices. Helices α1 and α5 including the β5α5 loop were identified as a dimerization interface bringing the phosphorylation sites of the monomers into close proximity. Interestingly, RcsB residue I14 being located in helix α1 in proximity to the active site, is inactive in all tested systems if mutated to alanine. Moreover the RcsB-I14A mutant appeared to be stable in the stability experiment (see chapter 2.3, Figure 13 and chapter 2.5, Figure 16). However, in the protein-protein interaction experiment *SPINE* RcsB mutant I14A was also found to interact with RcsB, BglJ, and RcsA, although the quantification of interaction proved to be difficult (see chapter 2.6, Figure 17). The surface equivalent to the α4β5α5 which is α4β6α6 in DesR was found to be involved in tetramerization. Analyses with mutated residues comprising both interfaces were used to study the capacity to regulate transcription showing that both surfaces are essential for transcriptional activation (Trajtenberg *et al.*, 2014). However, the findings that oligomerization of DesR brings the phosphorylation sites into close proximity correspond to our findings that the amino acids within RcsB that are important for activity are located within or in close vicinity to the active site.

3.5. The mechanism of transcriptional activation by BglJ-RcsB depends on the promoter

For repression of *flhDC*, the RcsA-RcsB heterodimer binds just downstream of the transcription start site (Francez-Charlot *et al.*, 2003). For *gadA* repression, RcsB binds the promoter region upstream of the -10 promoter element (Castanie-Cornet *et al.*, 2010). In

both cases it can be assumed that the bound transcription factors sterically prevent the RNA polymerase from binding the promoter. For transcriptional activation, the underlying mechanism most likely depends on the promoter. Recently, the BglJ-RcsB binding sites at different target promoters have been mapped (Salscheider *et al.*, 2013). Further analyses demonstrated a phasing dependent activation of the *molR* promoter and showed a BglJ-RcsB binding site in phase of the *ynbA* promoter, both located upstream of the core promoter with the RcsB subunit binding more proximal to the transcription start site (Salscheider *et al.*, 2013). This could indicate a mechanism in which BglJ-RcsB interacts with the RNA polymerase to activate the promoter. For the experiments the αCTD, αNTD, or full-length α subunit were plasmidically expressed in different reporter strains to study a potential BglJ-RcsB-αCTD interaction (see chapter 2.6.2., Figure 20). Initially it was hypothesized that in case of a mechanism in which BglJ-RcsB interacts with αCTD, the reporter expression should decrease upon αNTD expression (Figure 19B). However, P*molR* activation was still high upon αNTD overexpression, potentially due to the presence of the chromosomal *rpoA* gene and fully assembled wild-type RNA polymerase (Figure 21A). The results for P*molR*, in which the activation decreased upon αCTD expression and also upon full-length α domain expression, putatively indicate a pre-recruitment mechanism in which BglJ-RcsB binds the RNA polymerase before binding the promoter, supporting the hypothesis of a potential BglJ-RcsB-RNA polymerase interaction for activating the *molR* promoter (Figure 21B). Further analyses in which αCTD mutants were expressed that should impair a potential interaction with BglJ-RcsB, underscored this hypothesis (Figure 21C). Besides this proposed mechanism of activation by interaction with the RNA polymerase, BglJ-RcsB might activate expression by counteracting HNS, as it was suggested for activation of *yidL*, where the BglJ-RcsB binding site is in reverse orientation (Salscheider *et al.*, 2013) This counteraction could occur for example by simply competing with HNS for binding the DNA. Furthermore, a synergistic mechanism of BglJ-RcsB together with CRP has been demonstrated for *bgl* activation (Salscheider *et al.*, 2013). For *osmC*, RcsB was shown to recruit RNA polymerase to the promoter and therefore stimulate expression, potentially by a synergistic RcsB-RNA polymerase binding to the DNA (Davalos-Garcia *et al.*, 2001). However, the underlying molecular mechanism is unknown. Collectively, the mechanism of activation by BglJ-RcsB depends on the promoter and occurs by counteracting HNS repression (e.g. at P*yidL*),

presumably interaction with RNA polymerase (e.g. at P*molR*), or synergistically with CRP (e.g. at P*bgl*).

4. Materials and Methods

4.1. Material

4.1.1. Bacterial strains, plasmids and oligonucleotides

Escherichia coli strains are listed in Table 4, plasmids in Table 5 and oligonucleotides in Table 6.

Table 4. Strains

Strain	Summary	Source
CFT073	UPEC strain CFT073 (stored as KEC375)	(Welch *et al.*, 2002)
DH5α	supE44 ΔlacU159 (Φ80 lacZΔM15) hsdR17 recA1 endA1 gyrA96 thi-1 relA1, stored as S103	(Xia *et al.*, 2011)
BW30270	= MG1655 *rph*$^{+}$ (stored as S3839)	Laboratory collection
S3974	= MG1655 *rph*$^{+}$ *ilvG*$^{+}$ (not motile)	(Venkatesh *et al.*, 2010)
S4197	= S3974 Δ*lacZ*	(Venkatesh *et al.*, 2010)
T21/T22	= S4197 Δ*rcsB*$_{FRT}$	(Stratmann *et al.*, 2012)
T46	= S3839 *lac*O1-GCW	(Perfeito *et al.*, 2011)
T73	= S3974 Δ*rcsB*$_{FRT}$	(Stratmann *et al.*, 2012)
T175	= S3974 Δ*rcsB*$_{FRT}$ Δ*yjjPQ-bglJ*$_{FRT}$	(Stratmann *et al.*, 2012)
T768	= S4197 Δ(*rcsDB-rcsC*)$_{cmR}$	S4197/pKD46 x PCR T433/T329 (pKD3)
T903/T904	= S4197 Δ*rcsB*$_{FRT\ kanR}$PL-*rcsA*	x PCR T466/T467 (pKES263)
T905/T906	= S4197 Δ*rcsB*$_{FRT\ kanR}$P16-*rcsA*	x PCR T466/T468 (pKES262)
T1175/T1176	= S3974 Δ*rcsB*$_{FRT}$ Δ*hns*$_{kanR}$	T73 x T4GT7 (T208)
T1328/T1329	= BW30270 Δ*matA*$_{cmR}$	x PCR T748/T749 (pKD3)
T1330/T1331	= BW30270 Δ*dctR*$_{cmR}$	x PCR T750/T751 (pKD3)
T1338/T1339	= S3974 Δ*rcsB*$_{FRT}$ Δ*rcsA*$_{cmR}$	T73 x T4GT7 (T449)
T1341/T1342	= S3974 Δ*rcsB*$_{FRT}$ Δ*rcsA*$_{FRT}$	T1338 x pCP20
T1343/T1344	= BW30270 Δ*matA*$_{FRT}$	T1328 x pCP20
T1345/T1346	= BW30270 Δ*dctR*$_{FRT}$	T1330 x pCP20
T1561/T1562	= S3839 *rcsB*-3xFLAG$_{kanR}$	x PCR S819/T817 (pSUB11)
T1564/T1565	= S3839 *rcsB*-3xFLAG$_{FRT}$	T1561/T1562 x pCP20
T1574	= S3839 *rcsB*-3xFLAG$_{FRT}$ Δ(*yjjP-yjjQ-bglJ*)$_{cmR}$	T1564 x T4GT7 (T69)
T1599	= S3839 *rcsB*-3xFLAG$_{FRT}$ Δ*rcsA*$_{cmR}$	T1564 x T4GT7 (T449)
T1648	= S3839 *rcsB*-3xFLAG$_{FRT}$ Δ*matA*$_{cmR}$	T1564 x T4GT7 (T1328)
T1649	= S3839 *rcsB*-3xFLAG$_{FRT}$ Δ*dctR*$_{cmR}$	T1564 x T4GT7 (T1330)
T1800/T1801	= S4197 Δ*dctR*$_{cmR}$	S4197 x T4GT7 (T1330)
T1802/T1803	= S4197 Δ*rcsB*$_{FRT}$ Δ*dctR*$_{cmR}$	T21 x T4GT7 (T1330)

Strain	Summary	Source
T1819	= S3839 *rcsB*-3xFLAG$_{FRT}$ Δ(*yjjP-yjjQ-bglJ*)$_{FRT}$	T1574 x pCP20
T1832/T1833	= S4197 Δ*rcsB*$_{FRT\ kanR}$PL-*dctR*	T21 X PCR T964/T965 (pKES263)
T1839	= S4197 $_{kanR}$PL-*dctR*	PCR T964/T965 (pKES263)
T1840	= S4197 Δ*rcsB*$_{FRT\ FRT}$PL-*dctR*	T1832 x pCP20
T1841	= S4197 $_{FRT}$PL-*dctR*	T1839 x pCP20
T1819	= S3839 *rcsB*-3xFLAG$_{FRT}$ Δ(*yjjP-yjjQ-bglJ*)$_{FRT}$	T1574 x pCP20
T1832/T1833	= S4197 Δ*rcsB*$_{FRT\ kanR}$PL-*dctR*	T21/pKD46 x PCR T964/T965 (pKES263)
T1839	= S4197 $_{kanR}$PL-*dctR*	S4197/pKD46 x PCR T964/T965 (pKES263)
T1840	= S4197 Δ*rcsB*$_{FRT\ FRT}$PL-*dctR*	T1832 x pCP20
T1841	= S4197 $_{FRT}$PL-*dctR*	T1839 x pCP20
T1978	= S4197 $_{kanR}$PL-*matA*	S4197/pKD46 x PCR OA83/OA84 (pKES263)
T1985	= S4197 $_{FRT}$PL-*matA*	T1978 x pCP20
JW1224-1	Sex: F- Chromosomal Markers: Δ(araD-araB)567, ΔlacZ4787(::rrnB-3), λ-, ΔgalU745::kan, rph-1, Δ(rhaD-rhaB)568, hsdR514, stored as T2033	CGSC# 9110
T2035	= ER2507 (T679) Δ*rcsB*$_{cmR}$	T679 x T4GT7 (T1)
T2036	= ER2508 (T680) Δ*rcsB*$_{cmR}$	T680 x T4GT7 (T1)
T2041	= S4197 ΔgalU745$_{kanR}$	S4197 x P1(T2033)
T1241	= BW30270 *ilvG*$^{+}$ (motile)	BW30270 x T4GT7 (S3974)
U89	= T1241 Δ*rcsB*$_{cmR}$	T1241 x T4GT7 (T13)
U90	= T1241 Δ*rcsB*$_{cmR\ kanR}$PL-*matA*	U89 x T4GT7 (T1978)
U91	= T1241 $_{kanR}$PL-*matA*	T1241 x T4GT7 (T1978)
S1906	= S541 attB::(Spec^{R} P$_{UV5}$ *lac*O *lacZ*)	S541/pLDR8 x pKES99
S3432	CSH50 Δ*lacZ* Δ*bgl sulA*3 *lexA71*::Tn5 Δ*rcsB*$_{FRT}$ attB::(Spec^{R} *lacI*^{q} P$_{sulA}$ +/+ *lacZ*)	(Venkatesh *et al.*, 2010)
S3434	CSH50 Δ*lacZ* Δ*bgl sulA*3 *lexA71*::Tn5 Δ*rcsB*$_{FRT}$ Δ(*yjjP-yjjQ-bglJ*)$_{FRT}$ attB::(Spec^{R} *lacI*^{q} P$_{sulA}$ +/+ *lacZ*)	(Venkatesh *et al.*, 2010)
S3440	CSH50 Δ*lacZ* Δ*bgl sulA3 lexA71*::Tn5 Δ*rcsB*$_{FRT}$ attB::(Spec^{R} *lacI*^{q} P$_{sulA}$ 408/+ *lacZ*)	(Venkatesh *et al.*, 2010)
S3442	CSH50 Δ*lacZ* Δ*bgl sulA*3 *lexA71*::Tn5 Δ*rcsB*$_{FRT}$ Δ(*yjjP-yjjQ-bglJ*)$_{FRT}$ attB::(Spec^{R} *lacI*^{q} P$_{sulA}$ 408/+ *lacZ*)	(Venkatesh *et al.*, 2010)
T570	= S4197 attB::(Spec^{R} P*leuO* <u>*lacZ*</u>) *bglJ*$_{C}$	(Stratmann *et al.*, 2012)
T572	= S4197 attB::(Spec^{R} P*leuO lacZ*) Δ*rcsB*$_{FRT}$ *bglJ*$_{C}$	(Stratmann *et al.*, 2012)
T818/ T819	= S4197 Δ*rcsB*$_{FRT}$ attB::(Spec^{R} P$_{ftsA}$ *lacZ*)	T21/pLDR8 x pKES243
T864/T865	= S4197 Δ*rcsB*$_{FRT}$ attB::(Spec^{R} P$_{wza}$ *lacZ*)	S4197 x pKES260
T866/T867	= S4197 Δ*rcsB*$_{FRT}$ attB::(Spec^{R} P$_{ftsA}$ *lacZ*) Δ*rfaD::*mTn10$_{cmR}$	T818 x T4GT7 (T370)
T868/T869	= S4197 Δ*rcsB*$_{FRT}$ attB::(Spec^{R} P$_{ftsA}$ *lacZ*) Δ(*rcsDB-rcsC*)$_{cmR}$	T819 x T4GT7 (T768)
T919/T920	= S4197 Δ*rcsB*$_{FRT}$ attB::(Spec^{R} P$_{wza}$ *lacZ*) Δ*rfaD::*mTn10$_{cmR}$	T864 x T4GT7 (T370)
T921/T922	= S4197 Δ*rcsB*$_{FRT}$ attB::(Spec^{R} P$_{wza}$ *lacZ*) Δ(*rcsDB-rcsC*)$_{cmR}$	T864 x T4GT7 (T768)
T923/T924	= S4197 Δ*rcsB*$_{FRT}$ attB::(Spec^{R} P$_{wza}$ *lacZ*) $_{kanR}$PL-*rcsA*	T864 x T4GT7 (T903)
T925/T926	= S4197 Δ*rcsB*$_{FRT}$ attB::(Spec^{R} P$_{wza}$ *lacZ*) $_{kanR}$P16-*rcsA*	T864 x T4GT7 (T905)
T929/T930	= S4197 Δ*rcsB*$_{FRT}$ attB::(Spec^{R} P$_{wza}$ *lacZ*) $_{FRT}$P16-*rcsA*	T925 x pCP20
T961/T962	= S4197 Δ*rcsB*$_{FRT}$ attB::(Spec^{R} P$_{wza}$ *lacZ*) Δ(*rcsDB-rcsC*)$_{cmR\ kanR}$PL-*rcsA*	T921 x T4GT7 (T903)

Strain	Summary	Source
T963/T964	= S4197 Δ*rcsB*$_{FRT}$ attB::(Spec^{R} P$_{wza}$ *lacZ*) Δ(*rcsDB-rcsC*)$_{FRT\ FRT}$PL-*rcsA*	T961 x pCP20
T979/T980	= S4197 Δ*rcsB*$_{FRT}$ attB::(Spec^{R} P$_{wza}$ *lacZ*) $_{FRT}$P16-*rcsA* Δ(*rcsDB-rcsC*)$_{cmR}$	T929 x T4GT7 (T768)
T1052/T1053	= S4197 Δ*rcsB*$_{FRT}$ attB::(Spec^{R} P$_{rprA}$ *lacZ*)	T21/pLDR8 x pKES299
T1326	= S4197 Δ(*yjjPQ-bglJ*)$_{FRT}$ Δ*leuO*$_{FRT}$ *bglJ*$_{C}$ attB::(Spec^{R} P*ynbAB lacZ*)	(Salscheider *et al.*, 2013)
T1441	= S4197 Δ*leuO*$_{FRT}$ *bglJ*$_{C}$ (mTn10cm) attB::(Spec^{R} P$_{molR}$ *lacZ*)	(Salscheider *et al.*, 2013)
T1736	= S4197 Δ*rcsB*$_{FRT\ kanR}$PL-*rcsA* attB::(Spec^{R} P$_{rprA}$ *lacZ*)	T1052 x T4GT7 (T903)
T1743	= S4197 Δ*rcsB*$_{FRT\ FRT}$PL-*rcsA* attB::(Spec^{R} P$_{rprA}$ *lacZ*)	T1736 x pCP20
T1747/T1748	= S4197 Δ*rcsB*$_{FRT}$ attB::(Spec^{R} P$_{matA}$ *lacZ*)	T21/pLDR8 x pKEDP49
T1749/T1750	= S4197 attB::(Spec^{R} P$_{matA}$ *lacZ*)	S4197/pLDR8 x pKEDP49
T1751/T1752	= S4197 Δ*rcsB*$_{FRT}$ *bglJ*$_{C\ FRT}$PL-*rcsA* attB::(Spec^{R} P$_{rprA}$ *lacZ*)	T1743 x T4GT7 (S1734)
T1804/T1805	= S4197 Δ*rcsB*$_{FRT}$ Δ*matA*$_{cmR}$ attB::(Spec^{R} P$_{matA}$ *lacZ*)	T1564 x T4GT7 (T1328)
T1979	= S4197 $_{kanR}$PL-*matA* attB::(Spec^{R} P$_{matA}$ *lacZ*)	T1749/pKD46 x PCR OA83/OA84 (pKES263)
T1984	= S4197 Δ*rcsB*$_{FRT\ kanR}$PL-*matA* attB::(Spec^{R} P$_{matA}$ *lacZ*)	T1747 x T4GT7 (T1978)
T1986	= S4197 $_{FRT}$PL-*matA* attB::(Spec^{R} P$_{matA}$ *lacZ*)	T1979 x pCP20
T1987	= S4197 Δ*rcsB*$_{FRT\ FRT}$PL-*matA* attB::(Spec^{R} P$_{matA}$ *lacZ*)	T1984 x pCP20
T2015	= S4197 Δ*rcsB*$_{FRT\ FRT}$PL-*dctR* attB::(Spec^{R} P$_{ygeF}$ *lacZ*)	T1840/pLDR8 x pKEDP61
T2016	= S4197 $_{FRT}$PL-*dctR* attB::(Spec^{R} P$_{ygeF}$ *lacZ*)	T1841/pLDR8 x pKEDP61
T2017	= S4197 attB::(Spec^{R} P$_{ygeF}$ *lacZ*)	S4197/pLDR8 x pKEDP61
T2023	= S4197 attB::(Spec^{R} P$_{rprA}$ *lacZ*)	S4197/pLDR8 x pKES299
T2037	= S4197 attB::(Spec^{R} P$_{wza}$ *lacZ*)	S4197/pLDR8 x pKES260
T2039	= S4197 $_{kanR}$PL-*rcsA* attB::(Spec^{R} P$_{wza}$ *lacZ*)	T2037 x T4GT7 (T903)
T2042	= S4197 ΔgalU745$_{kanR}$ attB::(Spec^{R} P$_{wza}$ *lacZ*)	T2037 x P1(T2033)
T2043	= S4197 Δ*galU*$_{FRT}$ attB::(Spec^{R} P$_{rprA}$ *lacZ*)	T2041 x pCP20
T2044	= S4197 Δ*galU*$_{FRT}$ attB::(SpecR P$_{wza}$ *lacZ*)	T2042 x pCP20
T2045	= S4197 $_{kanR}$PL-*rcsA* Δ*galU*$_{FRT}$ attB::(Spec^{R} P$_{wza}$ *lacZ*)	T2044 x T4GT7 (T903)
T861	pKES260 in DH5alpha (S103)	This work
T872	pKES262 in T585	This work
T873	pKES263 in T585	This work
T1051	pKES299 in DH5alpha (S103)	This work
T1081	pKEDP01 in DH5alpha (S103)	This work
T1082	pKEDP02 in DH5alpha (S103)	This work
T1083	pKEDP03 in DH5alpha (S103)	This work
T1084	pKEDP04 in DH5alpha (S103)	This work
T1085	pKEDP05 in DH5alpha (S103)	This work
T1086	pKEDP06 in DH5alpha (S103)	This work
T1087	pKEDP07 in DH5alpha (S103)	This work
T1088	pKEDP08 in DH5alpha (S103)	This work
T1089	pKEDP09 in DH5alpha (S103)	This work
T1132	pKEDP10 in DH5alpha (S103)	This work
T1133	pKEDP11 in DH5alpha (S103)	This work
T1134	pKEDP12 in DH5alpha (S103)	This work

Strain	Summary	Source
T1135	pKEDP13 in DH5alpha (S103)	This work
T1136	pKEDP14 in DH5alpha (S103)	This work
T1137	pKEDP15 in DH5alpha (S103)	This work
T1138	pKEDP16 in DH5alpha (S103)	This work
T1139	pKEDP17 in DH5alpha (S103)	This work
T1140	pKEDP18 in DH5alpha (S103)	This work
T1141	pKEDP19 in DH5alpha (S103)	This work
T1142	pKEDP20 in DH5alpha (S103)	This work
T1143	pKEDP21 in DH5alpha (S103)	This work
T1173	pKEDP22 in DH5alpha (S103)	This work
T1174	pKEDP23 in DH5alpha (S103)	This work
T1214	pKEDP24 in DH5alpha (S103)	This work
T1215	pKEDP25 in DH5alpha (S103)	This work
T1216	pKEDP26 in DH5alpha (S103)	This work
T1217	pKEDP27 in DH5alpha (S103)	This work
T1218	pKEDP28 in DH5alpha (S103)	This work
T1219	pKEDP29 in DH5alpha (S103)	This work
T1244	pKEDP30 in DH5alpha (S103)	This work
T1245	pKEDP31 in DH5alpha (S103)	This work
T1246	pKEDP33 in DH5alpha (S103)	This work
T1247	pKEDP34 in DH5alpha (S103)	This work
T1248	pKEDP35 in DH5alpha (S103)	This work
T1259	pKEDP32 in DH5alpha (S103)	This work
T1308	pKEDP36 in DH5alpha (S103)	This work
T1356	pKEDP37 in XL1-Blue (S3984)	This work
T1406	pKEDP38 in DH5alpha (S103)	This work
T1407	pKEDP39 in DH5alpha (S103)	This work
T1656	pKEDP40 in T572	This work
T1657	pKEDP41 in T572	This work
T1658	pKEDP42 in T572	This work
T1659	pKEDP43 in T572	This work
T1660	pKEDP44 in T572	This work
T1671	pKEDP45 in T572	This work
T1672	pKEDP46 in T572	This work
T1673	pKEDP47 in T572	This work
T1680	pKEDP48 in DH5alpha (S103)	This work
T1715	pKEDP49 in DH5alpha (S103)	This work
T1735	pKEDP50 in XL1-Blue (S3984)	This work
T1799	pBAD24 in DH5alpha (S103)	This work
T1813	pKEDP51 in DH5alpha (S103)	This work
T1824	pKEDP52 in DH5alpha (S103)	This work
T1825	pKEDP53 in DH5alpha (S103)	This work
T1826	pKEDP54 in DH5alpha (S103)	This work
T1827	pKEDP55 in DH5alpha (S103)	This work
T1837	pKEDP56 in DH5alpha (S103)	This work
T1848	pKEDP57 in DH5alpha (S103)	This work
T1939	pKEDP58 in DH5alpha (S103)	This work
T1940	pKEDP59 in DH5alpha (S103)	This work
T1941	pKEDP56 in DH5alpha (S103)	This work
T1983	pKEDP61 in DH5alpha (S103)	This work

Table 5. Plasmids

Plasmid	Relevant structure	Source
pCP20	cI_{857} λ-P_R *flp* in pSC101 rep^{ts} *bla*	(Datsenko & Wanner, 2000)
pKD46	*araC* P_{ara} γ-β-exo in pSC101-ori rep^{ts} *bla*	(Datsenko & Wanner, 2000)
pLDR8	cI_{857} P_R λ-int in pSC101-ori rep^{ts} *neo*	(Diederich *et al.*, 1992)
pKD13	KanR flanked by FRT sites, AmpR, R6K gamma repl. origin	(Datsenko & Wanner, 2000)
pKES262	P16 promoter in pKD13, R6K gamma repl. origin, KanR AmpR	annealed oligos T462/T463 cloned in pKD13
pKES263	P-L promoter in pKD13, R6K gamma repl. origin, KanR AmpR	cloned PCR fragment T464/T465 in pKD13
pKES243	P_{ftsA} *lacZ* p15A KanR SpecR attP	Laboratory collection
pKEDP49	P_{matA}(-608 to +12) *lacZ* p15A KanR SpecR attP	cloned PCR fragment T908/T909 of CFT073 in pKES268
pKES260	P_{wza} *lacZ* p15A p15A KanR SpecR attP	cloned PCR fragment T460/T461 in pKES243
pKEDP61	P_{ygeF} (-193 to +12 rel. to start codon) *lacZ* p15A KanR SpecR attP	cloned PCR fragment OA89/90 of S3839 in pKES268
pKEDP52	P_{arrS} (-311 to +10) *lacZ* p15A KanR SpecR attP	cloned PCR fragment T954/955 in pKES268
pKEDP53	P_{dpiBA}(-378 to +25) *lacZ* p15A KanR SpecR attP	cloned PCR fragment T958/959 in pKES268
pKEDP54	P_{acrEF} (-410 to +5) *lacZ* p15A KanR SpecR attP	cloned PCR fragment T956/957 in pKES268
pKEDP55	P_{caiT} (-471 to +11) *lacZ* p15A KanR SpecR attP	cloned PCR fragment T960/961 in pKES268
pKEDP56	P_{dcuC} (-588 to +9) *lacZ* p15A KanR SpecR attP	cloned PCR fragment T962/963 in pKES268
pKEDP22	$lacI^q$ P_{tac} 3xFLAG *neo* ori-p15A	annealed oligos T687/T688 cloned in pKESK22
pKEDP23	$lacI^q$ P_{tac} 3xHA *neo* ori-p15A	annealed oligos T689/T690 cloned in pKESK22
pDP804	P_{lacUV5} lexA-$408_{1\text{-}87}$-*jun* p15A *bla*	(Dmitrova *et al.*, 1998)
pMS604	P_{lacUV5} $lexA_{WT}$-*fos* pMB1 *tet*	(Dmitrova *et al.*, 1998)
pKES189	P_{lacUV5} *lexA*-$408_{1\text{-}87}$-*jun* in P15A *bla*	Laboratory collection
pKEDP58	P_{lacUV5} *lexA*-$408_{1\text{-}87}$-*dctR* in P15A *bla*	cloned PCR fragment OA29/30 of pKEDP31 in pKES189
pKEDP59	P_{lacUV5} *lexA*-$408_{1\text{-}87}$-*matA* in P15A *bla*	cloned PCR fragment OA27/28 of pKEDP30 in pKES189
pKEDP60	P_{lacUV5} *lexA*-$408_{1\text{-}87}$-*rcsA* in P15A *bla*	cloned PCR fragment OA25/26 of pKES192 in pKES189
pKESK22	$lacI^q$ P_{tac} MCS in p15A-ori *neo*	(Venkatesh et al., 2010)
pKETS6	$lacI^q$ P_{tac} *rcsB* in ori-p15A *neo*	(Venkatesh et al., 2010)
pKETS7	$lacI^q$ P_{tac} *rcsB*-D56E in ori-p15A *neo* (GAT→GAG)	(Venkatesh et al., 2010)
pKETS8	$lacI^q$ P_{tac} *rcsB*-D56N in ori-p15A *neo* (GAT→AAT)	(Venkatesh et al., 2010)
pKES229	$lacI^q$ P_{tac} *rcsB*-D66A in ori-p15A *neo* (GAT→GCG)	Laboratory collection
pKES230	$lacI^q$ P_{tac} *rcsB*-H77A in ori-p15A *neo* (CAT→GCG)	Laboratory collection
pKES231	$lacI^q$ P_{tac} *rcsB*-I14A in ori-p15A *neo* (ATA→GCA)	Laboratory collection

Plasmid	Relevant structure	Source
pKES232	*lacI*^{q} P_{tac} *rcsB*-M88A in ori-p15A *neo* (ATG→GCG)	Laboratory collection
pKES233	*lacI*^{q} P_{tac} *rcsB*-R76A in ori-p15A *neo* (CGC→GCC)	Laboratory collection
pKES234	*lacI*^{q} P_{tac} *rcsB*-Y64A in ori-p15A *neo* (TAC→GCC)	Laboratory collection
pKES235	*lacI*^{q} P_{tac} *rcsB*-D56A in ori-p15A *neo* (GAT→GCG)	(Venkatesh et al., 2010)
pKES271	*lacI*^{q} P_{tac} *rcsB*-D11A in ori-p15A *neo* (GAC→GCC)	Laboratory collection
pKES272	*lacI*^{q} P_{tac} *rcsB*- P60A in ori-p15A *neo* (CCT→GCT)	Laboratory collection
pKES273	*lacI*^{q} P_{tac} *rcsB*- G67A in ori-p15A *neo* (GGC→GCC)	Laboratory collection
pKES274	*lacI*^{q} P_{tac} *rcsB*- T87A in ori-p15A *neo* (ACT→GCT)	Laboratory collection
pKES275	*lacI*^{q} P_{tac} *rcsB*- K109A in ori-p15A *neo* (AAA→GCA)	Laboratory collection
pKES276	*lacI*^{q} P_{tac} *rcsB*- K180A in ori-p15A *neo* (AAA→GCA)	Laboratory collection
pKES277	*lacI*^{q} P_{tac} *rcsB*- S184A in ori-p15A *neo* (AGC→GCC)	Laboratory collection
pKES278	*lacI*^{q} P_{tac} *rcsB*-I199A in ori-p15A *neo* (ATC→GCC)	Laboratory collection
pKES279	*lacI*^{q} P_{tac} *rcsB*- N203A in ori-p15A *neo* (AAT→GCT)	Laboratory collection
pKESL111	*lacI*^{q} P_{tac} *rcsB*-L95A in ori-p15A *neo* (CTT→GCT)	Laboratory collection
pKESL112	*lacI*^{q} P_{tac} *rcsB*-L99A in ori-p15A *neo* (TTG→GCG)	Laboratory collection
pKESL113	*lacI*^{q} P_{tac} *rcsB*-D100A in ori-p15A *neo* (GAT→GCT)	Laboratory collection
pKESL114	*lacI*^{q} P_{tac} *rcsB*-E104A in ori-p15A *neo* (GAA→GCA)	Laboratory collection
pKESL115	*lacI*^{q} P_{tac} *rcsB*-I106A in ori-p15A *neo* (ATC→GCC)	Laboratory collection
pKESL116	*lacI*^{q} P_{tac} *rcsB*-L108A in ori-p15A *neo* (CTG→GCG)	Laboratory collection
pKESL117	*lacI*^{q} P_{tac} *rcsB*-T114A in ori-p15A *neo* (ACC→GCC)	Laboratory collection
pKESL118	*lacI*^{q} P_{tac} *rcsB*-K118A in ori-p15A *neo* (AAA→GCA)	Laboratory collection
pKESL119	*lacI*^{q} P_{tac} *rcsB*-S96A in ori-p15A *neo* (AGT→GCT)	Laboratory collection
pKESL120	*lacI*^{q} P_{tac} *rcsB*-D115A in ori-p15A *neo* (GAT→GCT)	Laboratory collection
pKEDP40	*lacI*^{q} P_{tac} *rcsB*-F162C ori-p15A *neo* (TTT→TGT)	cloned error-prone PCR fragment T358/T106 in pKESK22
pKEDP41	*lacI*^{q} P_{tac} *rcsB*-S58P ori-p15A *neo* (TCC→CCC)	cloned error-prone PCR fragment T358/T106 in pKESK22
pKEDP42	*lacI*^{q} P_{tac} *rcsB*-F162S ori-p15A *neo* (TTT→TCT)	cloned error-prone PCR fragment T358/T106 in pKESK22
pKEDP43	*lacI*^{q} P_{tac} *rcsB*-V98A ori-p15A *neo* (GTA→GCA)	cloned error-prone PCR fragment T358/T106 in pKESK22
pKEDP44	*lacI*^{q} P_{tac} *rcsB*-L41P ori-p15A *neo* (CTG→CCG)	cloned error-prone PCR fragment T358/T106 in pKESK22
pKEDP45	*lacI*^{q} P_{tac} *rcsB*-D11G ori-p15A *neo* (GAC→GGC)	cloned error-prone PCR fragment T358/T106 in pKESK22
pKEDP46	*lacI*^{q} P_{tac} *rcsB*-D66N ori-p15A *neo* (GAT→AAT)	cloned error-prone PCR fragment T358/T106 in pKESK22
pKEDP47	*lacI*^{q} P_{tac} *rcsB*-D62G ori-p15A *neo* (GAT→GGT)	cloned error-prone PCR fragment T358/T106 in pKESK22
pKEAP22	pFDY127 derivate with MCS	Laboratory collection
pKEAP38	*lacI*^{q} P_{tac} rcsB-HA *bla* pBR-ori	Laboratory collection
pKEDP01	*lacI*^{q} P_{tac} rcsB-D56A-HA *bla* pBR-ori	BglII, XhoI fragment of pKES244 cloned in pKEAP22
pKEDP02	*lacI*^{q} P_{tac} *rcsB*-H77A-HA *bla* pBR-ori	BglII, XhoI fragment of pKES245 cloned in pKEAP22
pKEDP03	*lacI*^{q} P_{tac} *rcsB*- I14A-HA *bla* pBR-ori	BglII, XhoI fragment of pKES246 cloned in pKEAP22

Plasmid	Relevant structure	Source
pKEDP04	*lacI*^{q} P_{tac} *rcsB*- R76A-HA *bla* pBR-ori	BglII, XhoI fragment of pKES248 cloned in pKEAP22
pKEDP05	*lacI*^{q} P_{tac} *rcsB*-Y64A-HA *bla* pBR-ori	BglII, XhoI fragment of pKES249 cloned in pKEAP22
pKEDP06	*lacI*^{q} P_{tac} *rcsB*-G67A-HA *bla* pBR-ori	BglII, XhoI fragment of pKES273 cloned in pKEAP22
pKEDP07	*lacI*^{q} P_{tac} *rcsB*-K109A-HA *bla* pBR-ori	BglII, XhoI fragment of pKES275 cloned in pKEAP22
pKEDP08	*lacI*^{q} P_{tac} *rcsB*-K180A-HA *bla* pBR-ori	BglII, XhoI fragment of pKES276 cloned in pKEAP22
pKEDP09	*lacI*^{q} P_{tac} *rcsB*-I199A-HA *bla* pBR-ori	BglII, XhoI fragment of pKES278 cloned in pKEAP22
pKEDP10	*lacI*^{q} P_{tac} *rcsB*-Strep in ori-p15A *neo*	cloned PCR fragment T358/T639 of pKETS06 in pKESK22
pKEDP11	*lacI*^{q} P_{tac} *rcsB*-I14A-Strep in ori-p15A *neo*	cloned PCR fragment T358/T639 of pKES231 in pKESK22
pKEDP12	*lacI*^{q} P_{tac} *rcsB*-D56A-Strep in ori-p15A *neo*	cloned PCR fragment T358/T639 of pKES235 in pKESK22
pKEDP13	*lacI*^{q} P_{tac} *rcsB*-D56E-Strep in ori-p15A *neo*	cloned PCR fragment T358/T639 of pKETS7 in pKESK22
pKEDP14	*lacI*^{q} P_{tac} *rcsB*-D56N-Strep in ori-p15A *neo*	cloned PCR fragment T358/T639 of pKETS8 in pKESK22
pKEDP15	*lacI*^{q} P_{tac} *rcsB*-Y64A-Strep in ori-p15A *neo*	cloned PCR fragment T358/T639 of pKES234 in pKESK22
pKEDP16	*lacI*^{q} P_{tac} *rcsB*-G67A-Strep in ori-p15A *neo*	cloned PCR fragment T358/T639 of pKES273 in pKESK22
pKEDP17	*lacI*^{q} P_{tac} *rcsB*-R76A-Strep in ori-p15A *neo*	cloned PCR fragment T358/T639 of pKES233 in pKESK22
pKEDP18	*lacI*^{q} P_{tac} *rcsB*-H77A-Strep in ori-p15A *neo*	cloned PCR fragment T358/T639 of pKES230 in pKESK22
pKEDP19	*lacI*^{q} P_{tac} *rcsB*-K109A-Strep in ori-p15A *neo*	cloned PCR fragment T358/T639 of pKES275 in pKESK22
pKEDP20	*lacI*^{q} P_{tac} *rcsB*-K180A-Strep in ori-p15A *neo*	cloned PCR fragment T358/T639 of pKES276 in pKESK22
pKEDP21	*lacI*^{q} P_{tac} *rcsB*-I199A-Strep in ori-p15A *neo*	cloned PCR fragment T358/T639 of pKES278 in pKESK22
pKEDP24	*lacI*^{q} P_{tac} *rcsB*- D11A-HA *bla* pBR-ori	cloned PCR fragment S682/S683 of pKES271 in pKEAP22
pKEDP25	*lacI*^{q} P_{tac} *rcsB*-P60A-HA *bla* pBR-ori	cloned PCR fragment S682/S683 of pKES272 in pKEAP22
pKEDP26	*lacI*^{q} P_{tac} *rcsB*-P66A-HA *bla* pBR-ori	cloned PCR fragment S682/S683 of pKES229 in

Plasmid	Relevant structure	Source
		pKEAP22
pKEDP27	*lacI*^{q} P_{tac} *rcsB*-D11A-Strep *neo* ori-p15A	cloned PCR fragment T358/T639 of pKES271 in pKESK22
pKEDP28	*lacI*^{q} P_{tac} *rcsB*-P60A-Strep *neo* ori-p15A	cloned PCR fragment T358/T639 of pKES272 in pKESK22
pKEDP29	*lacI*^{q} P_{tac} *rcsB*-D66A-Strep *neo* ori-p15A	cloned PCR fragment T358/T639 of pKES229 in pKESK22
pKEDP36	*lacI*^{q} P_{tac} *rcsA-HA bla* pBR-ori	cloned PCR fragment T721/T722 in pKEAP22
pKEDP37	*lacI*^{q} P_{tac} *bglJ-Strep bla* pBR-ori	cloned PCR fragment T757/T759 of pKETS1 in pKEAP22
pKERV12	*lacI*^{q} $P_{tac\ \varepsilon SD}$*bglJ-HA in* pKK *bla*	Laboratory collection
pKEHB17	*araC* P_{BAD} *bglJ*-3xHA amp P15A ori	Laboratory collection
pKEHB21	*lacI*^{q} P_{tac} *bglJ*-3xHA cm pSC ori	Laboratory collection
pKEDP30	*lacI*^{q} P_{tac} *matA neo* ori-p15A	cloned PCR fragment T691/T692 in pKESK22
pKEDP51	*araC* P_{BAD} *matA* ampR M13 ori pBR322 ori	cloned PCR fragment T691/T692 in pBAD24
pKEDP32	*lacI*^{q} P_{tac} *matA*-3xFLAG *neo* ori-p15A	cloned PCR fragment T691/T693 in pKEDP22
pKEDP33	*lacI*^{q} P_{tac} *matA*-3xHA *neo* ori-p15A	cloned PCR fragment T691/T693 in pKEDP23
pKEDP57	*araC* P_{BAD} *dctR* M13 pBR	cloned PCR fragment T694/695 of pKEDP31 in pBAD24
pKEDP31	*lacI*^{q} P_{tac} *dctR neo* ori-p15A	cloned PCR fragment T694/T695 in pKESK22
pKEDP34	*lacI*^{q} P_{tac} *dctR*-3xFLAG *neo* ori-p15A	cloned PCR fragment T694/T696 in pKEDP22
pKEDP35	*lacI*^{q} P_{tac} *dctR*-3xHA *neo* ori-p15A	cloned PCR fragment T694/T696 in pKEDP23
pAC λcI-β 831-1057	P_{lacUV5}, p15A-ori, cat, cloning vector for cI-α two-hybrid	(Dove & Hochschild, 2004)
pBR α-σ70 D581G	P_{lacUV5}, pBR-ori, bla, positive control for cI-α two-hybrid	(Dove & Hochschild, 2004)
pAC λcI	P_{lacUV5}, p15A-ori, cat, negative control for cI-α two-hybrid	(Dove & Hochschild, 2004)
pBR α (NTD)	P_{lacUV5}, pBR-ori, bla, negative control for cI-α two-hybrid	(Dove & Hochschild, 2004)
pKEDP38	P_{lacUV} cI-beta-*rcsB(131-216)*-fusion for two hybrid system, CmR ori P15A	cloned PCR fragment T762/T106 in pKEAP22 in pAC cI-beta831-1057
pKEDP39	P_{lacUV} cI-beta-*rcsB(142-216)*-fusion for two hybrid system, CmR ori P15A	cloned PCR fragment T763/T106 in pKEAP22 in pAC cI-beta831-1057
pKEDP50	P_{lacUV} cI-beta-*rpoA* (705-990)-fusion for two hybrid system, CmR ori P15A	cloned PCR fragment T923/T924 of pLEX185 in pAC cI-beta831-1057
pKEKD23	P_{lacUV} cI-beta-*rcsB*-fusion for two hybrid system, *cat* ori P15A	Laboratory collection
pKEKD24	P_{lacUV} αNTD-*rcsB*-fusion for two hybrid system, *bla* ori pBR	Laboratory collection
pLAX185	$P_{lpp\text{-}lac}$ *rpoA lacI* pBR ori *bla*	(Hayward *et al.*, 1991)
pLAD235	$P_{lpp\text{-}lac}$ *rpoA*(1-705 bp) *lacI* pBR ori *bla*	(Hayward *et al.*, 1991)

Plasmid	Relevant structure	Source
pREIIα	AmpR; ori-pBR322; IppP-'lacPUV5-rpoA	(Blatter *et al.*, 1994)
pHTf1α	AmpR; ori-pBR322; ori-fl; IppP-'lacPUV5-rpoA	(Tang *et al.*, 1994)
pKEDP48	$P_{lpp\text{-}lac}$ *rpoA* (705-990) *lacI* ori-pBR bla	cloned PCR fragment T894/T895 of pLAX185 in pLAX185
pKEDP62	$P_{lpp\text{-}lac}$ *rpoA*(705-990)-T285A *lacI* ori-pBR *bla*	PCR 1&2: T894/OA125 of pKEDP48 and OA124/OA140 in pLAX185
pKEDP63	$P_{lpp\text{-}lac}$ *rpoA*(705-990)-E286A *lacI* ori-pBR *bla*	PCR 1&2: T894/OA127 of pKEDP48 and OA126/OA140 in pLAX185
pKEDP64	$P_{lpp\text{-}lac}$ *rpoA*(705-990)-V287A *lacI* ori-pBR *bla*	PCR 1&2: T894/OA129 of pKEDP48 and OA128/OA140 in pLAX185
pKEDP65	$P_{lpp\text{-}lac}$ *rpoA*(705-990)-E288A *lacI* ori-pBR *bla*	PCR 1&2: T894/OA131 of pKEDP48 and OA130/OA140 in pLAX185
pKEDP66	$P_{lpp\text{-}lac}$ *rpoA*(705-990)-L290A *lacI* ori-pBR *bla*	PCR 1&2: T894/OA133 pKEDP48 and OA132/OA140 in pLAX185
pKEDP67	$P_{lpp\text{-}lac}$ *rpoA*(705-990)-G315A *lacI* ori-pBR *bla*	PCR 1&2: T894/OA135 of pKEDP48 and OA134/OA140 in pLAX185
pKEDP68	$P_{lpp\text{-}lac}$ *rpoA*(705-990)-R317A *lacI* ori-pBR *bla*	PCR 1&2: T894/OA137 of pKEDP48 and OA136/OA140 in pLAX185
pKEDP69	$P_{lpp\text{-}lac}$ *rpoA*(705-990)-L318A *lacI* ori-pBR *bla*	PCR 1&2: T894/OA139 of pKEDP48 and OA138/OA140 in pLAX185

Table 6. Oligonucleotides

Oligo	Sequence[a] (5' → 3')	Target/purpose
S93	CCGGGCCGACAACAAAGTCA	λ-*attB* region
S95	CATATGGGGATTGGTGGCGA	λ-*attP* plasmids
S96	CACTCTGCCAGATGGCGCAA	λ-*attB* region
S116	TGGCACGACAGGTTTCCCGA	pUC12
S118	TGCGGGCCTCTTCGCTATTA	*lacZ*
S123	TGTGGAATTGTGAGCGGATA	*tac* promoter
S150	CGACGGGATCAGTACCGACGG	pACYC plasmid
S164	GAGCAGGGGAATTGATCCGGTGGA	λ-*attB* region
S656	ATGTCAAGAGCTTGCTGTAGCAAGG	*rcsB*
S657	GACACTAACGCGTCTTATCTGGCC	*rcsB*
S682	CGAATTCAGATCTTTGCTGTAGCAAGGTAGCCTATTACAT	Cloning of *rcsB*-HA EcoRI, BglII in pKEAP22
S683	AGCTCGAGCTAGCTTAAGCGTAATCTGGAACATCGTATGGGTA GTCTTTATCTGCCGGACTTAAGGTC	Cloning of *rcsB*-HA XhoI, NheI in pKEAP22
S820	TGCCAGATAAGACACTAACGCGTCTTATCTGGCCTACAGGTGA TTACATATGAATATCCTCCTTAGTTCCTATTCC	Construction of *rcsB*-3xFLAG using pSUB11
T106	CAGGGATCCTCTAGATTAGTCTTTATCTGCCGGACTTAAGGTC AC	cI-*rcsB*-HTH fusion BamHI, XbaI cloning pKEDP38
T311	AAGGGATTCGGATGTGATGGTATG	*rfaD*
T312	ATGAGGAATACCCGCGAAGAAAG	*rfaD*
T327	ACTCTGACTGTCGGCATCTCTTTAATG	*rcsA*
T328	CGCTCGGCATCTGGTTCTTTAATG	*rcsA*
T331	GTGATGATTTCTCGGCGGTGTATC	*rcsBCD*
T334	ACGACGTTGTAAAACGACGGCAACACGAATGCGGAACGGTT	λ-*attP* plasmids, P-wza region in pKES260
T358	GACCGAATTCTTGCTGTAGCAAGGTAGCCTATTACATG	Cloning of *rcsB*-Strep in pACYC EcoRI
T369	CTTTGTAACGGAGTAGAGACGAAAGTG	P_L and P_{16} in pKES262 and pKES263
T430	TGTCCTACTCAGGAGAGCGTTCAC	*rcsB*-HA pMALc5
T434	ATGCAGGATGATAAATATCACGGGAG	*rcsBCD*
T460	AGCAGTCGACCTCACATTATCCCTGAATTAAAAGTGG	P_{wza} *lacZ,* SalI Cloning pKES260
T461	AGCGTCTAGATTACATCATTGTTTATTTATCACTTTGGCAG	P_{wza} *lacZ,* XbaI Cloning pKES260
T462	P-TCGACTCACCCTTTGACGTGGTGATATGGATGACGGATAAT CCCGCCTGAAGGGAAAG	P_{16} SalI (overhang) Cloning pKES262
T463	P-GATCCTTTCCCTTCAGGCGGGATTATCCGTCATCCATATCA CCACGTCAAAGGGTGAG	P_{16} BamHI (overhang) Cloning pKES262
T464	AGCAGTCGACCTCTCACCTACCAAACAATGCCC	P_L SalI Cloning pKES263
T465	AGCAGGATCCTCATGGTGGTCAGTGCGTCC	P_L BamHI Cloning pKES263
T466	AATACCTACGAACATCTTCCAGGATACTCCTGCAGCGAAATAT TGTGTAGGCTGGAGCTGCTTCG	Replacement of P_{rcsA} by P_L and P_{16}
T467	CATACCCTCACTCAATGCGTAACGATAATTCCCCTTACCTGAA TCATGGTGGTCAGTGCGTCC	Replacement of P_{rcsA} by P_L
T468	CATACCCTCACTCAATGCGTAACGATAATTCCCCTTACCTGAA TTTCCCTTCAGGCGGGATTAT	Replacement of P_{rcsA} by P_{16}
T471	CTTGCGGCAGCGTGAGC	pKD13
T563	AGCAGTCGACAATTGATATTTGCTTGCTCTTCCCC	P_{rprA} *lacZ* SalI Cloning pKES299
T564	AGCGTCTAGACCGTGAGCTAATAGTAGGCATACGG	P_{rprA} *lacZ* XbaI Cloning pKES299
T639	AGCATCTAGATTATTTTTCGAACTGCGGGTGGCTCCAGTCTTT ATCTGCCGGACTTAAGGTCA	Cloning of *rcsB*-Strep tag in pACYC XbaI
T687	P-CTAGAGACTACAAAGACCATGACGGTGATTATAAAGATCA TGATATCGACTACAAAGATGACGACGATAAATAAG	3xFLAG XbaI (overhang) Cloning pKEDP22
T688	P-GATCCTTATTTATCGTCGTCATCTTTGTAGTCGATATCAT GATCTTTATAATCACCGTCATGGTCTTTGTAGTCT	3xFLAG BamHI (overhang) Cloning pKEDP22

Oligo	Sequence[a] (5′ → 3′)	Target/purpose
T689	P-CTAGATACCCATACGATGTTCCTGACTATGCGGGCTATCCCTATGACGTCCCGGACTATGCAGGATCCTATCCATATGACGTTCCAGATTACGCTTAA	3xHA XbaI (overhang) Cloning pKEDP23
T690	P-GATCTTAAGCGTAATCTGGAACGTCATATGGATAGGATCCTGCATAGTCCGGGACGTCATAGGGATAGCCCGCATAGTCAGGAACATCGTATGGGTAT	3xHA BamHI (overhang) Cloning pKEDP23
T691	AGCAGAATTCAATTACAGGTTTGGAAAGTAGTGACATG	*matA* EcoRI Cloning pKEDP30
T692	AGCGTCTAGATTACTGAACCAACTTATATATTTTTGAGTACAGC	*matA* XbaI Cloning pKEDP30
T693	AGCGTCTAGACTGAACCAACTTATATATTTTTGAGTACAGCTT	*matA* XbaI (without Stop) Cloning pKEDP32
T694	AGCAGAATTCGTCCGCACCAGGAGTCGG	*dctR* EcoRI Cloning pKEDP31
T695	AGCGTCTAGATCACACCAGATAATCAATATGCTGATG	*dctR* XbaI Cloning pKEDP31
T696	AGCGTCTAGACACCAGATAATCAATATGCTGATGGC	*dctR* XbaI (without Stop) Cloning pKEDP34
T721	AGCAAGATCTGTTACGCATTGAGTGAGGGTATGC	*rcsA*-HA with native SD BglII Cloning pKEDP36
T722	AGCGCTCGAGTTAAGCGTAATCTGGAACATCGTATGGGTAGCGCATGTTGACAAAAATACCAT	*rcsA*-HA with native SD XhoI Cloning pKEDP36
T748	TAAGGAAACTGAATGCACCTGTAAAAATTACAGGTTTGGAAAGTAGTGTAGGCTGGAGCTGCTTCG	Construction of Δ*matA*
T749	CCAGTGAGTCATTTTTTAAAACTAACTTGCCTGGAGTTTACATATGAATATCCTCCTTAGTTCCTATTCC	Construction of Δ*matA*
T750	TTGGCAAACTGATTATAAAGTTAATGTCCGCACCAGGAGTCGGTTGTGTAGGCTGGAGCTGCTTCG	Construction of Δ*dctR*
T751	TGTGGCAGCGTAGCCAGACTCACCGTAAGCCTGAAATTCACATATGAATATCCTCCTTAGTTCCTATTCC	Construction of Δ*dctR*
T753	CACCGTTACCAGAGCTATTGCC	*matA*
T754	CCTTTTCCGTTCACATATTGACACTC	*matA*
T755	CTGAGCTGGTCAAATAACACCACC	*dctR*
T756	GGCAGGGGTGAAAGGCG	*dctR*
T762	AGCAGCGGCCGCAGAAAGCGTTTCTCGCCTGTTG	cI-*rcsB*-HTH NotI Cloning pKEDP38
T763	AGCAGCGGCCGCAGCTGGTGGTTACGGTGACAAG	cI-*rcsB*-HTH NotI Cloning pKEDP38
T817	GCTGAATTATCTCTCTTCAGTGACCTTAAGTCCGGCAGATAAAGACGACTACAAAGACCATGACGGTGATTATA	Construction of rcsB-3xFLAG
T894	AGCGTCTAGAGAGCTTACTACCCAAAGAGAGGACACAATGGATGTACGTCAGCCTGAAGTGAAAG	αCTD (amino acids 236-329) XbaI Cloning pKEDP48
T895	AGCAGGATCCTTACTCGTCAGCGATGCTTGC	αCTD (amino acids 236-329) BamHI Cloning pKEDP48
T908	AGCAGTCGACGCCATCGTTCCTGTGACAACTG	P_{matA} (from UPEC strain CFT073) *lacZ SalI* Cloning pKEDP49
T909	AGCGTCTAGATTGCCATGTCACTACTTTCCAAACC	P_{matA} (from UPEC strain CFT073) *lacZ XbaI* Cloning pKEDP49
T923	AGCAGCGGCCGCAGATGTACGTCAGCCTGAAGTGAAAG	cI-αCTD NotI Cloning pKEDP50
T924	AGCGGGATCCTTACTCGTCAGCGATGCTTGC	cI-αCTD BamHI Cloning pKEDP50
T954	AGCAGTCGACAACTTGCTCCTTAGCCGTTATCG	P_{arrS} *lacZ* SalI Cloning pKEDP52
T955	AGCGTCTAGAATCGGATTACATTTTAACTTTAGTAATATTCTTC	P_{arrS} *lacZ* XbaI Cloning pKEDP52
T956	AGCAGTCGACTCTTTTTGCCATGATTAATTATTCAGG	P_{acrEF} *lacZ* SalI Cloning pKEDP54
T957	AGCGTCTAGAGTCATTACTATTCCTCAAAAAACCAAAAG	P_{acrEF} *lacZ* XbaI Cloning pKEDP54
T958	AGCAGTCGACAATAAATAGTATCCTGAAGGTGCATGTTG	P_{dpiBA} *lacZ* SalI Cloning pKEDP53
T959	AGCGTCTAGAGTTTATTCTCGTTAAGCTGCAACATTG	P_{dpiBA} *lacZ* XbaI Cloning pKEDP53
T960	AGCAGTCGACTGCATCTCCAGAAATCATGAAGG	P_{caiT} *lacZ* SalI Cloning pKEDP55
T961	AGCGTCTAGATCATTCTTCATGAGTTAATTCCACTGTG	P_{caiT} *lacZ* XbaI Cloning pKEDP55

Oligo	Sequence[a] (5′ → 3′)	Target/purpose
T962	AGCAGTCGACTTGTGACCATAAAACATTTATCAAAAATCTACTAC	P_{dcuC} *lacZ* SalI Cloning pKEDP56
T963	AGCGTCTAGATGTCAGCATAATTTTTCCTGTCTCC	P_{dcuC} *lacZ* XbaI Cloning pKEDP56
T964	CACCTGAGCTGGTCAAATAACACCACCGAAAGATGCAGATGCGTGTAGGCTGGAGCTGCTTCG	Replacement of P_{dctR} by P_L
T965	ATCCCTGGTAATTATAAGAAACATAACCGACTCCTGGTGCGGTCATGGTGGTCAGTGCGTCC	Replacement of P_{dctR} by P_L
OA10	ATCTGGTGAATGAAGGAACGCTC	*yjbM* qPCR
OA11	ATTGTGGTGCAGCATCTCGC	*yjbM* qPCR
OA12	CTACCACTGCAACCATTAGTTCCTG	*ygeF* qPCR
OA13	ATGTGTTAGATATTTTCCTCCAAGAGATTC	*ygeF* qPCR
OA14	GAATGGGCAAATCAACTAAAACACG	*ygeG* qPCR
OA15	TACCCTTTTCATGGTAGTCGAATGC	*ygeG* qPCR
OA16	TTGTCATTATGGGAGCTGGAGAAC	*ypjC* qPCR
OA17	CAGGCTCACCAGAACTAACTAACTCG	*ypjC* qPCR
OA18	TCAAAGCGAGTGGTGAATGTGTC	*yjbI* qPCR
OA19	GGTGAAGTGCGAAGCGTAAAGA	*yjbI* qPCR
OA20	GCTGTTCCTGATTTCGTTACTTGG	*ycdU* qPCR
OA21	TGCTTGACATAACTGGTGCGG	*ycdU* qPCR
OA25	AGCACTCGAGTCAACGATTATTATGGATTTATGTAGTTACAC	$LexA_{408}$-*rcsA* XhoI Cloning pKEDP60
OA26	AGCGAGATCTTTAGCGCATGTTGACAAAAATACC	$LexA_{408}$-*rcsA* BglII Cloning pKEDP60
OA27	AGCACTCGAGACATGGCAAAGTGATTACAGTAGGGAC	$LexA_{408}$-*matA* XhoI Cloning pKEDP59
OA28	AGCGAGATCTTTACTGAACCAACTTATATATTTTTGAGTACAGCTT	$LexA_{408}$- *matA* BglII Cloning pKEDP59
OA29	AGCACTCGAGTTTCTTATAATTACCAGGGATACGATGTTC	$LexA_{408}$-*dctR* XhoI Cloning pKEDP58
OA30	AGCGAGATCTTCACACCAGATAATCAATATGCTGATG	$LexA_{408}$- *dctR* BglII Cloning pKEDP58
OA81	CGACTCTAGATTTTAACTGGATTAACGGATTTCTCTTC	*ygeF* XbaI 5′ RACE
OA82	CGACTCTAGATCCAATAAAAGCCTATCAGAATAAGTCC	*ycdU* XbaI 5′ RACE
OA83	TCTTCAATGACAGCTCATCATAGTTTTATATTCTATCCCTTAGTGTAGGCTGGAGCTGCTTCG	Replacement of P_{matA} by P_L
OA84	ACTGTAATCACTTTGCCATGTCACTACTTTCCAAACCTGTAATCATGGTGGTCAGTGCGTCC	Replacement of P_{matA} by P_L
OA85	CGACTCTAGAAATATAATTTAAACCAGACCCCATTGTGA	*ygeF* XbaI 5′ RACE
OA88	ATTTTGTGCGGCATGTTAATCC	*matA*
OA89	AGCAGTCGACTGTATACCTCACATTTTTACCGTGACTC	P_{ygeF} *lacZ SalI* Cloning pKEDP61
OA90	AGCGTCTAGATCGTGGCTTCATTTTACATTTCTC	P_{ygeF} *lacZ* XbaI Cloning pKEDP61
OA100	GGTGCTGATATACTGGGATGCG	*galU*
OA101	ACGGCGTCGATTGCTCAAC	*galU*
OA124	GGTACAGCGTgccGAGGTTGAGCTCCTTAAAACGC	αCTD mutagenesis T285A
OA125	CTCAACCTCggcACGCTGTACCAGATCACCGATATA	αCTD mutagenesis T285A
OA126	AGCGTACCgcgGTTGAGCTCCTTAAAACGCCTAA	αCTD mutagenesis Q286A
OA127	GAGCTCAACcgcGGTACGCTGTACCAGATCACCG	αCTD mutagenesis Q286A
OA128	CGTACCGAGgctGAGCTCCTTAAAACGCCTAACCT	αCTD mutagenesis V287A
OA129	TAAGGAGCTCagcCTCGGTACGCTGTACCAGATCA	αCTD mutagenesis V287A
OA130	TACCGAGGTTgcgCTCCTTAAAACGCCTAACCTTGG	αCTD mutagenesis Q288A
OA131	GTTTTAAGGAGcgcAACCTCGGTACGCTGTACCAG	αCTD mutagenesis Q288A
OA132	GGTTGAGCTCgctAAAACGCCTAACCTTGGTAAAAA	αCTD mutagenesis L290A
OA133	AGGCGTTTTagcGAGCTCAACCTCGGTACGCT	αCTD mutagenesis L290A
OA134	TGTCTCTGgccATGCGCCTGGAAAACTGGC	αCTD mutagenesis G315A
OA135	AGGCGCATggcCAGAGACAGTCCACGGGAAGC	αCTD mutagenesis G315A
OA136	GGGCATGgccCTGGAAAACTGGCCACCGG	αCTD mutagenesis R317A
OA137	GTTTTCCAGggcCATGCCCAGAGACAGTCCACG	αCTD mutagenesis R317A
OA138	CATGCGCgcgGAAAACTGGCCACCGGCA	αCTD mutagenesis L318A
OA139	CAGTTTTCcgcGCGCATGCCCAGAGACAGT	αCTD mutagenesis L318A
OA140	GCGTTGTATCGTCGGGCAG	pKEDP48 reverse

Oligo	Sequence[a] (5' → 3')	Target/purpose
T385	TGACCATCCGgcaGTCTTGTTCGGTATTCGCAAATCA	*rcsB* mutagenesis I14A
T386	CGAACAAGACTgccGGATGGTCATCGGCAATAAT	*rcsB* mutagenesis I14A
T387	GCGATAAGgccGGCGATGGCATTACCTTAATCAA	*rcsB* mutagenesis Y64A
T388	GCCATCGCCggcCTTATCGCCAGGCATGGAGAG	*rcsB* mutagenesis Y64A
T389	AAGTACGGCgcgGGCATTACCTTAATCAAGTACATCAAGC	*rcsB* mutagenesis D66A
T390	AGGTAATGCCcgcGCCGTACTTATCGCCAGGCA	*rcsB* mutagenesis D66A
T391	CATCAAGgccCATTTCCCAAGCCTGTCGATCA	*rcsB* mutagenesis R76A
T392	TGGGAAATGggcCTTGATGTACTTGATTAAGGTAA	*rcsB* mutagenesis R76A
T393	CATCAAGCGCgcgTTCCCAAGCCTGTCGATCA	*rcsB* mutagenesis H77A
T394	TGGGAAcgcGCGCTTGATGTACTTGATTAAGGTAA	*rcsB* mutagenesis H77A
T395	TGTTCTGACTgcgAACAACAACCCGGCGATTCTT	*rcsB* mutagenesis M88A
T396	GGTTGTTGTTcgcAGTCAGAACAATGATCGACAGGCTT	*rcsB* mutagenesis M88A
T397	TGTTGATTACCgcgCTCTCCATGCCTGGCGATAAG	*rcsB* mutagenesis D56A
T398	GCATGGAGAGcgcGGTAATCAACACATGCGCATCC	*rcsB* mutagenesis D56A
T489	P-AACAATATGAACGTAATTATTGCCgctGACCATCCGATAGT CTTGTTC	*rcsB* mutagenesis D10A
T490	P-ATATGAACGTAATTATTGCCGATgccCATCCGATAGTCTTG TTCGGT	*rcsB* mutagenesis D11A
T491	P-TTGATTACCGATCTCTCCATGgctGGCGATAAGTACGGCGA	*rcsB* mutagenesis P60A
T492	P-TTGATTACCGATCTCTCCATgccTGGCGATAAGTACGGCGA	*rcsB* mutagenesis G67A
T493	P-GCCTGTCGATCATTGTTCTGgctATGAACAACAACCCGGC	*rcsB* mutagenesis T87A
T494	P-TATCGAAGGGATCGTGCTGgcaCAAGGTGCACCGACCG	*rcsB* mutagenesis K105A
T495	P-TAAAAAGCTGAACCGCAGTATTgcaACCATCAGTAGCCAGA AGAAAT	*rcsB* mutagenesis K180A
T496	P-CCGCAGTATTAAAACCATCAGTgccCAGAAGAAATCTGCGA TGATG	*rcsB* mutagenesis S198A
T497	P-GCTGGGTGTCGAGAACGATgccGCCCTGCTGAATTATCTCT CT	*rcsB* mutagenesis I199A
T498	P-AACGATATCGCCCTGCTGgctTATCTCTCTTCAGTGACCTT AAGTCC	*rcsB* mutagenesis N203A
OA33	CGGCGATTgctAGTGCGGTATTGGATCTGGATATC	*rcsB* mutagenesis L95A
OA34	CGCACTagcAATCGCCGGGTTGTTGTTC	*rcsB* mutagenesis L95A
OA35	CGATTCTTgctGCGGTATTGGATCTGGATATCG	*rcsB* mutagenesis S96A
OA36	CCAATACCGCagcAAGAATCGCCGGGTTGTTGT	*rcsB* mutagenesis S96A
OA37	GTGCGGTAgcgGATCTGGATATCGAAGGGATCGT	*rcsB* mutagenesis L99A
OA38	TCCAGATCcgcTACCGCACTAAGAATCGCCG	*rcsB* mutagenesis L99A
OA39	AGTGCGGTATTGgctCTGGATATCGAAGGGATCGTG	*rcsB* mutagenesis D100A
OA40	ATATCCAGagcCAATACCGCACTAAGAATCGCC	*rcsB* mutagenesis D100A
OA41	TCTGGATATCgcaGGGATCGTGCTGAAACAAGGT	*rcsB* mutagenesis E104A
OA42	ACGATCCCtgcGATATCCAGATCCAATACCGCACTA	*rcsB* mutagenesis E104A
OA43	CGAAGGGgccGTGCTGAAACAAGGTGCACCG	*rcsB* mutagenesis I106A
OA44	CAGCACggcCCCTTCGATATCCAGATCCAATAC	*rcsB* mutagenesis I106A
OA45	GGATCGTGgcgAAACAAGGTGCACCGACCG	*rcsB* mutagenesis L108A
OA46	CCTTGTTTcgcCACGATCCCTTCGATATCCAGA	*rcsB* mutagenesis L108A
OA47	TGCACCGgccGATCTGCCGAAAGCTCTCGC	*rcsB* mutagenesis T114A
OA48	CAGATCggcCGGTGCACCTTGTTTCAGC	*rcsB* mutagenesis T114A
OA49	ACCGACCgctCTGCCGAAAGCTCTCGCC	*rcsB* mutagenesis D115A
OA50	CGGCAGagcGGTCGGTGCACCTTGTTTCA	*rcsB* mutagenesis D115A
OA51	TCTGCCGgcaGCTCTCGCCGCGCTG	*rcsB* mutagenesis K118A
OA52	CGAGAGCtgcCGGCAGATCGGTCGGTG	*rcsB* mutagenesis K118A

a) Sites for restriction endonucleases are underlined. Mutated base triplets are indicated in lowercase.

4.1.2. Media, buffers and antibiotics

LB medium
For 1000 ml: 10 g BactoTryptone, 5 g BactoYeast extract, 5 g NaCl

LB agar plates
LB medium with 1.5 % (w/v) BactoAgar

LB X-gal agar plates
LB medium with 1.5 % (w/v) BactoAgar, 40 µg/ml X-gal

X-gal (5-Brom-4-chlor-3-indoxyl-β-D-galactopyranoside)
Stock: 20 mg/ml in Dimethylformamide
Use: 40 µg/ml for plates

IPTG (Isopropyl-β-D-thiogalactopyranoside)
Stock: 100 mM in H_2O (filter sterilized)
Use: 0.2 mM for plates; 1 mM for cultures

LB soft agar plates
LB medium with 0.2 % (w/v) BactoAgar

SOB medium
For 1000 ml: 20 g BactoTryptone, 5 g BactoYeast extract, 0.5 g NaCl, 1.25 ml 2M KCl, adjust pH to 7.0 with NaOH, after autoclaving add 10 ml 1 M MgCl2

SOC medium
Add 19.8 ml 20% Glucose to 1000 ml SOB

TE buffer
For 1000 ml: 10 ml 1 M Tris-HCl (pH 8.0), 2 ml 0.5 M EDTA (ethylenediaminetetraacetic acid)

TEN buffer
20 mM Tris-HCl (pH 7.5), 1 mM EDTA, 50 mM NaCl

50x TAE buffer
For 1000 ml: 242 g Tris, 100 ml 0.5 M Na_2EDTA (pH 8.0), 57.1 ml glacial acetic acid

Z buffer, pH 7.0
60 mM Na_2HPO_4, 40 mM NaH_2PO_4, 10 mM KCl, 1 mM $MgSO_4$, 100 µg/ml chloramphenicol

ONPG (2-Nitrophenyl β-D-galactopyranoside)
4 mg/ml in 0.1 M phosphate buffer (pH 7.0) (60 mM Na_2HPO_4 + 40 mM NaH_2PO_4)

10x PBS buffer (phosphate-buffered saline) pH 7.4
For 1000 ml: 2 g KCl, 80 g NaCl, 17.8 g Na_2HPO_4 x$2H_2O$, 2.4 g KH_2PO_4

10x TBS buffer (Tris buffered saline) pH 7.5
For 1000 ml: 60.5 g Tris (50 mM) and 87.6 g NaCl (150 mM)

10x TBE buffer pH 8.0
For 1000 ml: 108 g Tris base 55 g boric acid 40 ml of 0.5 M EDTA

BTB agar
For 1000 ml: 15 g BactoAgar, 1 g YeastExtract, 1 g BactoTryptone, 5 g NaCl, 1 ml 1 M $MgSO_4$, 1 ml 0.1 M $CaCl_2$, 1 ml of 1 mg/ml Vitamin B1, 20 ml of 10 % (w/v) casamino acids, 50 ml of 10 % (w/v) salicin, 10 ml bromthymol blue stock solution (2 % bromthymol blue in 50 % EtOH, 0.1 N NaOH)

T4 top agar
For 1000 ml: 6 g of BactoAgar, 10 g of BactoTryptone, 8 g of NaCl, 2 g of trisodiumcitrate dihydrate, 3 g of glucose.

SPINE ZAP buffer pH 7.5
50 mM TRIS-HCl, 200 mM NaCl

SPINE washing buffer pH 8.0
100 mM TRIS-HCl, 150 mM NaCl, 1 mM EDTA

SPINE elution buffer
0,536 g D-Desthiobiotin in 100 ml washing buffer

Antibiotics
Antibiotics were used as following concentrations: ampicillin 50 µg/ml, chloramphenicol 15 µg/ml, kanamycin 25 µg/ml, spectinomycin 50 µg/ml, tetracyclin 12 µg/ml

4.1.3. Enzymes, kits and chemicals

Company	Article
5PRIME, Hamburg, Germany	Agarose GelExtract PCRExtract
Affymetrix, Ohio, USA	GeneChip® E. coli Genome 2.0
Ambion, Carlsbad, CA, USA	SUPERAse In RNase Inhibitor
Becton, Dickinson, and Company, Sparks, USA	BactoAgar BactoTryptone YeastExtract Difco MacConkey Agar Base
Epicentre, Madison, WI, USA	Tobacco Acid Pyrophosphatase (TAP) Ampligase
IBA Lifesciences, Göttingen, Germany	D-Desthiobiotin Streptactin Sepharose columns

Company	Article
Life Technologies, Carlsbad, CA, USA	FastDigest restriction enzymes T4 DNA ligase HighFidelity Enzyme Mix dNTPs DNA and RNA ladders RNaseH SuperScript III reverse transcriptase Platinum Taq DNA polymerase RNase OUT Pierce ECL Western Blotting Substrate
Macherey-Nagel, Düren, Germany	NucleoBond Gel and PCR clean-up NucleoSpin Plasmid EasyPure
New England Biolabs, Frankfurt am Main, Germany	T4 RNA ligase
Promega, Madison, WI, USA	Wizard Plus MaxiPrep GoTaq DNA polymerase qPCR master mix
Qiagen, Hilden, Germany	QIAquick Gel Extract QIAquick PCR extract RNeasy MiniKit RNAprotect Bacteria Reagent
Sigma-Aldrich, Taufkirchen, Germany	custom-made oligonucleotides chemicals

4.2. Methods

4.2.1. Standard molecular techniques

Standard molecular techniques that are not described below (agarose gel electrophoresis, PCR, cloning) were done according to published protocols (Ausubel, 2005). Sequencing was performed by GATC Biotech AG, Konstanz. The sequences were analyzed by the Software Vector NTI Advance 11 (Invitrogen).

4.2.2. $CaCl_2$ competent cells and transformation

To prepare competent cells, 25 ml LB medium was inoculated with 200 µl of a fresh overnight culture and incubated in a shaker at 37°C. The cultures were harvested on ice at OD_{600} = 0.3, transferred into pre-cooled centrifuge tubes and centrifuged for 10 minutes at 3000 rpm and 4°C. The pellet was resuspended in 12.5 ml ice-cold $CaCl_2$ solution and further incubated on ice for 20 minutes. After a second centrifuge step (10', 3000 rpm, 4°C), the pellet was resuspended in 1 ml $CaCl_2$ solution. These cells were ready for transformation.

Alternatively 100-200 µl aliquots of the cell solution were stored at -80°C supplemented with glycerol (15 % final concentration). For the transformation 1-12 ng of vector DNA was prepared on ice and filled up with TEN buffer to a volume of 50 µl. After adding 100 µl of the competent cells and incubation for 20 minutes on ice, the cells were heat-shocked for 2 minutes at 42°C. After 10 minutes further incubation on ice, 1 ml LB medium was added, the cultures were incubated for one hour at 37°C (plasmids with temperature sensitive replication origin at 28°C). Afterwards 100 µl or varying volumes of the cultures were plated on LB plates containing antibiotics for selection.

4.2.3. Electro-competent cells and electroporation

For preparation of electro-competent cells, 50 ml SOB medium was inoculated with 200 µl of an overnight culture. This culture was incubated in a shaker at 37 °C, harvested at OD_{600} = 0.6 – 0.7 and kept on ice for 1 hour. The first centrifuging step was done in a 4°C pre-cooled centrifuge at 3000 rpm for 15 minutes. The cell pellet was resuspended in 50 ml ice cold sterile H_2O. After the second centrifuging step (15 minutes, 3000 rpm, 4°C) the pellet was resuspended in 25 ml water. After a third centrifugation under the same conditions, the pellet was resuspended in 2 ml 10 % glycerol, again centrifuged at 6000 rpm (15 minutes, 4°C) and finally resuspended in 200 µl glycerol and used for transformation. Alternatively the cells were stored at -80°C. For electroporation 0.5 to 1 µl of plasmid DNA of different concentrations was prepared, 40 µl competent cells added and incubated for 10 minutes on ice. This preparation was transferred to a pre-chilled electro cuvette and electro shocked for 3 seconds at 1.8 kV. Immediately afterwards 1 ml SOC medium was pipetted in the cuvette and this solution incubated for 1 hour in a 37°C in a culture tube. Afterwards various dilutions were plated on selection plates.

4.2.4. Mutagenesis PCR

Site-directed mutagenesis to replace amino acid residues of RcsB or the CTD of the RNA polymerase alpha subunit was carried out by overlap extension PCR (Ho *et al.*, 1989). For each mutagenesis, three standard polymerase chain reactions A, B, and C were conducted. PCR A contained a forward primer flanking the gene upstream and a reverse primer including the mutation matching the region of mutagenesis. PCR B contained a reverse primer flanking the gene downstream and a forward primer including the mutation, matching the region of mutagenesis. The fragments obtained by PCR A and B were gel

purified and used as templates in equal measures for PCR C with the forward primer of PCR A and reverse primer of PCR B. Both oligonucleotides contain specific restriction sites. The PCR fragment was gel purified, digested with appropriate restriction enzymes and cloned into a specific vector.

4.2.5. Random mutagenesis screen

A non-saturated random mutagenesis screen was performed to find RcsB mutants that affect the activities of BglJ-RcsB, RcsA-RcsB and RcsB-RcsB. Random mutations within RcsB were introduced by an error-prone PCR utilizing the GoTaq DNA polymerase (Promega) that lacks a 3'-5' proofreading activity and has an error rate of about 10^{-5} errors per synthesized nucleotide (Zhou *et al.*, 1991). In brief, *rcsB* was amplified with oligos T358 and T106 using vector pKETS6 as template, the fragments purified, digested with restriction endonucleases EcoRI and XbaI and ligated into the vector pKESK22. For finding potential RcsB mutants, reporter strains T572 (P*leuO lacZ* Δ*rcsB* Δ*lacZ bglJ*$_C$), T963 (P*wza lacZ* Δ*rcsBCD* Δ*lacZ rcsA*$_{PL}$) and T1052 (P*rprA lacZ* Δ*rcsB* Δ*lacZ*) were transformed with each ligation, plated on LB X-gal plates (IPTG, kanamycin) and a blue/white screen was performed. In order to find particular amino acids that are important for the activity of RcsB related to a specific interaction partner, the screen focused on finding RcsB mutants with different Lac-phenotypes in the three reporter backgrounds. Thus, colonies exhibiting Lac-negative phenotype in one and Lac-positive phenotype in the other reporter system(s) were picked and the *rcsB* allele analyzed by sequencing.

4.2.6. Promoter replacement and gene deletion

The replacement of promoters or deletion of chromosomal genes was done according to (Datsenko & Wanner, 2000). By this method, a specific chromosomal locus was replaced by a linear DNA fragment mediated by the λ-Red recombination system. The linear DNA fragment was prepared by PCR by amplifying a sequence with a resistance cassette for selection, flanked by FRT (**F**lp **R**ecombinase **T**arget) sites. The oligonucleotides were designed to have around 40 nt long homologue sequences to the chromosomal locus that should be replaced. The cells were transformed with the temperature sensitive plasmid (pKD46) encoding for the λ-Red system under the control of the arabinose-inducible promoter. In parallel the PCR product was prepared using pKD3, pKD4 or derivatives carrying the resistance cassette flanked by FRT sites as template. The cells harboring the pKD46 helper plasmid were electro-

transformed with the gel purified PCR product (> 100 ng/µl in H_2O). Due to the temperature sensitivity of replication of the pKD46 plasmid, the electro-competent cells were prepared at 28°C in SOB medium containing 10 mM L-arabinose for induction of λ-recombinase expression. The recombinants were selected on LB plates containing the appropriate antibiotic at 37°C. The deletion of the target gene was analyzed by PCR and the loss of the helper plasmid confirmed by ampicillin sensitivity. The resistance cassettes were flipped out expressing the Flp recombinase from the plasmid pCP20. This plasmid has a temperature sensitive replication origin; transformants were selected at 28°C on LB ampicillin plates. Colonies were restreaked on LB and incubation at 42°C induced expression of the recombinase and repressed replication of the plasmid. The excision of the resistance cassette was confirmed by PCR with locus specific oligonucleotides and the loss of pCP20 was confirmed by ampicillin sensitivity.

4.2.7. Preparation of lysate and transduction

Generalized transduction was applied to transfer DNA between bacteria with the help of the bacteriophage T4GT7 (Wilson *et al.*, 1979). For the preparation of a phage lysate 100 µl of an overnight culture of the donor strain whose genes should be transduced, were incubated for 20 minutes at room temperature with different dilutions (e.g. 10^{-2}, 10^{-3} and 10^{-4} in LB) of a phage lysate. Afterwards 1 ml LB medium as well as 3 ml of liquid 42°C warm top agar was added, carefully mixed and plated on fresh LB plates. After 8 – 14 hours of incubation at 37°C those plates showing almost confluent lysis were chosen and the top agar transferred into a glass tube. After adding the same volume of chloroform, the mixture was homogenized with a glass pestle. The homogenate was centrifuged at 12.000 rpm for 3 minutes. The top phase was pipetted into a new tube, the same volume of chloroform is added, mixed and centrifuged again. The top phase was stored at 4°C. For the transduction 100 – 200 µl of an overnight culture of the acceptor strain was mixed with different volumes of the phage lysate (e.g. 0.2 µl, 1 µl, 3 µl, 10 µl), incubated for less than 20 minutes at room temperature and plated on selection plates. Colonies of transduced cells were restreaked three times as soon as possible and the transduced locus analyzed by PCR.

4.2.8. Chromosomal integration

The integration of reporter constructs into the chromosome at the *attB* site was done as described (Diederich *et al.*, 1992). For integration, cells of the desired strain were

transformed with the helper plasmid pLDR8 that encodes for the integrase. On the plasmid pLDR8 the integrase encoding gene is under the control of the λ promoter P_R and the temperature sensitive repressor cI_{857}. The origin of replication of pLDR8 is temperature sensitive. The transformants were selected on LB plates with kanamycin at 28°C. The next day LB medium containing kanamycin was inoculated with a single colony and incubated overnight in a shaker at 28°C. The next morning this culture was diluted 1:20 with fresh LB medium containing kanamycin. This culture was incubated in a shaker at 37°C for 90 minutes, harvested and chemo-competent cells prepared. In parallel the plasmid containing the promoter *lacZ* fusion was digested with BamHI, the fragment gel-purified and re-ligated. The competent cells were transformed with the re-ligation and incubated for one hour at 37°C. Afterwards 200 µl of the cultures were plated on LB spectinomycin plates and incubated at 42°C. This temperature fully induced the integrase expression and the replication of the plasmid was inhibited. For the analysis of integration, four colonies were analyzed by PCR with S93/S164 (analysis of attB/P' site), S95/S96 or S95/T912 (analysis of attP/B' site), S95/S164 (exclusion of dimers) and T334/S118 (analysis of the reporter construct). The colonies were analyzed for kanamycin sensitivity (loss of pLDR8) and two independent clones were stored.

4.2.9. RcsB structure prediction

The RcsB protein consists of 216 amino acids with the N-terminal receiver domain comprising residues 1 to 124, and the C-terminal DNA-binding domain comprising residues 144 to 209 (Majdalani & Gottesman, 2005). The structure of the DNA-binding domain was solved for RcsB derived from *Erwinia amylovora* (Pristovsek *et al.*, 2003) but the structure of the receiver domain has not been solved. The model of the RcsB receiver domain was predicted using the Phyre2 server (Kelley *et al.*, 2015). For this, amino acids 1 to 124 of RcsB derived from *E. coli* K-12 served as query sequence. The 3D model prediction is based on a comparison of the query sequence with templates having a solved structure through (1) gathering homologous sequences, (2) a fold library scan, (3) loop modeling and (4) side chain replacement (Kelley *et al.*, 2015). Through this, 20 models based on different templates have been predicted that are ranked according to raw alignment scores. The highest scoring model was based on the crystal structure of NarL (PDB# 3EUL) (Schnell *et al.*, 2008) with a sequence identity of 26 %, a coverage of 97 % and a confidence of 99.9 %. Coverage and confidence indicate that residues 4 to 124 of the query sequence (97 %) were aligned to the

template and have been modeled with a 99.9 % probability that query sequence and NarL template are homologous (Kelley *et al.*, 2015).

4.2.10. β-galactosidase assay

Expression analyses of promoter *lacZ* fusions were carried out according to (Miller, 1992). To this end, exponential cultures were inoculated from a fresh overnight culture to an OD_{600} = 0.05 in LB medium containing appropriate antibiotics for transformants. If required, IPTG was added to overnight and exponential culture for induction (1 mM final concentration). Bacteria were harvested on ice at an OD_{600} = 0.5. The assays were repeated at least three times from independent cultures. The standard deviations are indicated as error bars. The statistical significance was calculated by t-test with *p < 0.05; **p < 0.01; ***p < 0.001.

4.2.11. Motility assays

3 µl of a fresh overnight culture grown in LB medium (with 25 µg/ml kanamycin and 1 mM IPTG for transformants) was pipetted in the center of freshly poured LB soft agar plates (0.2 % agar, with 25 µg/ml kanamycin and 0.2 mM IPTG for transformants). The plates were incubated for 5 hours at 37°C and scanned using Epson Perfection V700 Photo transparency scanner. The motility radii were measured in mm.

4.2.12. RNA isolation

Exponential cultures were inoculated from a fresh overnight culture to an OD_{600} = 0.05 in LB medium containing appropriate antibiotics for transformants. If induction required, IPTG (1 mM final concentration) or arabinose (0.2 % final concentration) was added at an OD_{600} = 0.3 and harvested after 30 minutes further growth. Bacteria were harvested using the RNAprotect Bacteria Reagent (Qiagen). The total RNA was isolated using the RNeasy MiniKit system (Qiagen) according to manufacturer's instructions including an on-column DNaseI treatment. The RNA was analyzed by denaturing urea PAGE and by measuring the UV light absorption ratio 260/280 nm. The RNA concentration was measured at 260 nm and isolated RNA stored at -80°C in H_2O.

4.2.13. Urea PAGE

Isolated RNA was analyzed using urea-polyacrylamide gel electrophoresis under denaturing conditions. For this, 0.5 µg RNA was mixed with 2 x RNA loading dye (Life Technologies) to a total volume of 10 µl with H_2O. The RNA sample and Riboruler High Range RNA ladder (Life Technologies) were heated at 70°C for 10 minutes and separated on 5 % polyacrylamide gel

(19:1 acrylamide:bisacrylamide 40 % stock) containing 7 M UREA in 0.5 x TBE for 1.5 hours at 200 V. Subsequently, the gel was stained for 30 minutes in 0.5 x TBE containing 0.5 µg/ml ethidium bromide. The 23S rRNA (2904 nt) and 16S rRNA (1542 nt) bands served as reference for intact RNA without degradation products.

4.2.14. cDNA synthesis

For first strand cDNA synthesis, 1 µg of RNA was reverse transcribed with the SuperScript III First Strand Synthesis Kit (Life Technologies) according to the manufacturer's instructions. For this, RNA was mixed with random hexameric oligonucleotides as primers and dNTPs. The samples were heat-denatured at 65°C and cooled on ice. For reverse transcription, 200 U of SuperScript III reverse transcriptase and 40 U of RNaseOUT were used (final reaction volume was 20 µl). Samples were incubated at 25°C for 10 min, at 50°C for 60 min, at 85°C for 5 min and cooled on ice. 1 µl of RNase H (Fermentas) was added and samples were incubated for 20 min at 37°C. The cDNA was stored at -20°C.

4.2.15. Microarray analysis

For finding putative target genes regulated by MatA or DctR, *E. coli* strain BW30270 (S3839) was transformed with either pKEDP30 (MatA) or pKEDP31 (DctR) respectively. From a fresh overnight culture, 15 ml LB medium with Kanamycin was inoculated to an OD_{600} = 0.05 and incubated in a shaker at 37°C until the culture has reached an OD_{600} = 0.3. At this point, IPTG was added to a final concentration of 1 mM and the cultures were harvested after 30 minutes further incubation using the RNAprotect Bacteria Reagent (Qiagen). The total RNA was isolated as described above. As a control, the same procedure was done in parallel with S3839 harboring the empty control plasmid pKESK22 instead of pKEDP30 or pKEDP31. The Microarray analysis was performed by the Cologne Center for Genomics with the Affymetrix system (E. coli Genome 2). Differential expression levels between sample and control were calculated as fold change.

4.2.16. qPCR analysis

RNA was isolated from cultures grown in LB medium containing antibiotics. At an OD_{600} = 0.3 IPTG (1 mM final concentration) or arabinose (0.2 % final concentration) was added, the bacteria were harvested, and the total RNA was isolated as described above. The cDNA was synthesized using the SuperScript III First Strand Synthesis Kit (Invitrogen) using 1 mg of RNA and random hexameric oligonucleotides as primers. Quantitative PCR measurements were

carried out using gene specific oligonucleotide primers, SYBR Green I and a C1000 touch thermalcycler with optical reaction module CFX96 (Bio-Rad). The cDNA derived from 1 mg of total RNA was diluted 1:10 in DEPC-treated water. For one assay, 4 ml of dNTPs (1 mM each), 4 ml of 5x GoTaq buffer (Promega), 6.8 ml of DEPC treated water, 0.8 ml of DMSO, 0.2 ml of SYBR green (1:1000 in DMSO), 0.2 ml of GoTaq DNA Polymerase (Promega), and 1 ml of each primer (10 pmol/µl) were used. Two microliters of diluted cDNA served as the template. Assays were pipetted on 96-well PCR plates and sealed with optical quality adhesive film (Bio-Rad). Samples were prepared in triplicate. For PCR efficiency correction, a pool of cDNA samples served as calibration line. Gene *rpoD* served as reference for data normalization. Data were analyzed with Bio-Rad CFX Manager 3.1 Software applying a normalized expression (ΔΔCt) algorithm.

4.2.17. SDS PAGE and western blotting

The stability of RcsB mutant proteins was analyzed by western blot. For that reason Δ*rcsB* strain T21 was transformed with plasmids being able of IPTG inducible expression of C-terminally HA-tagged RcsB mutants (pKEAP38, pKEDP1-9). To estimate the RcsB concentration in the cells, cultures were grown without induction of rcsB-HA expression. At OD_{600} = 0.3 the first samples (1 ml each) were harvested on ice. At the same time the expression was induced by adding IPTG. The second sample was taken 30 minutes after induction. Immediately, chloramphenicol (200 µg/ml) was added to inhibit protein synthesis. After further 30 minutes the third sample was taken. The OD_{600} was documented in each case. The 1 ml aliquots were centrifuged (1 minute, 13.000 rpm), the supernatant discarded and the pellet resuspended in appropriate volume of sample buffer (OD_{600} x 200 = volume of sample buffer in µl) or alternatively frozen at -20°C. These samples were boiled for 5 minutes at 95°C, spun down and 5 or 10 µl per slot were loaded on 15 % polyacrylamide gels (5 µl LifeTechnologies Prestained Protein Ladder). The gels were run at 100 V, 40 mA until the blue loading dye had reached the separation gel. At this point the voltage was increased to 150 V for around 1.5 hours until the dye has reached the end of the gel. The blotting was done on Nitrocellulose or PVDF membrane in a semi-dry transfer chamber for at least 1 hour at 50 V and 0.8 mA/cm^2. Afterwards the membrane was rinsed with distilled water, blocked for 1 hour at RT or overnight at 4°C in TBS or PBS containing 3-5 % skimmed milk powder. The primary antibody staining occurred as listed below for at least 1 hour. After the primary antibody staining the membrane was washed 3 x 10 minutes in TBS-T or PBS-T, the blot

stained with secondary antibodies (see below) for 1 hour and washed again. The detection was done according to the secondary antibodies with Odyssey (Li-Cor) for fluorescence coupled antibodies or with ImageQuant (GE Healthcare) for HRP coupled antibodies. Before developing the blot by ImageQuant, the membranes were treated with ECL chemiluminescence reagent from Pierce according to the manual.

Table 7. Western blot staining and developing conditions

	HA tag staining	Strep tag staining	FLAG tag staining
Membrane	Nitrocellulose	Nitrocellulose or PVDF (activate in MeOH)	Nitrocellulose
Blocking	TBS, 3% skimmed milk powder, 1 h gently shaking	PBS, 3 % BSA, 0.5 % TWEEN or PBS, 1% skimmed milk powder 1 h gently shaking	PBS, 3% skimmed milk powder, 1 h gently shaking
Washing		3 x for 5 min with PBS-T (0,05% Tween)	3 x for 5' with PBS-T (0,05% Tween)
1° Antibody	rat anti HA in TBS, 3% skimmed milk powder (1:500 or 1:1000) 1 h gently shaking	StrepMAB classic HRP conj. in PBS-T (0,2% BSA, 0,1% Tween) (1:30.000) When blocking with milk powder: add 4 µl undiluted StrepMAB classic HRP conj. In blocking buffer (1:4000) 1 h gently shaking	anti FLAG polyclonal from rabbit PBS, 3% skimmed milk (1:1000) 1 h gently shaking
Washing	3 x for 10 min with TBS-T	2 x for 1 min with PBS-T and 2 x for 1' with PBS	3 x for 5 min with PBS-T
2° Antibody	rat anti HA (1:500 or 1:1000) 1 h gently shaking		anti rabbit in PBS-T (1:2000) 1 h gently shaking
Washing	Wash membrane 3 x for 10 min with TBS-T		3 x for 5' with PBS-T (0,05% Tween)
Detection	Fluorescence detection with Odyssey	Proceed to the chromogenic reaction (Pierce ECL)	Fluorescence detection with Odyssey

4.2.18. Strep-protein interaction experiment (SPINE)

For analyzing the interaction of proteins the *SPINE* (***S****trep-****P****rotein-****I****nteraction-****E****xperiment*) method according to (Herzberg *et al.*, 2007) was applied. For this purpose Δ*rcsB* strain (T73) was transformed with two different low-copy expression vectors. One harboring an HA tagged RcsB version, the other one the Strep tagged dimerization partner. In brief, 1 liter LB medium containing the appropriate antibiotics was inoculated with a fresh overnight culture of the transformants. This culture was incubated in a shaker at 37°C until the OD_{600} has reached 0.8. At this time point the induction of *rcsB* expression was induced with IPTG (1 mM final concentration) and further incubated for 1 hour. Then the crosslinking agent formaldehyde was added (0.4 % final concentration) and the incubation continued for 20 minutes. After harvesting the cells on ice they were centrifuged (5000 rpm, 15 minutes, 4°C), resuspended in 15 ml ZAP buffer, again centrifuged, resuspended in 15 ml ZAP buffer and disrupted with an EmulsiFlex french press. The crude extracts were centrifuged for 1 hour at 19.000 rpm and the obtained protein lysates loaded onto a Streptactin Sepharose column (IBA Lifesciences) to isolate the cross-linked protein complexes. The columns were washed

four times with 10 ml washing buffer and eluted with three times 1 ml elution buffer. The eluate was subsequently analyzed by western blot.

5. References

Aiso, T., M. Murata & S. Gamou, (2011) Transcription of an antisense RNA of a gadE mRNA is regulated by GadE, the central activator of the acid resistance system in Escherichia coli. *Genes Cells* **16**: 670-680.

Al-Bassam, M.M., M.J. Bibb, M.J. Bush, G. Chandra & M.J. Buttner, (2014) Response Regulator Heterodimer Formation Controls a Key Stage in *Streptomyces* Development. *PLoS Genet.* **10**: 10.1371/journal.pgen.1004554.

Ausubel, F.M., R. Brent, R. E. Kingston, D. D. Moore, J. G. Seidman, J. A. Smith & K. Struhl, (2005) Current Protocols in Molecular Biology. In. Hoboken, NJ: John Wiley & Sons, Inc., pp.

Blatter, E.E., W. Ross, H. Tang, R.L. Gourse & R.H. Ebright, (1994) Domain organization of RNA polymerase alpha subunit: C-terminal 85 amino acids constitute a domain capable of dimerization and DNA binding. *Cell* **78**: 889-896.

Bourret, R.B., (2010) Receiver domain structure and function in response regulator proteins. *Curr. Opin. Microbiol.* **13**: 142-149.

Carballes, F., C. Bertrand, J.P. Bouche & K. Cam, (1999) Regulation of *Escherichia coli* cell division genes *ftsA* and *ftsZ* by the two-component system *rcsC-rcsB*. *Mol. Microbiol.* **34**: 442-450.

Castanie-Cornet, M.P., K. Cam, B. Bastiat, A. Cros, P. Bordes & C. Gutierrez, (2010) Acid stress response in *Escherichia coli*: mechanism of regulation of *gadA* transcription by RcsB and GadE. *Nucleic Acids Research* **38**: 3546-3554.

Castanie-Cornet, M.P., K. Cam & A. Jacq, (2006) RcsF is an outer membrane lipoprotein involved in the RcsCDB phosphorelay signaling pathway in Escherichia coli. *J. Bacteriol.* **188**: 4264-4270.

Cho, B.K., C.L. Barrett, E.M. Knight, Y.S. Park & B.O. Palsson, (2008) Genome-scale reconstruction of the Lrp regulatory network in Escherichia coli. *Proc. Natl. Acad. Sci. U.S.A.* **105**: 19462-19467.

Cho, S.H., J. Szewczyk, C. Pesavento, M. Zietek, M. Banzhaf, P. Roszczenko, A. Asmar, G. Laloux, A.K. Hov, P. Leverrier, C. Van der Henst, D. Vertommen, A. Typas & J.F. Collet, (2014) Detecting Envelope Stress by Monitoring β-Barrel Assembly. *Cell* **159**: 1652-1664.

Clarke, D.J., (2010) The Rcs phosphorelay: more than just a two-component pathway. *Future Microbiol* **5**: 1173-1184.

Datsenko, K.A. & B.L. Wanner, (2000) One-step inactivation of chromosomal genes in *Escherichia coli* K-12 using PCR products. *Proc. Natl. Acad. Sci. U.S.A.* **97**: 6640-6645.

Davalos-Garcia, M., A. Conter, I. Toesca, C. Gutierrez & K. Cam, (2001) Regulation of osmC gene expression by the two-component system rcsB-rcsC in Escherichia coli. *J. Bacteriol.* **183**: 5870-5876.

Diederich, L., L.J. Rasmussen & W. Messer, (1992) New cloning vectors for integration in the lambda attachment site *attB* of the *Escherichia coli* chromosome. *Plasmid* **28**: 14-24.

Dmitrova, M., G. Younes-Cauet, P. Oertel-Buchheit, D. Porte, M. Schnarr & M. Granger-Schnarr, (1998) A new LexA-based genetic system for monitoring and analyzing protein heterodimerization in *Escherichia coli*. *Mol. Gen. Genet.* **257**: 205-212.

Dove, S.L. & A. Hochschild, (2004) A bacterial two-hybrid system based on transcription activation. *Methods Mol. Biol.* **261**: 231-246.

Dreck, K., (2013) Functional characterization of the transcription factor YjjQ in Escherichia coli (PhD thesis). Institut für Genetik. Universität zu Köln

Ebel, W. & J.E. Trempy, (1999) *Escherichia coli* RcsA, a Positive Activator of Colanic Acid Capsular Polysaccharide Synthesis, Functions To Activate Its Own Expression. *J. Bacteriol.* **181**: 577-584.

Evans, K.L., S. Kannan, G. Li, M.A. de Pedro & K.D. Young, (2013) Eliminating a Set of Four Penicillin Binding Proteins Triggers the Rcs Phosphorelay and Cpx Stress Responses in *Escherichia coli*. *J. Bacteriol.* **195**: 4415-4424.

Fabisch, M., (2008) Wechselwirkung von Transkriptionsfaktoren des LuxR-Typs in *Escherichia coli* (Diplomarbeit) Institut für Genetik. Universität zu Köln

Farris, C., S. Sanowar, M.W. Bader, R. Pfuetzner & S.I. Miller, (2010) Antimicrobial peptides activate the Rcs regulon through the outer membrane lipoprotein RcsF. *J. Bacteriol.* **192**: 4894-4903.

Ferrieres, L., S.N. Aslam, R.M. Cooper & D.J. Clarke, (2007) The *yjbEFGH* locus in *Escherichia coli* K-12 is an operon encoding proteins involved in exopolysaccharide production. *Microbiology (Reading, Engl.)* **153**: 1070-1080.

Francez-Charlot, A., M.P. Castanie-Cornet, C. Gutierrez & K. Cam, (2005) Osmotic regulation of the Escherichia coli bdm (biofilm-dependent modulation) gene by the RcsCDB His-Asp phosphorelay. *J. Bacteriol.* **187**: 3873-3877.

Francez-Charlot, A., B. Laugel, G.A. Van, N. Dubarry, F. Wiorowski, M.P. Castanie-Cornet, C. Gutierrez & K. Cam, (2003) RcsCDB His-Asp phosphorelay system negatively regulates the *flhDC* operon in *Escherichia coli*. *Mol. Microbiol.* **49**: 823-832.

Gao, R., T.R. Mack & A.M. Stock, (2007) Bacterial response regulators: versatile regulatory strategies from common domains. *Trends Biochem. Sci.* **32**: 225-234.

Gao, R. & A.M. Stock, (2010) Molecular Strategies for Phosphorylation-Mediated Regulation of Response Regulator Activity. *Curr. Opin. Microbiol.* **13**: 160-167.

Girgis, H.S., Y. Liu, W.S. Ryu & S. Tavazoie, (2007) A Comprehensive Genetic Characterization of Bacterial Motility. *PLoS Genet.* **3**: 1644-1660.

Gottesman, S., P. Trisler & A. Torres-Cabassa, (1985) Regulation of Capsular Polysaccharide Synthesis in *Escherichia coli* K-12: Characterization of Three Regulatory Genes. *J. Bacteriol.* **162**: 1111-1119.

Grainger, D.C., D. Hurd, M. Harrison, J. Holdstock & S.J. Busby, (2005) Studies of the distribution of Escherichia coli cAMP-receptor protein and RNA polymerase along the E. coli chromosome. *Proc. Natl. Acad. Sci. U.S.A.* **102**: 17693-17698.

Gupte, G., C. Woodward & V. Stout, (1997) Isolation and characterization of rcsB mutations that affect colanic acid capsule synthesis in Escherichia coli K-12. *J. Bacteriol.* **179**: 4328-4335.

Haiko, J. & B. Westerlund-Wikstrom, (2013) The role of the bacterial flagellum in adhesion and virulence. *Biology (Basel)* **2**: 1242-1267.

Hayward, R.S., K. Igarashi & A. Ishihama, (1991) Functional specialization within the alpha-subunit of Escherichia coli RNA polymerase. *J. Mol. Biol.* **221**: 23-29.

Henikoff, S., J.C. Wallace & J.P. Brown, (1990) Finding protein similarities with nucleotide sequence databases. *Meth. Enzymol.* **183**: 111-132.

Herzberg, C., L.A. Weidinger, B. Dorrbecker, S. Hubner, J. Stulke & F.M. Commichau, (2007) SPINE: a method for the rapid detection and analysis of protein-protein interactions in vivo. *Proteomics* **7**: 4032-4035.

Hinchliffe, S.J., S.L. Howard, Y.H. Huang, D.J. Clarke & B.W. Wren, (2008) The importance of the Rcs phosphorelay in the survival and pathogenesis of the enteropathogenic yersiniae. *Microbiology (Reading, Engl.)* **154**: 1117-1131.

Ho, S.N., H.D. Hunt, R.M. Horton, J.K. Pullen & L.R. Pease, (1989) Site-directed mutagenesis by overlap extension using the polymerase chain reaction. *Gene* **77**: 51-59.

Hommais, F., E. Krin, J.Y. Coppee, C. Lacroix, E. Yeramian, A. Danchin & P. Bertin, (2004) GadE (YhiE): a novel activator involved in the response to acid environment in Escherichia coli. *Microbiology (Reading, Engl.)* **150**: 61-72.

Hu, L.I., B.K. Chi, M.L. Kuhn, E.V. Filippova, A.J. Walker-Peddakotla, K. Basell, D. Becher, W.F. Anderson, H. Antelmann & A.J. Wolfe, (2013) Acetylation of the response regulator RcsB controls transcription from a small RNA promoter. *J. Bacteriol.* **195**: 4174-4186.

Kelley, L.A., S. Mezulis, C.M. Yates, M.N. Wass & M.J. Sternberg, (2015) The Phyre2 web portal for protein modeling, prediction and analysis. *Nat Protoc* **10**: 845-858.

Kelley, L.A. & M.J. Sternberg, (2009) Protein structure prediction on the Web: a case study using the Phyre server. *Nat Protoc* **4**: 363-371.

Krin, E., A. Danchin & O. Soutourina, (2010) Decrypting the H-NS-dependent regulatory cascade of acid stress resistance in Escherichia coli. *BMC Microbiol.* **10**: 273.

Lara-Gonzalez, S., J.J. Birktoft & C.L. Lawson, (2010) Structure of the Escherichia coli RNA polymerase alpha subunit C-terminal domain. *Acta Crystallogr. D Biol. Crystallogr.* **66**: 806-812.

Lasaro, M., Z. Liu, R. Bishar, K. Kelly, S. Chattopadhyay, S. Paul, E. Sokurenko, J. Zhu & M. Goulian, (2014) Escherichia coli isolate for studying colonization of the mouse intestine and its application to two-component signaling knockouts. *J. Bacteriol.* **196**: 1723-1732.

Laubacher, M.E. & S.E. Ades, (2008) The Rcs Phosphorelay Is a Cell Envelope Stress Response Activated by Peptidoglycan Stress and Contributes to Intrinsic Antibiotic Resistance. *J. Bacteriol.* **190**: 2065-2074.

Lehti, T.A., P. Bauchart, U. Dobrindt, T.K. Korhonen & B. Westerlund-Wikstrom, (2012a) The fimbriae activator MatA switches off motility in *Escherichia coli* by repression of the flagellar master operon *flhDC*. *Microbiology (Reading, Engl.)* **158**: 1444-1455.

Lehti, T.A., P. Bauchart, J. Heikkinen, J. Hacker, T.K. Korhonen, U. Dobrindt & B. Westerlund-Wikstrom, (2010) Mat fimbriae promote biofilm formation by meningitis-associated Escherichia coli. *Microbiology (Reading, Engl.)* **156**: 2408-2417.

Lehti, T.A., P. Bauchart, M. Kukkonen, U. Dobrindt, T.K. Korhonen & B. Westerlund-Wikstrom, (2013) Phylogenetic group-associated differences in regulation of the common colonization factor Mat fimbria in *Escherichia coli*. *Mol. Microbiol.* **87**: 1200-1222.

Lehti, T.A., J. Heikkinen, T.K. Korhonen & B. Westerlund-Wikstrom, (2012b) The response regulator RcsB activates expression of Mat fimbriae in meningitic Escherichia coli. *J Bacteriol*.

Majdalani, N. & S. Gottesman, (2005) The Rcs phosphorelay: A Complex Signal Transduction System. *Annu. Rev. Microbiol.* **59**: 379-405.

Majdalani, N., M. Heck, V. Stout & S. Gottesman, (2005) Role of RcsF in signaling to the Rcs phosphorelay pathway in Escherichia coli. *J. Bacteriol.* **187**: 6770-6778.

Majdalani, N., D. Hernandez & S. Gottesman, (2002) Regulation and mode of action of the second small RNA activator of RpoS translation, RprA. *Mol. Microbiol.* **46**: 813-826.

Maris, A.E., M.R. Sawaya, M. Kaczor-Grzeskowiak, M.R. Jarvis, S.M. Bearson, M.L. Kopka, I. Schroder, R.P. Gunsalus & R.E. Dickerson, (2002) Dimerization allows DNA target site recognition by the NarL response regulator. *Nat. Struct. Biol.* **9**: 771-778.

Martinez-Santos, V.I., A. Medrano-Lopez, Z. Saldana, J.A. Giron & J.L. Puente, (2012) Transcriptional Regulation of the *ecp* Operon by EcpR, IHF, and H-NS in Attaching and Effacing *Escherichia coli*. *J. Bacteriol.* **194**: 5020-5033.

Masuda, N. & G.M. Church, (2003) Regulatory network of acid resistance genes in *Escherichia coli*. *Mol. Microbiol.* **48**: 699-712.

Mates, A.K., A.K. Sayed & J.W. Foster, (2007) Products of the *Escherichia coli* Acid Fitness Island Attenuate Metabolite Stress at Extremely Low pH and Mediate a Cell Density-Dependent Acid Resistance. *J. Bacteriol.* **189**: 2759-2768.

Miller, J.H., (1992) A short course in bacterial genetics. A laboratory manual and handbook for *Escherichia coli* and related bacteria. In. Cold Spring Harbor Laboratory, NY: Cold Spring Harbor Laboratory Press, pp.

Parker, C.T., A.W. Kloser, C.A. Schnaitman, M.A. Stein, S. Gottesman & B.W. Gibson, (1992) Role of the rfaG and rfaP genes in determining the lipopolysaccharide core structure and cell surface properties of Escherichia coli K-12. *J. Bacteriol.* **174**: 2525-2538.

Pegues, J.C., L.S. Chen, A.W. Gordon, L. Ding & W.G. Coleman, Jr., (1990) Cloning, expression, and characterization of the *Escherichia coli* K-12 *rfaD* gene. *J. Bacteriol.* **172**: 4652-4660.

Perfeito, L., S. Ghozzi, J. Berg, K. Schnetz & M. Lassig, (2011) Nonlinear fitness landscape of a molecular pathway. *PLoS Genet.* **7**: e1002160.

Pristovsek, P., K. Sengupta, F. Lohr, B. Schafer, M.W. von Trebra, H. Ruterjans & F. Bernhard, (2003) Structural Analysis of the DNA-binding Domain of the *Erwinia amylovora* RcsB Protein and Its Interaction with the RcsAB box. *J. Biol. Chem.* **278**: 17752-17759.

Salscheider, S.L., A. Jahn & K. Schnetz, (2013) Transcriptional regulation by BglJ-RcsB, a pleiotropic heteromeric activator in Escherichia coli. *Nucleic Acids Res*.

Savery, N.J., G.S. Lloyd, S.J. Busby, M.S. Thomas, R.H. Ebright & R.L. Gourse, (2002) Determinants of the C-terminal domain of the Escherichia coli RNA polymerase alpha subunit important for transcription at class I cyclic AMP receptor protein-dependent promoters. *J. Bacteriol.* **184**: 2273-2280.

Savery, N.J., G.S. Lloyd, M. Kainz, T. Gaal, W. Ross, R.H. Ebright, R.L. Gourse & S.J. Busby, (1998) Transcription activation at Class II CRP-dependent promoters: identification of determinants in the C-terminal domain of the RNA polymerase alpha subunit. *EMBO J.* **17**: 3439-3447.

Sayed, A.K. & J.W. Foster, (2009) A 750 bp sensory integration region directs global control of the Escherichia coli GadE acid resistance regulator. *Mol. Microbiol.* **71**: 1435-1450.

Scharf, B.E., (2010) Summary of useful methods for two-component system research. *Curr. Opin. Microbiol.* **13**: 246-252.

Schnell, R., D. Agren & G. Schneider, (2008) 1.9 A structure of the signal receiver domain of the putative response regulator NarL from *Mycobacterium tuberculosis*. *Acta Crystallogr. Sect. F Struct. Biol. Cryst. Commun.* **64**: 1096-1100.

Sledjeski, D. & S. Gottesman, (1995) A small RNA acts as an antisilencer of the H-NS-silenced *rcsA* gene of *Escherichia coli*. *Proc. Natl. Acad. Sci. U.S.A.* **92**: 2003-2007.

Soutourina, O.A. & P.N. Bertin, (2003) Regulation cascade of flagellar expression in Gram-negative bacteria. *FEMS Microbiol. Rev.* **27**: 505-523.

Soutourina, O.A., E. Krin, C. Laurent-Winter, F. Hommais, A. Danchin & P.N. Bertin, (2002) Regulation of bacterial motility in response to low pH in Escherichia coli: the role of H-NS protein. *Microbiology (Reading, Engl.)* **148**: 1543-1551.

Stephenson, K., Y. Yamaguchi & J.A. Hoch, (2000) The mechanism of action of inhibitors of bacterial two-component signal transduction systems. *J. Biol. Chem.* **275**: 38900-38904.

Stock, A.M., V.L. Robinson & P.N. Goudreau, (2000) Two-component signal transduction. *Annu. Rev. Biochem.* **69**: 183-215.

Stout, V. & S. Gottesman, (1990) RcsB and RcsC: a two-component regulator of capsule synthesis in Escherichia coli. *J. Bacteriol.* **172**: 659-669.

Stout, V., A. Torres-Cabassa, M.R. Maurizi, D. Gutnick & S. Gottesman, (1991) RcsA, an Unstable Positive Regulator of Capsular Polysaccharide Synthesis. *J. Bacteriol.* **173**: 1738-1747.

Stratmann, T., S. Madhusudan & K. Schnetz, (2008) Regulation of the *yjjQ-bglJ* Operon, Encoding LuxR-Type Transcription Factors, and the Divergent *yjjP* Gene by H-NS and LeuO. *J. Bacteriol.* **190**: 926-935.

Stratmann, T., U. Pul, R. Wurm, R. Wagner & K. Schnetz, (2012) RcsB-BglJ activates the *Escherichia coli leuO* gene, encoding an H-NS antagonist and pleiotropic regulator of virulence determinants. *Mol. Microbiol.* **83**: 1109-1123.

Sturny, R., K. Cam, C. Gutierrez & A. Conter, (2003) NhaR and RcsB Independently Regulate the *osmCp1* Promoter of *Escherichia coli* at Overlapping Regulatory Sites. *J. Bacteriol.* **185**: 4298-4304.

Tang, H., K. Severinov, A. Goldfarb, D. Fenyo, B. Chait & R.H. Ebright, (1994) Location, structure, and function of the target of a transcriptional activator protein. *Genes Dev.* **8**: 3058-3067.

Tao, K., S. Narita & H. Tokuda, (2012) Defective lipoprotein sorting induces lolA expression through the Rcs stress response phosphorelay system. *J. Bacteriol.* **194**: 3643-3650.

Thao, S., C.-S. Chen, H. Zhu & J.C. Escalante-Semerena, (2010) N^{ϵ}–Lysine Acetylation of a Bacterial Transcription Factor Inhibits Its DNA-Binding Activity. *PLoS ONE*: 10.1371/journal.pone.0015123.

Tobe, T., H. Ando, H. Ishikawa, H. Abe, K. Tashiro, T. Hayashi, S. Kuhara & N. Sugimoto, (2005) Dual regulatory pathways integrating the RcsC-RcsD-RcsB signalling system control enterohaemorrhagic Escherichia coli pathogenicity. *Mol. Microbiol.* **58**: 320-333.

Torres-Cabassa, A.S. & S. Gottesman, (1987) Capsule synthesis in Escherichia coli K-12 is regulated by proteolysis. *J. Bacteriol.* **169**: 981-989.

Trajtenberg, F., D. Albanesi, N. Ruetalo, H. Botti, A.E. Mechaly, M. Nieves, P.S. Aguilar, L. Cybulski, N. Larrieux, D. de Mendoza & A. Buschiazzo, (2014) Allosteric activation of bacterial response regulators: the role of the cognate histidine kinase beyond phosphorylation. *mBio*: 10.1128/mBio.02105-02114.

Tramonti, A., M. De Canio & D. De Biase, (2008) GadX/GadW-dependent regulation of the Escherichia coli acid fitness island: transcriptional control at the gadY-gadW divergent promoters and identification of four novel 42 bp GadX/GadW-specific binding sites. *Mol. Microbiol.* **70**: 965-982.

Tucker, D.L., N. Tucker & T. Conway, (2002) Gene expression profiling of the pH response in Escherichia coli. *J. Bacteriol.* **184**: 6551-6558.

Tucker, D.L., N. Tucker, Z. Ma, J.W. Foster, R.L. Miranda, P.S. Cohen & T. Conway, (2003) Genes of the GadX-GadW regulon in Escherichia coli. *J. Bacteriol.* **185**: 3190-3201.

Venkatesh, G.R., F.C. Kembou Koungni, A. Paukner, T. Stratmann, B. Blissenbach & K. Schnetz, (2010) BglJ-RcsB Heterodimers Relieve Repression of the *Escherichia coli bgl* Operon by H-NS. *J. Bacteriol.* **192**: 6456-6464.

Vianney, A., G. Jubelin, S. Renault, C. Dorel, P. Lejeune & J.C. Lazzaroni, (2005) Escherichia coli tol and rcs genes participate in the complex network affecting curli synthesis. *Microbiology (Reading, Engl.)* **151**: 2487-2497.

Wang, D., S.S. Korban & Y. Zhao, (2009) The Rcs phosphorelay system is essential for pathogenicity in Erwinia amylovora. *Mol. Plant Pathol.* **10**: 277-290.

Wang, Q., Y. Zhao, M. McClelland & R.M. Harshey, (2007) The RcsCDB signaling system and swarming motility in *Salmonella enterica serovar typhimurium*: dual regulation of flagellar and SPI-2 virulence genes. *J. Bacteriol.* **189**: 8447-8457.

Wehland, M. & F. Bernhard, (2000) The RcsAB box. Characterization of a new operator essential for the regulation of exopolysaccharide biosynthesis in enteric bacteria. *J. Biol. Chem.* **275**: 7013-7020.

Welch, R.A., V. Burland, G. Plunkett, 3rd, P. Redford, P. Roesch, D. Rasko, E.L. Buckles, S.R. Liou, A. Boutin, J. Hackett, D. Stroud, G.F. Mayhew, D.J. Rose, S. Zhou, D.C. Schwartz, N.T. Perna, H.L. Mobley, M.S. Donnenberg & F.R. Blattner, (2002) Extensive mosaic structure revealed by the complete genome sequence of uropathogenic *Escherichia coli*. *Proc. Natl. Acad. Sci. U.S.A.* **99**: 17020-17024.

Wiebe, H., D. Gurlebeck, J. Gross, K. Dreck, D. Pannen, C. Ewers, L.H. Wieler & K. Schnetz, (2015) YjjQ represses transcription of flhDC and additional loci in Escherichia coli. *J. Bacteriol.*

Wilson, G.G., K.Y.K. Young, G.J. Edlin & W. Konigsberg, (1979) High-frequency generalised transduction by bacteriophage T4. In., pp. 80-82.

Xia, X.X., Z.G. Qian & S.Y. Lee, (2011) Comparative proteomic and genetic analyses reveal unidentified mutations in Escherichia coli XL1-Blue and DH5alpha. *FEMS Microbiol. Lett.* **314**: 119-124.

Yamanaka, Y., T. Oshima, A. Ishihama & K. Yamamoto, (2014) Characterization of the YdeO regulon in *Escherichia coli*. *PLoS ONE*: 10.1371/journal.pone.0111962.

Zhou, Y.H., X.P. Zhang & R.H. Ebright, (1991) Random mutagenesis of gene-sized DNA molecules by use of PCR with Taq DNA polymerase. *Nucleic Acids Research* **19**: 6052.

Abbreviations

amp	ampicillin
ara	arabinose
bp	base pairs
BTB	bromothymol blue
cam	chloramphenicol
CRP	cAMP receptor protein
DMSO	dimethyl sulfoxide
dNTP	deoxynucleoside triphosphate
EDTA	ethylenediaminetetraacetic acid
EHEC	enterohaemorrhagic *E. coli*
εSD	epsilon Shine-Dalgarno sequence
FRT (FRT site)	Flp recombinase target site
HTH	helix-turn-helix (motif)
IM	inner membrane of the bacterial cell wall
IPTG	isopropyl-β-D-thiogalactopyranosid
kan	kanamycin
LPS	lipopolysaccharide
nt	nucleotide
NMEC	newborn meningitis-associated *E. coli*
NTP	nucleoside triphosphate
OD_X	optical density at X nm wavelength
OM	outer membrane of the bacterial cell wall
ONPG	o-nitrophenyl-β, D-galactopyranoside
PAGE	polyacrylamide gel electrophoresis
PCR	polymerase chain reaction
PG	peptidoglycan
rpm	revolutions per minute
RR	response regulator
RT	room temperature
spec	spectinomycin
TAP	tobacco acid pyrophosphatase
TCS	two-component system
tet	tetracycline
UPEC	uropathogenic *E. coli*
v/v	volume per volume
w/v	weight per volume
wt	wild-type
X-gal	5-bromo-4-chloro-3-indolyl-β-D-galactopyranoside

Figure Index

Figure 1. Model of activation and phosphotransfer of the Rcs phosphorelay 5
Figure 2. Targets of RcsB homo- and heterodimers in *E. coli*. 9
Figure 3. Homo- and heterodimer formation by RcsB, BglJ, RcsA, MatA and DctR. 13
Figure 4. Analysis of the P*ftsA lacZ* reporter in different strain backgrounds.....16
Figure 5. P*rprA lacZ* as a reporter for studying activation by RcsB 17
Figure 6. P*wza lacZ* as a reporter for studying activation by RcsA-RcsB 19
Figure 7. The mucoid phenotype depends on RcsB and RcsA. 21
Figure 8. Sequence alignment of *matA* upstream region of *E. coli* strains IHE3034, CFT073 and MG1655.....23
Figure 9. MatA-RcsB activates the $matA_{CFT073}$ promoter. 25
Figure 10. MatA-RcsB inhibits motility. 26
Figure 11. Influence of DctR and pH on expression. 28
Figure 12. Triple reporter system for RcsB mutagenesis screen 29
Figure 13. Structural model of the receiver domain of RcsB.....32
Figure 14. Effects of active site and surface exposed residues on transcriptional activation. 35
Figure 15. Effects of residues in DNA-binding domain and residues located in loop regions or non-exposed residues on transcriptional activation. 37
Figure 16. Stability assays of RcsB and its mutants by western blot analysis. 39
Figure 17. RcsB protein interaction studies by *SPINE*.....41
Figure 18. Experimental setup, used plasmids and results for RcsB-RNA polymerase interaction by bacterial two-hybrid analyses. 44
Figure 19. Idea of overexpressing RNA polymerase α subunit and αNTD in case of αCTD BglJ-RcsB interaction. 45
Figure 20. Effects of overexpression of the RNAP α subunit on different promoters.....46
Figure 21. Potential model of P*molR* activation by BglJ-RcsB. 48
Figure 22. Effects of overexpression of αCTD mutants on P*molR*, P*ynbA*, and P*yidL*. 50
Figure 23. Model of RcsB involved in different regulatory networks. 54

Table Index

Table 1. Cellular roles of RcsB homo- and heterodimers 8
Table 2. Summary of MatA microarray analysis results 22
Table 3. DctR upregulated loci determined by microarray analysis 27
Table 4. Strains 61
Table 5. Plasmids 65
Table 6. Oligonucleotides 70
Table 7. Western blot staining and developing conditions 85

Danksagung

Ich bedanke mich zuallererst bei Karin Schnetz für die Überlassung des interessanten Projektes, ihr Vertrauen und ihre Unterstützung während der gesamten Zeit.

Ich bedanke mich bei Jürgen Dohmen als Mitglied meines *Thesis Committees* und für die Übernahme des Zweitgutachtens dieser Arbeit. Zudem danke ich Kay Hofmann ebenfalls für seine Mitwirkung im *Thesis Committee* und Jan Riemer für seine Bereitschaft den Prüfungsvorsitz zu übernehmen.

Bei Richard Gourse und Wilma Ross bedanke ich mich für die Bereitstellung einiger Plasmide.

Darüber hinaus möchte ich mich bei Selman Öztürk, Julia Eckhoff, Markus Doll, Lisa Gausling und allen Studenten bedanken, die zu diesem Projekt beigetragen haben. Meinen ehemaligen und derzeitigen Kollegen Lilia, Kostja, Thomas, Katrin, Hannes, Susann und Aathmaja danke ich für die Unterstützung im Labor, die Diskussionen in der Mensa und die Abende im Sozialraum.

Ich danke meinen Eltern und meiner Schwester, auf deren Unterstützung ich immer zählen kann. Zuletzt danke ich Eva, die mir immer wieder die sonnigen Seiten des Lebens aufzeigt.

Erklärung

Ich versichere, dass ich die von mir vorgelegte Dissertation selbständig angefertigt, die benutzten Quellen und Hilfsmittel vollständig angegeben und die Stellen der Arbeit − einschließlich Tabellen, Karten und Abbildungen −, die anderen Werken im Wortlaut oder dem Sinn nach entnommen sind, in jedem Einzelfall als Entlehnung kenntlich gemacht habe; dass diese Dissertation noch keiner anderen Fakultät oder Universität zur Prüfung vorgelegen hat; dass sie − abgesehen von unten angegebenen Teilpublikationen − noch nicht veröffentlicht worden ist, sowie, dass ich eine solche Veröffentlichung vor Abschluss des Promotionsverfahrens nicht vornehmen werde. Die Bestimmungen der Promotionsordnung sind mir bekannt. Die von mir vorgelegte Dissertation ist von Prof. Dr. Karin Schnetz betreut worden.

_____

Hans Derk Pannen